Sumoylation of Nuclear Transport Receptors and the small GTPase Ran

Dissertation
for the award of the degree
"Doctor rerum naturalium"
of the Georg-August-Universität Göttingen

submitted by
Volkan Sakin

born in
Diyarbakir / TURKEY

Göttingen 2012

Members of the Thesis Committee:

1) Prof. Dr. Frauke Melchior (Reviewer)
DKFZ-ZMBH Alliance, ZMBH, Heidelberg

2) Prof. Dr. Nils Brose (Reviewer)
Dept. of Molecular Neurobiology, Max Planck Institute for Experimental Medicine, Göttingen

3) Prof. Dr. Gerhard Braus
Dept. of Molecular Microbiology and Genetics, Institute for Microbiology and Genetics, Georg August University Göttingen

Date of Oral Examination: 22 October 2012

Affidavit:

I hereby declare that this submission is my own work and that to my best knowledge and belief all extrinsic sources and aid are appropriately quoted.

Volkan Sakin

LIST of PUBLICATIONS

Moutty, M.C., Sakin, V., and Melchior, F. (2011). Importin α/β mediates nuclear import of individual SUMO E1 subunits and of the holo-enzyme. Mol Biol Cell. 22(5): 652-60.

Sakin V., Eskiocak U., Kars M.D., Iseri O.D., Gunduz U. (2008). hTERT gene expression levels and telomerase activity in drug-resistant MCF-7 cells. Exp Oncol. 30(3): 202-5

TABLE of CONTENTS

ACKNOWLEDGEMENTS

I am deeply grateful to Heidi Ehret not only for the technical helps she provided but also for her efforts and patience to teach me german. She brings so much energy and laughter to the lab, and it was such a privilage for me to be working next to her everyday even though my pipettes or ethanol solutions went for a walk from time to time. Du bist der beste Heidi. Vielen Dank für alles.

I also want to thank all former and current Melchior lab members for providing such a friendly working atmosphere as well as for all the fun times we had not only in the lab but also outside.

Special thanks from my heart go to my friend Dönem Avcı, for sharing the tea, lunch or ice-cream breaks as well as for the countless activities we have done together including getting our German driving licences, buying our first cars, and having road trips. Thanks for all the joy you brought to my life.

I am also grateful to my friend Christian, who has been a great listener many times. I owe him a lot for helping me cope with many stressful days during my Phd and also for the wise piece of advice and the support he has given.

I also would like to thank to my friend Miro for the countless unaccessible papers he has provided me with during the course of my PhD as well as his friendship.

I would also like to thank to my brother Caglar Sakin, for his support and friendship. He is always very understanding and motivating, and it has always been a pleasure to include each other in our dreams. Now, time to make them real!

Last but not least, I am truely thankful to my family. Knowing that you are there for me whenever I need is such a comforting feeling. Without your support and love, this work could not be achieved.

Son olarak sevgili aileme, ve özellikle de beni kosulsuz seven ve destekleyen canim anneme, tesekkür etmek istiyorum. Sizin desteginizi, sevginizi hissetmeden bu işi asla başaramazdım. Sizi cok seviyorum ve iyi ki varsiniz.

ABSTRACT

Sumoylation has been linked to nucleocytoplasmic transport since the discovery of SUMO as a modifier of vertebrate RanGAP1, which is targeted to the nuclear pore complex (NPC) after sumoylation. The link between sumoylation and nucleocytoplasmic transport has been strengthened even more with the discovery that the major component of NPC cytoplasmic filaments, RanBP2, acts as a SUMO E3 ligase. RanBP2 is in stable complex with Ubc9 and sumoylated RanGAP1, and it was recently discovered that it is the RanBP2 complex which acts as a multisubunit E3 ligase in cells. One fascinating feature of the RanBP2 complex is the very close proximity of the E3 ligase region and the binding site for sumoylated RanGAP1, both of which are embedded between binding sites for nuclear transport receptors and RanGTP. Consequently, nuclear transport receptors and the small GTPase Ran are candidates for RanBP2 dependent sumoylation. In line with this idea, in recent mass spectrometry based screens several nuclear transport receptors and Ran were found to be potential candidates for sumoylation. In this work, I aimed to test whether nuclear transport receptors and/or Ran are subjected to RanBP2-dependent sumoylation and to further investigate the mechanistics and the functional consequences of this modification. Indeed, upon enrichment of endogenously sumoylated proteins from HeLa cells by IP/peptide elution, in vivo sumoylation of Crm1, Impβ, and Imp5 could be confirmed. Although Ran sumoylation could not be detected by IPs, I could demonstrate that it is sumoylated in the context of semi-permeabilized cells. Subsequent in vitro sumoylation experiments revealed that an 80kDa RanBP2 fragment as well as the reconstituted RanBP2/Ubc9/RanGAP1-SUMO1 complex could stimulate the sumoylation of Ran, whereas PIAS E3 ligases could not. Large scale in vitro sumoylation of Ran by RanBP2 fragment followed by mass spectrometric analysis identified K130, 132, and 134 as SUMO acceptor sites. Mutation of these three lysines into arginines allowed to investigate functional consequences. While Ran triple mutant was predominantly nuclear and behaved identical to wild type in the canonical Imp α/β-dependent import, it showed a striking stimulation in Imp13-dependent import. Intriguingly, the sumoylation deficient Ran mutant lost dependency on its import receptor NTF2, suggesting that it may enrich in the nucleus by other means. In a side project, I could show that the import of the SUMO E1 enzyme subunit, Aos1, is not supported by transportin or Imp13 and demonstrate that Imp α/β interacts with the E1 heterodimer mainly via the Uba2 NLS. These findings complemented the study published as "Imp α/β mediates nuclear import of individual SUMO E1 subunits and of the holo-enzyme" (Moutty M.C., Sakin V., Melchior F., 2011 MBoC).

LIST of FIGURES

INTRODUCTION

The abundance or the function of proteins in cells can be regulated at DNA, mRNA, or protein level. Regulations at protein level are mediated by posttranslational modifications (PTMs) that allow a fast and reversible way of changing the biochemical features of proteins. For many years, PTMs were regarded as covalent attachment of small chemical moieties (phosphate, acetyl, methyl, etc.) to the proteins. However, this deep-rooted perception changed with the discovery that proteins themselves can also be used as modifiers. The first example of such a protein modifier was ubiquitin (Ub), which is a very small protein with only 76 amino acids. The canonical function of this peptidic modifier turned out to be targeting proteins for proteasomal degradation, although many other regulatory functions have been reported since its discovery (reviewed in Hershko and Ciechanover, 1998; Hicke and Dunn, 2003; Welchman et al., 2005; Komander and Rape, 2012). The idea that proteins can be used as modifiers led to the discovery of plethora of other peptidic modifiers such as ISG15, Urm1, Nedd8, SUMO, etc., which are currently categorized as Ubiquitin-like modifiers (Ubls). Most Ubls are covalently attached to proteins via lysine residues, and the mechanism for conjugation is similar. They use an enzymatic cascade specific for the modifier.

1. SUMO (Small Ubiquitin-like Modifier)

The best investigated Ubl beside ubiquitin is SUMO, which is a small protein (~11kDa). Although SUMO and ubiquitin share only ~18% sequence homology, the structures of the two proteins look very similar to each other (Bayer et al., 1998) SUMO proteins are highly conserved among eukaryotes. While *S.cerevisiae*, *D.melanogaster*, and *C.elegans* have only a single SUMO gene, plants and vertebrates have more than one. Human genome, for instance, encodes for four SUMO proteins: SUMO2 and SUMO3 are almost identical, differing only in 3 amino acids. These paralogs are commonly referred to as SUMO2/3 since there is currently no evidence that the two proteins have distinct targets. SUMO1 and SUMO2/3, on the other hand, share only ~50% sequence identity. The functionality of SUMO4 in vivo is currently enigmatic (Bohren et al., 2004; Owerbach et al., 2005) since it is unclear whether SUMO4 can be processed or conjugated in cells.

The SUMO pathway is essential in almost all eukaryotic organisms, exceptions being *S.pombe* and *A.nidulans.* In fission yeast when the only SUMO protein, PMT3, is deleted, cells are still viable but they develop severe growth problems (Tanaka et al., 1999). Similarly in filamentous fungi *A.nidulans*, the deletion of the SUMO-encoding gene sumO does not affect the viability. However, the mutant strain exhibits impaired growth and reduced conidiation (Wong et al., 2008). In budding yeast, on the other hand, the only SUMO protein, SMT3, is indispensable for cell viability (Johnson et al., 1997; Giaever et

al., 2002). In higher organisms, sumoylation is also required, which was shown by deleting the only SUMO conjugating enzyme, Ubc9. Ubc9 knockdown in chicken DT40 lymphocyte cell line, for instance, resulted in mitotic abnormalities followed by cell death (Hayashi et al., 2002). Similarly, Ubc9-knockout mice died during early embryogenesis due to mitotic abnormalities (Nacerddine et al., 2005). Whereas the requirement for sumoylation in eukaryotic cells is well-accepted in the field, the necessity for SUMO1 is currently controversial. In one study, the authors produced homozygous and heterozygous mice for SUMO1. All of the homozygous mice died during embryogenesis whereas surviving heterozygous mice developed cleft lip and palate (Alkuraya et al., 2006). In another study, it was shown that both homozygous and heterozygous knock-out mice for SUMO1 developed congenital heart defects, and the reexpression of SUMO1 in cardiac tisse rescued the phenotype (Wang et al., 2011). On the other hand, in two papers, SUMO1-knockout mice were reported to be alive without obvious phenotype (Evdokimov et al., 2008; Zhang et al., 2008a), which suggested that the absence of SUMO1 can be compensated by SUMO2/3.

1.1. SUMOylation and its machinery

The covalent attachment of SUMO proteins to the targets is called sumoylation, which comes in different forms such as monosumoylation, multiple monosumoylation, or polysumoylation (Ulrich, 2008). In humans, polysumoylation occurs with SUMO2/3 proteins due to the presence of SUMO-acceptor sites in their N-terminal regions. Although SUMO1 is known to form chains in vitro, in vivo data is currently missing. Sumoylation requires an enzymatic cascade comprising an E1 activating enzyme, E2 conjugating enzyme, and in most cases E3 ligases (summarized in Fig. 1). In the first step of conjugation, mature SUMO is recognized by the E1 activating enzyme, the heterodimer of SAE1/SAE2 in mammals, which activates SUMO in an ATP-dependent reaction (Gong et al., 1997; Desterro et al., 1999). Activation leads to a SUMO-adenylate intermediate, which is followed by the formation of a thioester bond between the carboxy terminus of SUMO and the catalytic cysteine of the SAE2 subunit of the heterodimer. The SUMO~E1 thioester bond is recognized by the only E2 conjugating enzyme, Ubc9, and SUMO is transferred to the catalytic cysteine of Ubc9 by thioester bond formation (Lee et al., 1998; Saitoh et al., 1998; Schwarz et al., 1998). In some cases, Ubc9, by itself, can catalyze the formation of an isopeptide bond between the carboxy terminus of SUMO and the ε-amino group of the target lysine residue. This is due to a consensus sumoylation motif in target proteins, which canbe directly recognized by Ubc9 (Sampson et al., 2001; Bernier-Villamor et al., 2002). The consensus motif is a short stretch of four amino acids with the sequence
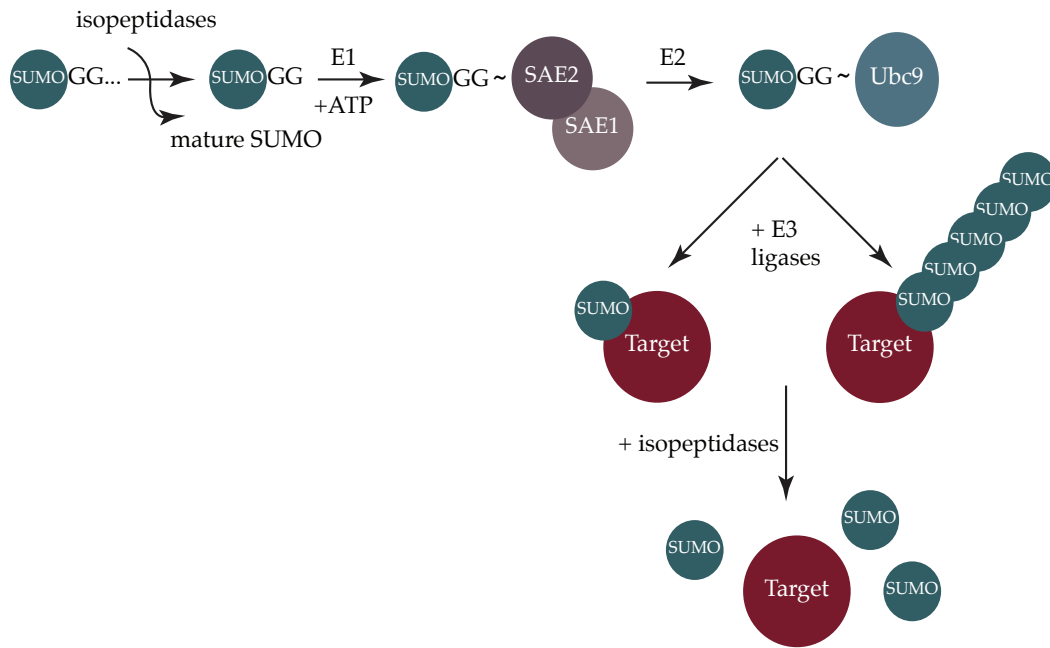
Fig. 1: Schematic overview of SUMO conjugation and deconjugation. The newly synthesized SUMO protein is first processed by isopeptidases to form the mature SUMO having the di-glycine (GG) motif at its C-terminus. Mature SUMO is then covalently linked to the SAE2 subunit of the E1 heterodimer via a thioester bond (~) in an ATP-dependent reaction. Next, SUMO is transferred from E1 enzyme to the E2 conjugating enzyme, Ubc9, through thioester bond formation. In the final step, SUMO is covalently linked to lysine residues of target proteins, in most cases with the help of E3 ligases. The final outcome of sumoylation might be either a single SUMO moiety or SUMO chains attached to the target proteins. The modification is reversed by the actions of several isopeptidases in cells.

of ψKxE (ψ: bulky hydrophobic amino acid, x: any amino acid) (Desterro et al., 1998; Rodriguez et al., 1999). In most cases, however, Ubc9 recognition by itself is not sufficient, and SUMO E3 ligases are required for efficient target sumoylation. Although the list of identified SUMO substrates is rapidly growing, the knowledge about E3 ligases is still rather limited.

There are two types of well-studied SUMO E3 ligases: The first and the largest group is characterized by the presence of a SP-RING domain, which is structurally similar to the RING domains of Ub E3 ligases. The members of this group recognize the target and Ubc9 directly. PIAS (Protein inhibitors of activated STATs) family of proteins (Johnson and Gupta, 2001; Schmidt and Muller, 2002), hMms21 (Potts and Yu, 2005), and Zip3 (Cheng et al., 2006) comprise the SP-RING domain SUMO E3 ligases. The PIAS family of proteins has two members in yeast: Siz1 (Takahashi et al., 2001) and Siz2 (Johnson and Gupta, 2001) whereas in mammals, there are five members: PIAS1, PIAS3, PIASxα, PIASxβ, and

PIAS4 (reviewed in Rytinki et al., 2009). The second group is comprised of only one unique member, RanBP2 protein, which is discussed in great detail in the following chapter (Introduction/Section 3.1.). Besides these two groups, many other proteins have been reported to show SUMO E3 ligase activity. A few examples are Pc2 (Kagey et al., 2003) (Kagey et al., 2003), HDAC4 (Grégoire and Yang, 2005; Lee et al., 2009), RHES (Subramaniam et al., 2009), TOPORS (Weger et al., 2005), MAPL (Braschi et al., 2009), TLS (Oh et al., 2010), and TRAF7 (Morita et al., 2005). However, the mechanisms underlying how these proteins function need to be further investigated.

Sumoylation is a very dynamic modification which is reversed by SUMO-specific isopeptidases. Most of these enzymes are equipped with two distinct enzymatic activities: Hydrolase activity, which is responsible for the processing of the C-terminus of SUMO to expose a di-glycine motif (Gly-Gly) required for conjugation and the isopeptidase activity, which cleaves SUMO from either target proteins or chains. In yeast, there are only two SUMO isopeptidases, which are Ulp1 (Ubiquitin like protease 1) and Ulp2, whereas in mammals the number is still increasing although the SENP (SUMO/Sentrin specific proteases) family of proteases is well-defined with currently seven members: SENP1, 2, 3, 5, 6, 7, and 8. Although classified in this family, SENP8 is not specific for SUMO but for Nedd8 (Gan-Erdene et al., 2003; Mendoza et al., 2003; Wu et al., 2003). All the other members are specific for SUMO, some showing paralog specificity for SUMO2/3. Very recently, the first examples of SUMO-isopeptidases which do not belong to the SENP family of proteases has been described, and the enzymes are named as DeSI1 (DeSumoylating Isopeptidase 1) (Shin et al., 2012) and Uspl-1 (Ubiquitin-specific protease-like 1) (Schulz et al., 2012).

Noncovalent interactions with SUMO proteins contribute both to modification and to downstream events. At the moment, a single, yet prominent SUMO interaction motif (SIM) is known. SIMs are short stretches of hydrophobic amino acids, V/I-X-V/I-V/I, which are often flanked by negative charges, which can either be provided by acidic amino acids or phosphorylated serine residues (Song et al., 2004; Hannich et al., 2005; Hecker et al., 2006; Stehmeier and Muller, 2009). They are also found in SP-RING E3 ligases. Functionally, they might be involved in the stimulation of target sumoylation (Meulmeester et al., 2008) as well as the assembly of many PML proteins into PML nuclear bodies (Shen et al., 2006).

1.2. Functional outcomes of SUMOylation

There are hundreds of proteins, mostly being nuclear, modified with SUMO (Golebiowski et al., 2009). Therefore, a wide range of cellular processes such as transcription, DNA repair, DNA replication, nucleocytoplasmic transport, signalling, and cell cycle are regulated by sumoylation. The functional consequences of sumoylation are very diverse and hard to predict. Yet, most of them can be explained at molecular level by three major changes in protein-protein interactions: First, sumoylation can promote protein-protein interactions since additional surfaces are introduced with SUMO. The prototypical example for such change is the sumoylation of RanGAP1, which targets the protein to the cytoplasmic filaments of nuclear pore complexes (Matunis et al., 1996; Mahajan et al., 1997) by promoting its interaction with RanBP2. Another well-known example is the sumoylation of PML, which is required for the formation of PML nuclear bodies (Zhong et al., 2000). Secondly, it can disrupt the already existing protein-protein interactions as in the case of E2-25K and Usp25 sumoylation. Sumoylation of E2-25K inhibits the interaction of the enzyme with the ubiquitin E1 enzyme, thereby decreasing its ubiquitination activity (Pichler et al., 2005). Similarly, USP25 can no longer interact with ubiquitin chains upon sumoylation, which results in decrease in deubiquitinating activity (Meulmeester et al., 2008). Lastly, sumoylation can change the conformation of the protein as observed for the DNA repair enzyme, thymine DNA glycosylase. Upon sumoylation, the enzyme changes its conformation, which facilitates the release from DNA (Hardeland et al., 2002; Baba et al., 2005). Overall, different types of molecular changes due to sumoylation might change the subcellular/subnuclear localization, the activity, or the stability of proteins (reviewed in Geiss-Friedlander and Melchior, 2007).

2. Nucleocytoplasmic transport

In eukaryotes, the genetic material is physically separated from the rest of the cell in the nucleus. The eukaryotic nucleus is surrounded by the nuclear envelope which is composed of two membranes separated by the ER lumen. The outer nuclear membrane is continuous with the endoplasmic reticulum membrane. Compartmentalization of genetic material allows cells to perform different cellular processes at differing subcellular environments. As a result of that DNA replication and transcription are nuclear processes, whereas protein translation occurs in the cytoplasm. Such organization of cells, on one hand, provide the cells with additional ways of regulating the flow of information, but on the other hand, requires that proteins and RNAs are continuously shuttled between cytoplasm and nucleus. Such transport is accommodated by nuclear pore complexes (NPCs), which are the sole openings between the two compartments.

2.1. The structure of nuclear pore complexes

NPCs have been extensively studied since their discovery in the 1950s (reviewed in Hoelz et al., 2011). They are proteinaceous structures formed at the regions where outer and inner nuclear membranes are fused and allow passive diffusion of small molecules such as ions, metabolites, or small proteins with a diameter less than 9nm (Paine et al., 1975; Bonner et al., 1978). Proteins bigger than ~40kDa, however, require transport signals which are recognized by nuclear transport receptors (NTRs) that facilitate the passage through the pores (Kiseleva et al., 1998). With the help of NTRs, transport of proteins up to 39nm in diameter could be achieved (Panté and Kann, 2002), which is approximately four times bigger than diffusion can accommodate.

NPCs are composed of approximately 30 different proteins, collectively called nucleoporins (nups), which are present in multiples of eight copies. Due to this eight-fold symmetrical architecture of the pore complexes through the central axis of the pore, there are approximately 500-1000 protein molecules in a given NPC (Hoelz et al., 2011), which makes NPCs huge protein assemblies. In *Dictyostelium discoideum*, the outer diameter and the length of the pores were determined as ~125nm and ~150nm, respectively (Beck et al., 2004; 2007), although NPCs are different in size in different organism. For instance, in budding yeast they have a mass of ~66MDa (Rout and Blobel, 1993) whereas in higher eukaryotes they are ~125Mda (Reichelt et al., 1990). Although individual proteins show little sequence homology among yeast and vertebrates (Adam, 2001), the overall structure of NPCs seem to be evolutionarily conserved (Yang et al., 1998). The number of NPCs, on the other hand, usually varies depending on the size and the transport needs of the cell. A typical proliferating human cell contains ~3000-5000 NPCs (Görlich and Kutay, 1999) whereas yeast cells have only ~190 (Rout and Blobel, 1993).

2.2 Nuclear transport receptors (NTRs)

NTRs are soluble components of the nucleocytoplasmic transport machinery that can carry cargo proteins and RNAs through the NPC. The best studied family of NTRs is the importin β (Imp β) superfamily of receptors, which has at least 21 members in humans and 14 members in budding yeast (reviewed in Görlich and Kutay, 1999). The name of the family comes from the founding member, Imp β, which was the first transport receptor identified (Enenkel et al., 1995; Görlich et al., 1995). Imp β-like transport receptors share some common features, although the sequence homology among them is relatively low (~15-20%) (Cook et al., 2007). They are made up of tandemly repeated HEAT motifs, which are ~50 aa long occuring in a wide range of eukaryotic proteins (Andrade et al., 2001). They all have a similar size (~100kDa) and isoelectric point (average ~5.1) (Fornerod et al., 1997; Görlich et al., 1997). Imp β-like transport receptors are intrinsically

flexible, which is believed to help them recognize a wide range of different cargos (Conti et al., 2006). They can interact with FG repeats of nucleoporins (Ohno et al., 1998; Damelin and Silver, 2000), which allows them to go through the complex milieu of the central channel of nuclear pores. Finally, they all bind to the small GTPase Ran (discussed in great detail below in Section 2.3.) via their N-terminal regions.

Depending on the direction they carry their respective cargo, Imp-β superfamily of transport receptors are divided into two groups: importins and exportins. Importins interact with their respective cargos in the cytoplasm and carry them to the nuclear compartment, whereas exportins function the other way around (reviewed in Macara, 2001). Importins and exportins recognize signal sequences on their respective cargos either directly or indirectly via adaptor proteins such as Importin α (Impα) and snurportin. These sequences are called nuclear localization sequences (NLSs) and nuclear export sequences (NESs) for import and export, respectively. There exists different types of NLSs but the best characterized one is the classical NLS (cNLS). It is comprised of basic amino acids and can be either mono- or bipartite. In case of bipartite cNLSs, the second cluster of basic amino acids is usually separated from the first cluster with a linker of varying size (~10-12 aa) (reviewed in Lange et al., 2007). Nuclear export sequences, on the other hand, are usually comprised of hydrophobic amino acids. The best characterized NES so far is the leucine-rich NES originally discovered in the HIV-1-Rev protein (Fischer et al., 1995) and PKI (Wen et al., 1995). The leu-rich NES is specifically recognized by the well-studied exportin, Crm1 (chromosome region maintenance 1), although it is known that Crm1 can also recognize some of its cargos independent of a leu-rich NES. Such an interaction occurs, e.g., between Crm1 and snurportin (Paraskeva et al., 1999).

2.3. Ran

2.3.1. Biochemical features of Ran

Ran (Ras-related nuclear protein) is a small GTPase (~25kDa) which belongs to the superfamily of Ras proteins. It shares homology to Ras in its guanine nucleotide binding domain (G-domain). Unlike many other G-proteins, Ran is predominantly nuclear, and a small pool of it can also be found in cytoplasm. In contrast to other members of the Ras superfamily, which are modified by fatty acids or isoprenoids that usually target the proteins to membranes, Ran is not modified and hence soluble. All eukaryotic cells contain Ran, and it has been highly conserved throughout evolution (Rush et al, 1996). It is an extremely abundant protein (~10^7 copies/cell) and makes up of ~0.4% of the total cellular protein (Bischoff and Ponstingl, 1991). As a small GTPase, Ran has intrinsic GTPase activity, which is however very slow, and it requires the help of a GTPase activating protein for full catalytic activity. Therefore, Ran is considered to be an

incomplete enzyme. Ran has a strong affinity towards guanine nucleotide, which is Mg^{2+}-dependent (pM-nM range), and the dissociation of the nucleotide from the protein is very slow.

2.3.2. Ran GTPase cycle

Like all other G-proteins, Ran cycles between GDP- and GTP-bound conformations. The conformational change between these two different states is striking and occurs in three different regions of Ran named as switch I (aa 37-45), switch II (aa 69-85), and the C-terminal acidic tail (Scheffzek et al., 1995). Due to its biochemical properties discussed above, Ran requires two accessory proteins in order to switch between the two conformations: In mammals, these are RanGAP1 (Ran GTPase activating protein 1) and RCC1 (Regulator of chromosome condensation 1) (Fig. 2). RanGAP1 increases the intrinsic GTPase activity of Ran by a factor of 10^5 in vitro (Bischoff et al., 1994), thereby converting RanGTP to RanGDP. RCC1, on the other hand, stimulates the nucleotide exchange on Ran by up to five orders of magnitude (Bischoff and Ponstingl, 1991), allowing Ran to bind GTP since free GTP concentrations in cells are 10-fold higher than GDP (Bourne et al., 1991). Interestingly, RanGAP1 and RCC1 are localized to different compartments in cells. RanGAP1 is localized to the cytoplasm and the cytoplasmic filaments of nuclear pore complexes, the latter being mediated via sumoylation of RanGAP1 as mentioned previously (Matunis et al., 1996; Mahajan et al., 1997). RCC1, on the other hand, is a chromatin-bound protein, which interacts with the core nucleosome components H2A and H2B (Ohtsubo et al., 1987; Nemergut et al., 2001). Differential localization of the two effectors of Ran results in a steep gradient of RanGTP to RanGDP in the direction of nucleus to cytoplasm, which is essential for the directionality of nucleocytoplasmic transport (Izaurralde et al., 1997). Attempts to measure this gradient by FRET-based experiments led to the estimation that the RanGTP concentration in the nucleus is 100-fold higher than in the cytoplasm (Kalab et al., 2002).

Despite the continuous efflux of Ran (10^5 mol/sec per nucleus) from the nucleus (Smith et al., 2002; Görlich et al., 2003) due to shuttling importins and exportins, Ran is still predominantly nuclear (Moore and Blobel, 1994). This is mainly due to the active import of Ran to the nucleus by its import receptor, NTF2 (Nuclear transport factor 2) (Ribbeck et al., 1998; Smith et al., 1998). NTF2 is a homodimeric import receptor, which does not belong to the Imp β superfamily of transport receptors. NTF2 forms a complex with Ran in GDP-bound state and passes through the nuclear pores since it has the intrinsic ability to interact with nucleoporins via their FG-repeats (Bayliss et al., 2002). On the

nucleoplasmic side, probably the nucleotide exchange reaction with RCC1 triggers the dissociation of Ran from NTF2 since it can not interact with Ran in GTP-bound conformation (Stewart et al., 1998).

2.3.3. Functions of Ran in nuclear transport and beyond

Ran is an essential protein with several important functions. Besides its well-established role to regulate the directionality of nucleocytoplasmic transport Ran is also involved in two other key cellular processes: Spindle formation and nuclear envelope reassembly. RanGTP in the nucleus interacts with importin-cargo complexes, releasing the cargos in the nucleus, and helping the importins recycle back to the cytoplasm. It also interacts with exportins, increasing their affinity towards their respective cargos, which results in trimeric export complex formation. Molecular details of such regulation is discussed in detail in Section 2.4. RanGTP also regulates the spindle assembly around the vicinity of chromatin by releasing spindle assembly factors such as TPX2 and NuMA from Imp α/β inhibition in a similar way how it releases the cargo proteins from Imp α/β in the nucleus (Nachury et al., 2001; Wiese et al., 2001; Gruss et al., 2002). The RanGTP gradient around the mitotic chromosomes (Kalab et al., 2002) spatially controls microtubule formation and stabilization. The role of Ran in nuclear envelope formation, on the other hand, is not yet fully understood but it is known that both nucleotide exchange and GTP hydrolysis are required for the process (Hetzer et al., 2000; Zhang and Clarke, 2000).
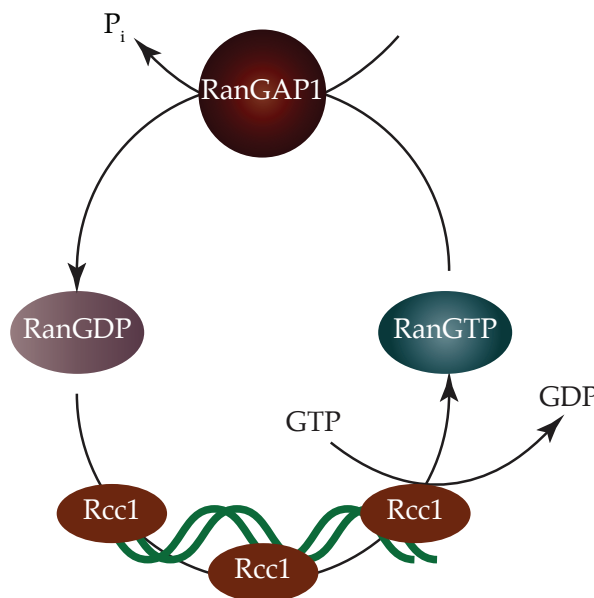
Fig. 2: Schematic representation of the Ran cycle. Ran cycles between two different conformations with the help of two accessory proteins. The nucleotide exchange factor, RCC1, is responsible for the exchange of GDP with GTP in the nuclear compartment since it is a chromatin-bound enzyme. RanGTP hydrolysis to RanGDP, on the other hand, is carried out with the help of the cytoplasmic RanGAP1.

2.4. Molecular mechanisms of nucleocytoplasmic transport

Nucleocytoplasmic transport is a remarkably fast and complicated process, which enables ~100-1000 cargos to go through a single pore complex every minute (Ribbeck and Görlich, 2001). Most of the transport processes are mediated via the Imp β-superfamily of nuclear transport receptors although alternative transport mechanisms were described as well. Nucleocytoplasmic transport is a combination of biochemical reactions (refer to Fig. 3), which can be grouped into four distinct steps (reviewed in Stewart, 2007): In the first step, transport complexes are formed between transport receptors and cargo proteins. In case of import, importins recognize their respective cargo proteins in the cytoplasm directly or with the help of adaptor proteins such as Imp α and snurportin. In export, however, the interaction between exportins and cargo proteins is not strong enough and requires stabilization by RanGTP. Therefore, export complexes can only form in the nucleus, where high RanGTP concentrations are available. In the second step, transport complexes formed on either side of the nuclear envelope translocate through the nuclear pores. This step is energy-independent and non-directional (facilitated diffusion) (Schwoebel et al., 1998; Englmeier et al., 1999; Ribbeck et al., 1999). Although several models such as „virtual gate model" (Rout et al., 2003), „the spaghetti oil model" (Macara, 2001), and „selective phase model" (Ribbeck and Görlich, 2001) have been suggested to account for the movement of transport complexes through the pores, the exact underlying mechanisms remain still enigmatic. In the third step, the directionality of the cargo transport is established by compartment-specific dissociation of cargo proteins. For import, it is the high RanGTP concentrations in the nucleus that promote cargo dissociation. RanGTP interacts with all importins via their N-terminal region (Vetter et al., 1999; Lee et al., 2005), which, in turn, leads to the release of respective cargo molecules in the nucleoplasm. For export, it is the RanGTP hydrolysis on the cytoplasmic filaments or in the cytoplasm, which leads to the dissociation of trimeric export complexes. The directionality of the translocation is not dependent on the composition of nuclear pores but on the dissociation of cargo-carrier complexes which was nicely documented by changing the direction of the transport by inverting the Ran gradient (Nachury and Weis, 1999). In the final step, importins recycle back to the cytoplasm in complex with RanGTP. Hydrolysis of RanGTP by RanGAP1 sets them free for another round of import. This fast step is however complicated by the fact that transport receptors can block the hydrolysis of RanGTP by RanGAP1, which is exemplified in case of Imp β (Floer and Blobel, 1996). This inhibition is released by either cytoplasmic RanBP1 protein or the RanBP1-homology domains of RanBP2 at the cytoplasmic filaments. In case of RanGTP-Imp β complex, even the presence of RanBP1 or RanBP2 is not sufficient for GTP hydrolysis, and the reaction also requires the presence of Imp α and NLS-containing cargo (Yaseen and Blobel, 1999).
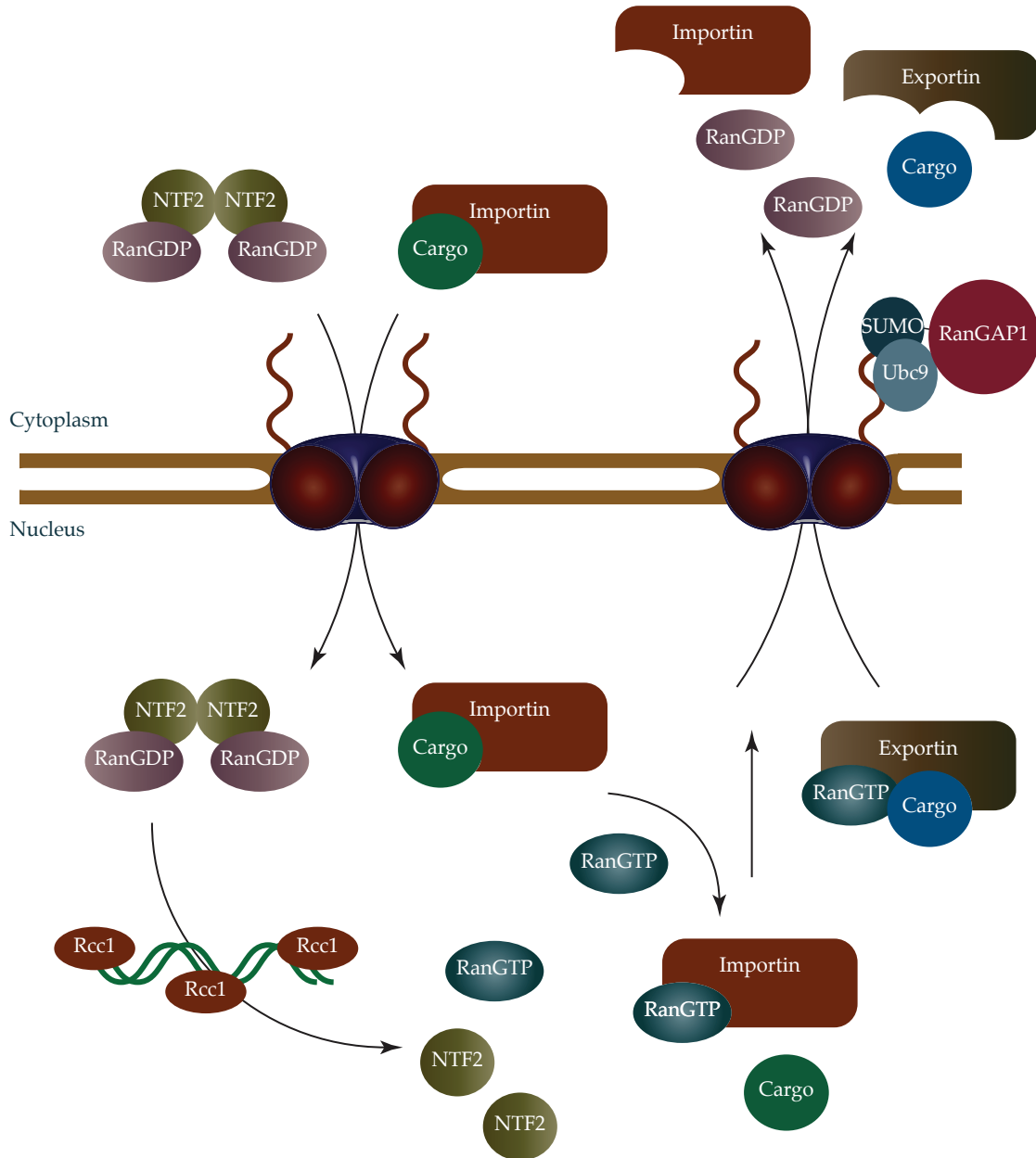
Fig. 3: Schematic representation of nucleocytoplasmic transport mechanisms. Different nucleocytoplasmic transport mechanisms are illustrated in the scheme. One is the canonical cargo transport via the Imp β superfamily of nuclear transport receptors and the other one is the import of Ran via NTF2, which does not belong to the Imp β superfamily. In case of importin- or exportin-dependent transport, receptor-cargo complexes form either in the cytoplasm or nucleus, respectively. These complexes then translocate through the NPCs. In case of import, importins interact with the nuclear RanGTP, which, in turn, releases the bound cargo in the nucleoplasm. In case of export, trimeric export complexes disassemble on the cytoplasmic side of NPCs upon RanGTP hydrolysis by RanGAP1. Importins recycle in complex with RanGTP whereas exportins by themselves. To recycle Ran, dimeric NTF2 interacts with two RanGDP molecules in the cytoplasm. The tetrameric complex then translocates through the NPCs. In the nucleus, chromatin-associated nucleotide exchange factor, RCC1, converts RanGDP into RanGTP, which possibly initiates the dissociation of RanGTP from NTF2.

Exportins, on the other hand recycle back to the nucleus in their free form by facilitated diffusion.

3. Intriguing links between sumoylation and nucleocytoplasmic transport

SUMO has been linked to nucleocytoplasmic transport ever since its discovery as a modifier of vertebrate RanGAP1, which is targeted to the nuclear pore complex (NPC) after sumoylation (Matunis et al., 1996; Mahajan et al., 1997; Lee et al., 1998; Mahajan et al., 1998). The interplay between sumoylation and nucleocytoplasmic transport has rapidly become evident with several papers describing either sumoylation or nucleocytoplasmic transport being a prerequisite for the other. Nuclear import of several proteins such as Sp100, PML, and Rad52 was essential for their efficient sumoylation (Duprez et al., 1999; Sternsdorf et al., 1999; Ohuchi et al., 2008). In line with these findings, it was also reported that the sumoylation of a consensus motif fused to a carrier protein was only possible when the protein was forced to the nucleus by addition of an NLS (Rodriguez et al., 2001). While many proteins required active nuclear import to be sumoylated, many others required sumoylation to enrich in the nucleus. For instance, sumoylation of the viral protein E1B-55kDa (Endter et al., 2001) and bovine papillomavirus E1 (Rangasamy et al., 2000) was shown to change the localization of the proteins from the cytoplasm to the nucleus. Similarly, Drosophila cells, which had a mutation in the semushi gene, the homolog of Ubc9, had a defect in the import of the transcription factor bicoid, indicating a correlation between sumoylation and nuclear import (Epps and Tanda, 1998). Although many examples indicate a link between sumoylation and import, nuclear export has also been observed to be regulated by sumoylation. For example, it was shown for the transcriptional repressor TEL that the mutations which impair sumoylation lead to the accumulation of the TEL in nucleus due to the defects in its nuclear export (Wood et al., 2003). Besides the individual examples where nucleocytoplasmic transport and sumoylation are interlinked, there has been a more global regulation described when Kathrin Stade and her colleagues reported that cNLS-dependent import was impaired in temperature sensitive *ulp1* or *uba2* yeast strains (Stade et al., 2002). They also showed that the importin α homolog in yeast, Srp1, accumulates in the nucleus in those yeast strains. This study clearly indicated that in the absence of sumoylation in yeast, Imp α/β-dependent import is defected. However, the underlying mechanisms for why Imp α accumulates in nucleus and the contribution of SUMO remained elusive.

Over the last decade, some components of the SUMO pathway have been discovered to be localized to NPCs (reviewed in Palancade and Doye, 2008), which strengthened the link between sumoylation and nucleocytoplasmic transport (Fig. 4). The first example was

the discovery of the yeast isopeptidase Ulp1 (Li and Hochstrasser, 1999), which was found to be localized to the nuclear basket via interactions with nucleoporins (Takahashi et al., 2000; Li and Hochstrasser, 2003). Localizing a SUMO isopeptidase to nuclear pore complexes turned out to be highly conserved during evolution. Ulp1's orthologs in *S.pompe, D. melanogaster*, *A.thaliana*, and mammals were discovered to localize to the NPCs as well (Hang and Dasso, 2002; Taylor et al., 2002; Zhang et al., 2002; Murtas et al., 2003; Smith et al., 2004). Another example came with the discovery that RanBP2/Nup358, the main component of the cytoplasmic filaments of NPCs, is a SUMO E3 ligase (Pichler et al., 2002). Intriguingly, a small fraction of the otherwise nuclear SUMO E2 conjugating enzyme Ubc9, was found to be in complex with RanBP2 together with sumoylated RanGAP1 (Saitoh et al., 1997; Swaminathan et al., 2004; Zhu et al., 2006). RanBP2 or RanGAP1 localization at the cytoplasmic face of the NPCs, however, is not completely conserved during evolution. The RanGAP1 ortholog in budding yeast, Rna1, for instance, is not sumoylated and exclusively cytoplasmic (Hopper et al., 1990). Interestingly in plants, RanGAP localizes to NPCs although it lacks the C-terminal tail region (Pay et al., 2002), which is sumoylated and necessary for targeting mammalian RanGAP1 to the
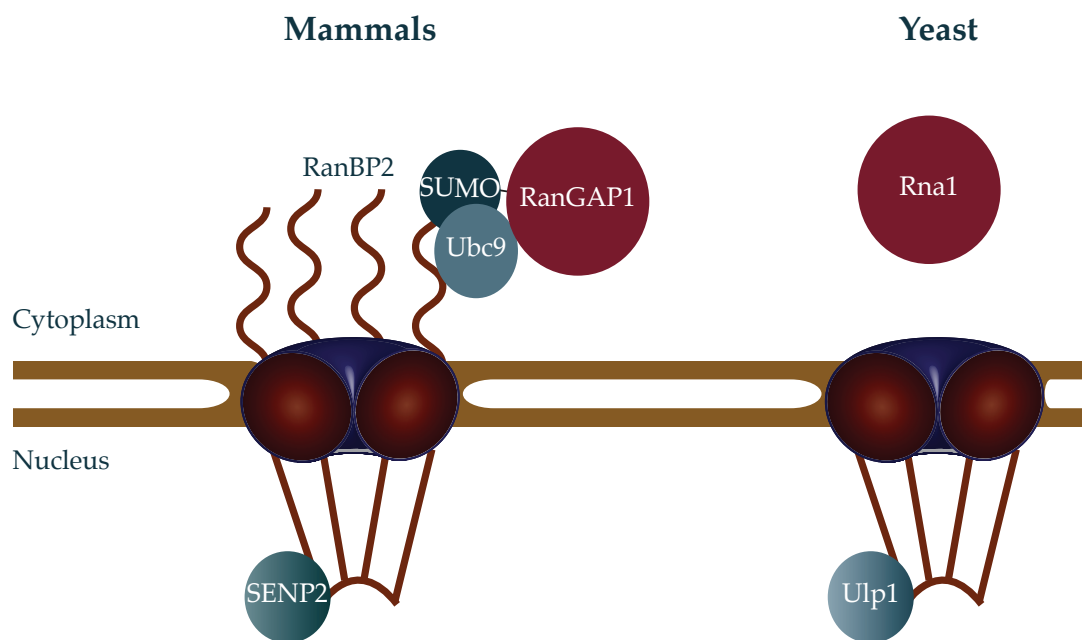
Fig. 4: Components of the SUMO pathway are localized at nuclear pore complexes in yeast and human. In mammals, RanBP2, which forms the cytoplasmic filaments of nuclear pore complexes, interacts with sumoylated RanGAP1 and Ubc9 and has SUMO E3 ligase activity. Similarly, the SUMO isopeptidase SENP2 is localized to the nuclear basket. In yeast, however, RanBP2 protein does not exist. The yeast ortholog of RanGAP1, which is Rna1, is not sumoylated and localized to the cytoplasm. Localizing a SUMO isopeptidase to the nuclear basket, on the other hand, is conserved: Mammalian SENP2 and yeast Ulp1 are enriched at nuclear pore complexes.

NPCs. Instead, RanGAP in *A.thaliana* has a plant-specific N-terminal extension responsible for the localization of RanGAP at nuclear pores. RanBP2 orthologs, on the other hand, do not exist in yeast or plant genome (Rout et al., 2000; Miller et al., 2010). Finally, during the course of this work, there have been many screens in which sumoylated proteins from total cell extracts were affinity purified and identified by mass spectrometry. Amongst hundreds of candidates in the resulting lists are several nuclear transport receptors including Crm1, Imp β, CAS, Imp α, and Importin 5. In two of these screens (Golebiowski et al., 2009; Bruderer et al., 2011) heat shock was used to increase sumo conjugation globally. It is known that cellular stress conditions such as heat shock increase the levels of sumoylated proteins especially modified with SUMO2/3 (Saitoh and Hinchey, 2000). Recently, one possible mechanism for this was suggested by the observation that the activities of several SENPs including SENP1-3 and SENP7 decrease upon heat shock (Pinto et al., 2012). In line with these observations, during the last year of my PhD work, the first nuclear transport receptor was shown to be sumoylated in yeast (Rothenbusch et al., 2012). In this work, Rothenbusch and her colleagues demonstrated that the yeast Kap114 (Imp 9 homolog) is sumoylated by the E3 ligase Mms21, and sumoylation/desumoylation cycles were required for proper recycling of the import receptor.

3.1. Multisubunit SUMO E3 ligase RanBP2

RanBP2/Nup358 is a giant nucleoporin (~358kDa) in vertebrates, and localizes to the cytoplasmic filaments of nuclear pore complexes during interphase (Wu et al., 1995; Yokoyama et al., 1995). It has several domains including a zinc finger domain, four Ran-binding domains, a leucine-rich domain, an E3 ligase region, a cyclophilin-homology domain as well as several FG and FxFG repeats (refer to Fig. 5). Via its Ran-binding domains and FG repeats, RanBP2 provides a transient interaction platform for RanGTP and nuclear transport receptors, respectively. It interacts stably with sumoylated RanGAP1 and Ubc9 (RanBP2 complex) (Mahajan et al., 1997; Saitoh et al., 1997; Lee et al., 1998; Pichler et al., 2002), which stays as a soluble entity in mitosis after nuclear envelope disassembly (Swaminathan et al., 2004). Of note, within the stable RanBP2 complex, sumoylated RanGAP1 is resistant to SUMO isopeptidases (Zhu et al., 2009), which makes RanGAP1 a unique SUMO substrate.

During the last year of this work, it was discovered in our lab that there is no free RanBP2 in cells neither in interphase nor in mitosis, and that the RanBP2 complex acts as a multi-subunit SUMO E3 ligase (Werner et al., 2012). This discovery is very crucial to study RanBP2-dependent sumoylation since biochemical features of small RanBP2 fragments in isolation and the RanBP2 complex differ significantly. RanBP2 is a unique SUMO E3

ligase (Pichler et al., 2002) without homology to other known ubiquitin or SUMO E3 ligases (Pichler et al., 2004). The E3 ligase activity of RanBP2 was mapped to a small region comprised of internal repeat 1 (IR1) and internal repeat 2 (IR2), which are 50 aa each and separated by a short linker region called M region (20 aa) (Fig. 5). Both IR1 and IR2 regions can interact with Ubc9 and stimulate sumoylation, although IR2 is much less efficient than IR1 in vitro (Pichler et al., 2004; Tatham et al., 2005). Surprisingly, sumoylated RanGAP1 and Ubc9, as part of the stable RanBP2 complex, occupy the IR1 region both in vitro and in vivo (Reverter and Lima, 2005; Werner et al., 2012). Therefore, it was initially suggested that in vivo RanBP2 complex can not be active and only represents an inactive trapped E2/E3 complex (Reverter and Lima, 2005). This idea was first challenged with the identification of the two in vivo targets of RanBP2: Topoisomerase IIα and Borealin (Dawlaty et al., 2008; Klein et al., 2009), both of which are sumoylated during mitosis, when a pool of RanBP2/Ubc9/RanGAP1*SUMO complex enriches at kinetochores and mitotic spindles (Joseph et al., 2002). The molecular explanation how RanBP2 complex shows activity was later shown in our lab. It turned out
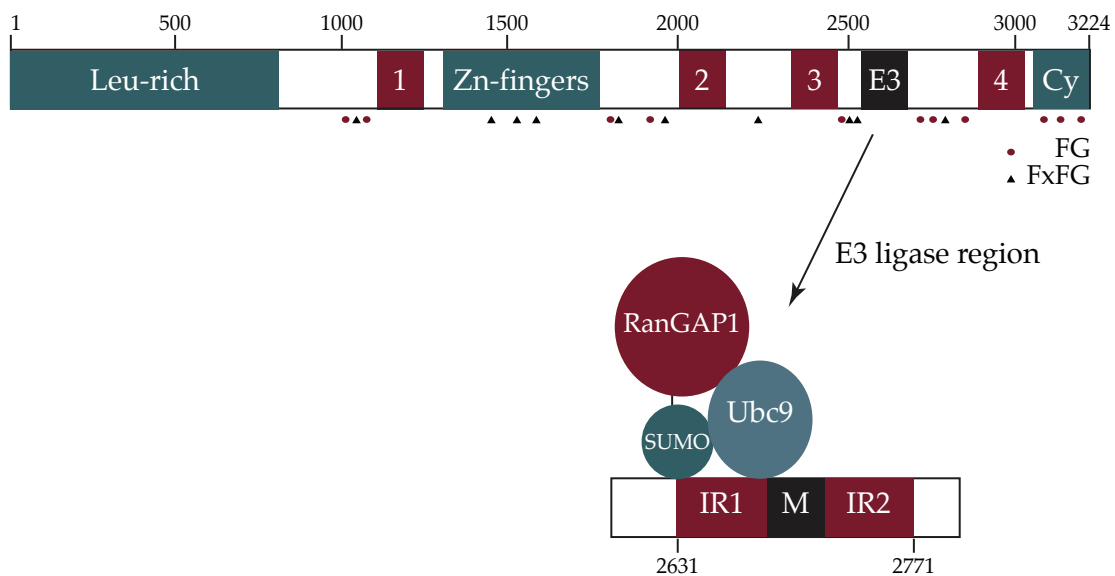
Fig. 5: The domain structure of ~358kDa RanBP2. The scheme shows several different domains of the nucleoporin RanBP2: N-terminal leucine rich domain (Leu-rich), four Ran-binding domains (numbered as 1-4), zinc-finger domain (Zn-fingers), E3 ligase region (E3), cyclophilin-homology domain (Cy), and several FG and FxFG (x: any amino acid) repeats, which are represented by small circles and triangles, respectively. Amino acid positions are shown as numbers at the top of the figure. The E3 ligase region (aa 2631-2771) is enlarged to visualize the binary interactions of the components of RanBP2 complex. This region of RanBP2 has two internal repeats (IR1 and IR2), 50 amino acids each, separated by a 20 amino acid middle region (M). Sumoylated RanGAP1 and the SUMO E2 conjugating enzyme, Ubc9, bind to the IR1+M region as depicted.

that upon complex formation, the catalytic center switches from IR1 to IR2, enabling IR2 to catalyze the in vitro sumoylation of physiological substrates such as Borealin much more efficiently than IR2 in free RanBP2 (Werner et al., 2012).

RanBP2 is part of the cytoplasmic filaments of NPCs and actively involved in nucleocytoplasmic transport. Different groups tried to adress the exact role of RanBP2 in transport with sometimes conflicting answers. Initially, it was shown that extensive blocking of RanBP2 with gold particles or NPCs formed from Xenopus egg extracts depleted for RanBP2 did not have any effect on Imp α/β- and transportin-depedendent import (Walther et al., 2002). On the other hand, it was shown that the cells depleted for RanBP2 had dramatically reduced rates for Imp α/β- and transportin-dependent import with model cargos (Hutten et al., 2008; 2009), although the import was not inhibited completely. Protein export, however, was only slightly affected by RanBP2 knockdown (Hutten and Kehlenbach, 2006). Studies with embryonic fibroblasts from RanBP2 conditional knockout mice clearly indicated that RanBP2 is required for cell viability, and it is the transport-related functions rather than mitotic functions that were indispensable (Hamada et al., 2011). Moreover, RanBP2 was also recently shown to affect the nuclear localization of a subset of cellular proteins (Wälde et al., 2012), without affecting the import of many others.

5. Aims of this work:

In light of the above mentioned links between sumoylation and nucleocytoplasmic transport, preliminary mass spectrometry evidence, and the intriguing architecture of the RanBP2 complex, the nuclear transport receptors and/or the small GTPase Ran may be regulated by RanBP2-dependent sumoylation. In this work, I aimed to test this hypothesis and further investigate the mechanistics and the functional consequences of nuclear transport receptors and/or Ran sumoylation during interphase.

MATERIALS & METHODS

1. MATERIALS

1.1. Technical Equipment

Axioskop 2 Fluorescence Microscope	Zeiss
Axiocam digital camera	Zeiss
Bacterial incubator ISF-1-w, ISF-1-x	Kühner
Balance PC4400	Mettler
BD FACSCanto™ II	BD Biosciences
Cell culture hood Hera Safe	Heraeus
Cell culture incubator Hera cell	Heraeus
Cell culture incubator Incucell	MMM medcenter
Centrifuge Allegra X-22R	Beckman Coulter
Centrifuge Heraeus Multifuge 1S	Thermo Scientific
Centrifuge RC 3BP+, RC 6+	Sorvall
Centrifuges 5415C, 5430, 5417R	Eppendorf
Chromatography system Äkta Purifier	GE Healthcare
Electrophoresis Power Supply EPS300/301	Pharmacia Biotech
Electrophoresis Power Supply Power Pac HC	Bio-rad
Electrophoresis and blotting chambers	Workshops at MPI, Martinsried and Biochemistry I, Göttingen
EmulsiFlex-C5	Avestin
Film developing machine Curix60	Agfa
Film developing machine X-OMAT 2000 Processor	Kodak
Freezers, Refrigerators	Liebherr
Gelfiltration columns:	GE Healthcare
Superdex200 10/300 GL	
MonoQ 5/50 GL	
HiLoad™ 26/60 Superdex™ 75 prep grade	
HiLoad™ 26/60 Superdex™ 200 prep grade	
Heating blocks	Störk-Tronic
HeraFreeze	Thermo Scientific
Icemachine	Scotsman
Incubation water bath 1008	GFL
Leica DMIL LED microscope	Leica
Leica SP2 confocal miscroscope	Leica
Luminescent Image Analyzer LAS-4000	Fujifilm
Magnetic stirrer MR Hei-Mix L	Heidolph
Microwave R-93ST-A	Sharp

NanoDrop ND-1000	Thermo Scientific
pH-meter 720	WTW
UV/Visible SpectroPhotometer Ultraspec 3100 pro	Amersham Biosciences
Pipettes	Gilson, Eppendorf
Precision balance TE601, Mettler PC4400, Micro balance CP 60-OCE	Sartorius
Reciprocating shaker 3005, 3015	GFL
Rotor S45A	Sorvall
Rotors TLA45, Type45Ti, Type70.1Ti	Beckman Coulter
Rotors: FiberLite F13 – 14x50cy, F9-4x1000y F10-6x500y	Piramoon Technologies Inc.
Scanner 4990 Photo, V700 Photo	Epson
Shaker DRS-12	Neolab
Sonifier Sonopuls GM 200	Bandelin
Thermocycler Primus	MWG Biotech
Thermocycler T3000 and Tprofessional	Biometra
Thermomixer Compact	Eppendorf, Hamburg
Ultracentrifuge Discovery™ 90SE, M120 SE	Sorvall
Ultrasonic bath Sonorex RK 100	Bandelin
UV-table UVT-20L	Herolab
UV-transilluminator	Peqlab Biotechnologie GmbH
Vacuum pump Laboport N480.3FTP	KNF Neuberger
Vortex 7-2020	Neolab
Water purification system MembraPure	MembraPure GmbH

1.2. Software

Adobe Acrobat 9 Pro	Adobe
Adobe Creative Suite 4	Adobe
DNASTAR Lasergene	DNAStar Inc.
Papers 2.1.12	Mekentosj
Image Reader LAS 4000	Fujifilm
Image J 1.43u	Wayne Rasband, National Institutes of Health, USA
MacPyMOL	DeLano Scientific LLC
Microsoft Office	Microsoft

1.3. Consumables

Autoradiography Films (Hyperfilm™ ECL, SuperRX)	GE Healthcare, Fujifilm
Canulas, syringes (different sizes)	Braun, Discardit II, Mediware
Cell culture consumables	Sarstedt, TPP
Centrifugal filter units	Millipore, Vivaspin
Dialysis tubing Spectra-Por	Roth
Disposable plastic columns Bio-Spin, Poly-Prep, Econo-Pac	Bio-Rad
Filter paper 3MM Whatman	Whatman
Glass slides, coverslips	Roth
Glassware	Schott
Gloves (Rotiprotect-LATEX, -NITRIL, Peha-soft)	Roth, Hartmann
Pipette tips (combi tips, filter tips)	Sarstedt, Eppendorf, Nerbe, Plus, Biozym Ratiolab
Plastic pasteur pipettes	Roth
Protein low binding reaction tubes	Sarstedt, Eppendorf
PROTRAN Nitrocellulose	Schleicher & Schuell
Reaction tubes	Sarstedt, Eppendorf
Scalpels	Lance Paragon LTD
Sterile filters and membranes (0.22-0.45μm)	Millipore, Pall, Sartorius
5mm Polystyrene Round-Bottom tubes	BD Falcon™

1.4. Chemicals, reagents, and enzymes

Common chemicals were obtained from AppliChem, CARL ROTH GmbH, Merck, Serva, and Sigma-Aldrich. Some selected chemicals, reagents, and enzymes are listed below:

Acrylamide solution (30%)	AppliChem
Alexa Fluor 488 C_5 Maleimide	Invitrogen
Aprotinin	Biomol
Apyrase	Sigma-Aldrich
ATP	Sigma-Aldrich
BSA, fraction V	AppliChem
Creatine Phosphate, Dipotassium Salt	Calbiochem
Creatine Phosphokinase	Calbiochem
Cyanogen bromide-activated sepharose 4B	Sigma-Aldrich
Digitonin, high purity	Calbiochem
DEAE Sepharose®	Sigma-Aldrich
DMEM (high glucose)	Gibco, PAA
DMSO	AppliChem

DMP	Thermo Scientific
dNTPs	Fermentas, Roche
ECL (Pierce ECL Western Blotting Substrate, Immobilon Western Chemiluminescent HRP Substrate)	Millipore, Pierce
Ethidium bromide	AppliChem
Fetal bovine serum (FBS)	Gibco
Formaldehyde Solution, 37%	AppliChem
Fugene® HD transfection reagent	Promega
GDP & GTP	Sigma-Aldrich
GeneRuler DNA ladder (1kb)	Fermentas
Glutamine (cell culture grade)	Gibco
Glutathione Sepharose	GE Healthcare, Macherey & Nagel
Glycerol 87% (Glycerin)	AppliChem
GMP-PNP	Sigma-Aldrich
Hexokinase	Sigma-Aldrich
HyClone® RNase-free water	Thermo Scientific
IPTG	Fermentas
Joklik's modified minimal essential medium	Sigma-Aldrich
Leupeptin	Biomol
Lipofectamine® RNAiMAX reagent	Invitrogen
N-Ethylmaleimide (NEM)	Sigma-Aldrich
Newborn calf serum (NCS)	Gibco
Ni-NTA agarose	Qiagen
Normal mouse IgG	Invitrogen
Oligonucleotides	Operon, Sigma-Aldrich
OptiMEM	Invitrogen
Ovalbumin	Sigma-Aldrich
PageRuler prestained protein ladder	Fermentas
PageRuler unstained protein ladder	Fermentas
PD10-column	GE Healthcare
Penicillin/Streptomycin	Gibco, PAA
Pepstatin	Biomol
Phusion polymerase	Finnzymes, NEB
PMSF	Sigma
Protein G agarose	Roche
Restriction enzymes	Fermentas, NEB
Slow Fade® Gold antifade reagent	Invitrogen

T4 DNA ligase	Fermentas
TEMED	AppliChem
Trypsin/EDTA	Gibco, PAA

1.5. Kits

NucleoBond® PC100, PC500	Macherey & Nagel
660nm Pierce Protein Detection Kit and Ionic detergent compatibility reagent (IDCR)	Pierce
Nucleospin® Extract II	Macherey & Nagel
Nucleospin® Plasmid	Macherey & Nagel
QIAquick® Gel Extraction Kit	Qiagen
QIAquick® PCR Purification Kit	Qiagen
Quick Start™ Bradford Protein Assay	Bio-Rad

1.6. Buffers and Stock Solutions

Buffers and stock solutions were prepared using deionized water unless noted otherwise. Setting the pH was carried out by titrating either NaOH or HCI unless noted otherwise. Stock solutions were either stored at -20°C as aliquots or prepared freshly.

Buffers

DNA Loading dye (6X)	60mM EDTA, 60% (v/v) glycerol, 0.2% (w/v) bromophenol blue, 0.2% (w/v) xylencyanol
Colloidal Coomassie dye stock solution	2% (v/v) ortho-phosphoric acid, 10% (w/v) ammonium sulfate, 0.1% (w/v) Coomassie G-250
Coomassie Destainer	10% (v/v) acetic acid, 45% (v/v) methanol
Coomassie staining solution	0.25% (w/v) Coomassie brilliant blue R-250, 10% (v/v) acetic acid, 45% (v/v) methanol
Laemmli running buffer	25mM Tris, 192mM glycine, 0.05% (v/v) SDS, prepared as 10x stock solution
Phosphate buffered saline (PBS)	140mM NaCI, 2.7mM KCI, 10mM Na_2HPO_4 1.5mM KH_2PO_4, pH 7.3; prepared as 10x stock solution
PBS-Tween	PBS supplemented with 0.2% (v/v) Tween20

Ponceau-S	0.5% (w/v) Ponceau-S, 1% (v/v) acetic acid
RIPA buffer	20mM Na_2HPO_4 pH 7.4, 150mM NaCI, 1% (v/v) Triton-X100 0.5% (w/v) Na-deoxycholat, 0.1% (v/v) SDS
SDS sample buffer	50mM Tris/HCI pH 6.8, 2% (v/v) SDS, 0.1% (w/v) bromophenol blue, 10% (v/v) glycerol, 100mM DTT prepared as 1x, 2x, and 4x stock solutions
Sumoylation Assay Buffer (SAB)	TB supplemented with 0.2mg/mL ovalbumine, 0.05% (v/v) Tween20, 1mM DTT, $1\mu g$/mL AP and LP
TAE (Tris-Acetate-EDTA) Buffer	40mM Tris pH 7.7, 1mM EDTA, 0.1% (v/v) acetic acid, prepared as 50x stock solution
Transport Buffer (TB)	110mM K-acetate, 2mM Mg-acetate, 1mM EGTA 20mM HEPES pH 7.3 titrated with KOH prepared as 10x stock solution
Western blot Buffer (WB)	25mM Tris/HCI, 193mM glycine, 20% (v/v) methanol, 0.04% (v/v) SDS prepared as 10x stock solution

Stock Solutions

Ampicillin	100mg/mL
Aprotinin (1000x)	1mg/mL
ATP	100mM ATP, 100mM Mg-acetate, 20mM HEPES, pH 7.4
Chloramphenicol (1000x)	30mg/mL
Digitonin	10% (w/v) in DMSO
Dithiothreitol (DTT)	1M
GDP/GTP	10mM GDP/GTP, 10mM $MgCI_2$, 20mM HEPES pH 7.4 titrated with NaOH
Hoechst 33258	1mg/mL
Kanamycin (1000x)	30mg/mL
Leupeptin/Pepstatin (LP) (1000x)	1mg/mL each, in DMSO
N-ethylmaleimide (50x)	500mM in DMSO, prepared freshly

Nocodazole	5mg/mL in DMSO
Pefabloc (100x)	100mM
PMSF	100mM in 2-propanol

1.7. Media

Bacterial media were sterilized by autoclaving whereas mammalian cell culture media were sterile-filtered.

Bacterial cell culture media

LB Medium	1% (w/v) bacto-tryptone, 0.5% (w/v) yeast extract, 1% (w/v) NaCI, pH 7. LB was supplemented with 1.5% (w/v) bacto-agar for agar plates
SOC Medium	2% (w/v) tryptone, 5% (w/v) yeast extract, 50mM NaCI, 2.5mM KCI, 10mM $MgCI_2$, 10mM $MgSO_4$

Mammalian cell culture media

Supplemented DMEM	Dulbecco's modified eagle medium (DMEM), 10% (v/v) FBS, Penicillin/Streptomycin (0.1 U/mL/100 μg/mL) 2mM L-glutamine

Jokliks Medium

Jokliks medium was prepared by dissolving Jokliks MEM powder (Sigma), 20g sodium hyrogen carbonate ($NaHCO_3$), and 23.8g HEPES in 10L ultrapure water. The pH of the medium was titrated to 7.1 with sodium hydroxide followed by filter-sterilization. The medium was stored at 4°C protected from light.

Other cell culture media and supplements were obtained commercially.

1.8. Cell lines

Bacterial strains

DH5α	F-φ80lacZ ΔM15 (lacZYA-argF) U169 deoR recA1 endA1 hsdR7 (r_k-, m_k+) phoA supE44 thi-1 gyrA96 relA1 λ-
BL21 (DE3)	F- ompT $hsdS_B$ (r_B- m_B-) gal dcm λ(DE3)
BL21 (DE3) pLysS	F- ompT $hsdS_B$ (r_B- m_B-) gal dcm λ(DE3), pLysS(Cm_R)
TOP10	F-mcrAΔ (mrr-hsdRMS-mcrBC) φ80lacZΔM15 ΔlacX74 recA1 araD139Δ (ara-leu) 7697 galU galK rpsL (Str^R) endA1 nupG λ-
Rosetta2 (DE3)	F- ompT $hsdS_B$(r_B- m_B-) gal dcm (DE3) pRARE2 (Cm^R)
JM109	e14- ($McrA^-$), endA1, recA1, gyrA96, thi-1 hsdR17 (r_k^-, m_k^+), relA1 supE44, Δ(lac-proAB), (F´ traD36, proAB, $lacI^qZ$ΔM15)

Mammalian cell lines

HEK 293T   Human embryonic kidney cell line

HeLa (obtained from Francis Barr)   Human cervix carcinoma cell line

HeLa suspension cells (CSH HeLa strain)   Human cervix carcinoma cell line

1.9. Oligonucleotides, vectors, and plasmids

DNA oligonucleotides for cloning		
Number in common stocks	Name	Sequence (5'-3')
1493	Impβ_BamHI_F	GAAGGATCCATGGAGCTGATCACCATT
1494	Impβ_NotI_R	GAAGCGGCCGCTCAAGCTTGGTTCTTCAG
1956	BamHI_mUbc9	ACTGGGATCCATGTCGGGGATCGCCCTCAG
1957	XhoI_mUbc9	CTTACTCGAGTTATGAGGGGGCAAACTTCTTCG
2180	SacI_Ran_For	CTGGAGCTCATGGCTGCGCAGGGAGAGCC
2181	Ran_EcoRI_Rev	GTAGAATTCTCACAGGTCATCATCCTCATCCG
DNA oligonucleotides for mutagenesis		
1666	RanK130,132,134R_For	GGATATTAAGGACAGGAGAGTGAGGGCGAGATCCATTGTCTTCC
1667	RanK130,132,134R_Rev	GGAAGACAATGGATCTCGCCCTCACTTTCCTGTCCTTAATATCC
1670	Imp13K856R_For	GGAAGTAGAGTCTGTGGGAAGGGTGGTACAGGAAGACGG
1671	Imp13K856R_Rev	CCGTCTTCCTGTACCACCCTTCCCACAGACTCTACTTCC
1672	Imp13K553R_For	CTCTTCTGTGTCCACCCTCAAGAGGATCTGCCGAGAGTGC
1673	Imp13K553R_Rev	GCACTCTCGGCAGATCCTCTTGAGGGTGGACACAGAAGAG

Vectors for bacterial expression		
Name	Features	Origin
pET11d	T7-tag, Amp^R	New England Biolabs
pET3		New England Biolabs
pET23a(+)	T7-tag, C-term. His-tag, Amp^R	Novagen
pET28a	N-term. and C-term.His-tag, Kan^R	Novagen
pET28b	N-term. and C-term.His-tag, Kan^R	Novagen
prSET-B	N-term. 6xHis-tag, Amp^R	Invitrogen
pQE-80L	N-term. His-tag, Amp^R	Qiagen
pQE-60	C-term. 6xHis-tag, Amp^R	Qiagen
pQE-32	N-term. His-tag, Amp^R	Qiagen
pGEX-6P-1	N-term. GST-tag, Amp^R	GE Healthcare
Vectors for mammalian expression		
pEGFP-C1	N-term. EGFP-tag, Kan^R,Neo^R	Clontech

Plasmids for bacterial expression		
Name	Features	Origin
pET11d-Ran wt	untagged Ran wt	Lab common stock Melchior F. et al., 1993
pET11d-Ran K130,132,134R	untagged RanK130,132,134R	this work
pET3-RanQ69L	untagged RanQ69L	Prof. Ralph Kehlenbach*
pET23a-Impβ	Impβ-His	this work
prSET-B-Impα	His-Impα	Prof. Ralph Kehlenbach*
pQE80-Imp13 wt	His-Imp13 wt	Prof. Ralph Kehlenbach*
pQE80-Imp13 K553R	His-Imp13 K553R	this work
pQE80-Imp13 K856R	His-Imp13 K856R	this work

pQE80-Imp13 K553,856R	His-Imp13 K553,856R	this work
pQE32-Transportin	His-Transportin	Prof. Ralph Kehlenbach*
pET28a-EYFP-M9	His-EYFP-M9	Prof. Ralph Kehlenbach*
pQE60-Crm1	Crm1-His	Prof. Ralph Kehlenbach*
pGEX-6P-1-Ubc9	GST-Ubc9	this work
pGEX-TEV-Rcc1	GST-Rcc1	Dr. Annette Flotho*
pET-NTF2	untagged NTF2	Prof. Dr. Dirk Görlich*
pET28a-Aos1	His-ECFP-Aos1	Dr. Marie-Christine Moutty*, PhD Thesis
pET28b-Uba2	Uba2-EYFP-His	Dr. Marie-Christine Moutty*, PhD Thesis
Plasmids for mammalian expression		
pEGFP-C1-Ran wt	EGFP-Ran wt	this work
pEGFP-C1-Ran K130,132,134R	EGFP-Ran mutant	this work

1.10. Proteins

Recombinant Protein	Source
His-Aos1/Uba2 (SUMO E1 enzyme)	Lab common stock^
Ubc9 (SUMO E2 enzyme)	Lab common stock^
His-RanBP2 fragment	Dr. Andreas Werner*
His-RanBP2/Ubc9/RanGAP1*SUMO1 complex	Dr. Andreas Werner*
His-RanBP2/Ubc9/acidic RanGAP1 tail - SUMO1 complex	Dr. Andreas Werner*
SUMO1	Dr. Andreas Werner*
SUMO2	Dr. Andreas Werner*
Strep-TEV-HA-SUMO3-Vme (Trap)	Dr. Erik Meulmeester*
YFP-SUMO1	Dr. Andreas Werner*

YFP-SUMO2	Dr. Andreas Werner*
His-Crm1	this work
His-Impβ	this work
His-Impα	this work
His-Imp13 wt	this work
His-Imp13 K553	this work
His-Imp13 K856R	this work
His-Imp13 K553,856R	this work
His-Transportin	this work
His-Imp5	Prof. Ralph Kehlenbach*
His-Imp9	Prof. Ralph Kehlenbach*
Ran wt	this work
Ran K130,132,134R	this work
RanQ69L	this work
CFP-Aos1	this work
Uba2-YFP	this work
GST-Ubc9-Alexa488	this work
FITC-BSA-NLS	Lab common stock^
YFP-M9	this work
NTF2	this work
GST-Rcc1	this work
GST	Dr. Andreas Werner*
Ovalbumin	Sigma
GST-PIAS1, GST-PIASxα , PIASxβ, PIAS3 GST-PIASy	Lab common stock^
GST-p53	Lab common stock^

* These people are current or former members of Melchior lab except for following people:

Prof. Dr. Ralph Kehlenbach, University of Göttingen

Prof. Dr. Dirk Görlich, MPIbpc, Göttingen

^ These proteins were purified by various members of Melchior lab and are available as common stocks in the lab.

1.11. Antibodies

Primary Antibodies

Antibody	Immunogen	Origin/Reference	Concentration	Dilutions
mouse anti-Ran	hRan aa. 7-171	BD Transduction Laboratories™	0.25 mg/mL	WB 1:4000 IF 1:2000
goat anti-Crm1	hCrm1-His	this work affinity purified	0.25 mg/mL	WB 1:500
rabbit anti-Imp13	hImp13	Proteintech	0.13 mg/mL	WB 1:2000
rabbit anti-Imp β	hImpβ	serum provided by Dr.Ralph Kehlenbach affinity purified	0.38 mg/mL	WB 1:1000
rabbit anti-Imp5	hImp5 aa 1-300	Santa Cruz (sc-11369)	0.2 mg/mL	WB 1:200
rabbit anti-GFP (FL)	*A.victoria* GFP aa 1-238	Santa Cruz (sc-8334)	0.2 mg/mL	WB 1:1000
mouse anti-SUMO1	hHis-SUMO1	Developmental studies Hybridoma Bank Uni. of Iowa (Matunis et al., 1996)	serum	WB 1:10

goat anti-SUMO2/3	RanGAP1 tail conjugated to SUMO2	Melchior Lab Bossis & Melchior, 2006	0.75 mg/mL	WB 1:500
goat anti-Aos1	His-hAos1	Melchior Lab	0.8 mg/mL	WB 1:1000
goat anti-Uba2	His-hUba2	Melchior Lab	0.5 mg/mL	WB 1:1000 IF: 1:200
rabbit anti-Ubc9	GST-Ubc9	Melchior Lab	0.2 mg/mL	WB 1:1000
rabbit anti-SENP1	peptide from hSENP1 sequence not provided by company	Epitomics	not provided	WB 1:5000
rabbit anti-TRIM28	synthetic peptide corresponding to aa surrounding Pro585 of Human TIF1β	Cell Signaling #4124	unknown	WB 1:1000

rabbit anti-PARP1	synthetic peptide corresponding to the caspase cleavage site	Cell Signaling #9542	unknown	WB 1:500
mouse anti-α-tubulin	Chicken brain tubulin	Sigma Clone DM 1A	unknown provided as ascites	WB 1:1000
mouse anti-Penta His	unknown	Qiagen	unknown	WB 1:1000
mouse anti-p53	human p53 aa 11-25	Santa Cruz (sc-126)	0.2 mg/mL	WB 1:1000

Secondary Antibodies

Horseradish peroxidase-conjugated secondary antibodies for western blot analysis were obtained from Jackson ImmunoResearch Laboratories distributed by Dianova and used at a dilution of 1:10000. Secondary antibodies for immunofluorescence conjugated to Alexa488 and Alexa594 were obtained from Molecular Probes (as 2mg/mL stock solutions) and were used at 2 μg/mL final concentration.

1.12. siRNAs

Name	5' to 3' Sequence	Reference
Uba2	AUAGACCAGUGCAGAACAAuu	PhD Thesis, Dr. Tina Lampe*

* Former member of Melchior lab

2. METHODS

Standard procedures in molecular biology, biochemistry, and cell biology were performed on the basis of „Molecular Cloning: A Laboratory Manual" Maniatis T., Fritsch E.F., Sambrook J. (Cold Spring Harbor Laboratory, New York, 1982), „Current Protocols in Protein Science" Coligan, J.E., Dunn B.M., Speicher, D.W., Wingfield, P.T. (John Whiley & Sons, 2003), and "Current Protocols in Cell Biology" Bonifacino, J.S., Dasso, M., Harford, J.B., Lippincott-Schwartz, J., Yamada, K.M. (John Whiley & Sons, 2000).

2.1. Molecular biology techniques

2.1.1. Culturing and storage of bacteria

Bacteria were cultured at 37°C in LB medium supplemented with the required antibiotics (ampicillin 100μg/mL, kanamycin 30μg/mL or chloramphenicol 30μg/mL for liquid cultures, half the concentration for plates) to maintain the transformed plasmid. Liquid cultures were shaken constantly at 180 rpm. For long-term storage, cultures were grown overnight, and supplemented with 50% glycerol followed by flash freezing in liquid nitrogen. Glycerol stocks were stored at -80°C.

2.1.2. Plasmid preparation

Plasmids were prepared mostly from DH5α bacteria at different scales (mini-, midi-, and maxi-preps) depending on the following applications such as cloning, clone screening via restriction enzyme digestion, mutagenesis, sequencing, storage, or transfection into mammalian cells. All plasmid purifications were performed with Macherey-Nagel DNA purification kits according to the manufacturer's instructions. In short, cells were grown overnight at 37°C, and harvested by centrifugation. Collected cells were resuspended in 50mM Tris-HCI, pH 8.0 supplemented with 10mM EDTA and 100μg/mL RNase A, and lysed with alkaline lysis buffer (200mM NaOH, 1% (v/v) SDS) (described by Birnboim and Doly, 1979). Cell debris and proteins were precipitated by the addition of neutralization buffer (2.8M KAc, pH 5.1). The soluble fraction was separated from the precipitated material by either loading the bacterial lysate onto filters and collecting the flow through or by centrifugation. The DNA was precipitated out of the solution by adding room-temperature isopropanol. The precipitated DNA was collected by centrifugation, washed with 70% (v/v) ethanol, dried, and reconstituted in TE buffer (10mM Tris-HCI, pH 8.0, 0.1mM EDTA) or sterile deionized H_2O. DNA concentration and the purity were determined by measuring the absorption at 230, 260, and 280nm by Nanodrop ND-1000 spectrophotometer.

2.1.3. Cloning

Polymerase chain reaction (PCR) techniques

PCR reactions were set up in a final volume of $50\mu L$ using up to 10ng plasmid DNA as a template, $0.5\mu M$ final concentration of forward and reverse primer (can be varied in a range of 0.2-$1\mu M$), $200\mu M$ of each dNTPs, and 1 unit of Phusion polymerase (Finnzymes) in Phusion HF buffer. The annealing temperature (Tm) for the primers used was calculated according to the online calculators,

(Phusion: http://www.finnzymes.com/tm_determination.html).

For primers > 20nt, 3°C was added to the calculated temperature whereas for primers < 20nt, calculated temperature for the primer with the lower Tm value was used. If the Tm values were at least 69°C (for primers >20nt) or 72°C (for primers <20nt), a 2-step protocol was used with the combined annealing/extension step at 72°C even when the Tm values of primers exceeded 72°C. Annealing time for Phusion polymerase was usually used in the range of 10-30 seconds, whereas the extension time was calculated depending on the length of the amplicon (15 seconds per 1kb of DNA). In most cases, the following 2-step program was used:

Initial Denaturation	98°C	30 sec	
Denaturation	98°C	5 sec	
Annealing	72 °C	20 sec	30 cycles
Elongation	72 °C	15 sec / kb	
Final elongation	72 °C	10 min	
Hold	4 °C		

Restriction of DNA by endonucleases

Restriction enzymes were obtained from New England Biolabs. Digestion reactions were set up either in $20\mu L$ or $50\mu L$ reactions depending on whether vector DNA or amplified PCR fragment is to be cut. For vector DNA, in general 2-$5\mu g$ DNA were cut, whereas for the amplified PCR fragments, everything that could be purified was used for the reaction. In most cases, 20 units of the restriction enzymes were used, and under no circumstances should the volume of the enzyme exceed 1/10th of the reaction volume. In case of double restrictions, the appropriate buffer was chosen with the „Double digest finder" tool from the website of NEB. Where necessary, reactions were supplemented with BSA and incubated in 37°C room for at least 2hours.

Agarose gel electrophoresis and DNA extraction

The amplified PCR fragments or digested plasmid DNAs were resolved by agarose gel electrophoresis. In most cases, 1-2% (w/v) agarose gels, chosen to provide optimal resolution, were prepared by dissolving the required amount of agarose powder in TAE buffer (refer to section 1.6. Buffers and Stock solutions) upon heating. The solution was allowed to cool down in a special chamber with combs to form the agarose gel. DNA samples were supplemented with 6x DNA loading dye (60mM EDTA, 60% (v/v) glycerol, 0.2% (w/v) bromophenol blue, 0.2% (w/v) xylenecyanol in H_2O) to have a final concentration of 1x, loaded into the pockets of the gel, and resolved at 80-100 Volts for 1-2 hours. Afterwards, the gel was incubated for ~30 min in a TAE bath supplemented with $1\mu g/mL$ ethidiumbromide to stain the DNA. Visualization of the DNA was performed using UV light (365nm), and the exposure time was kept minimal to avoid DNA damage. The DNA fragments of interest were excised from the agarose gels with sterile scalpels and extracted with Nucleospin® Extract II Kit from Macherey-Nagel according to the manufacturer's instructions.

DNA ligation

Ligation of DNA fragments were carried out in $10\mu L$ reaction volumes. In most cases, 50-400ng of linear vector together with an amount of insert DNA that provides a molar ratio of 3:1 (insert/vector) were incubated together with $1\mu L$ of T4 DNA ligase (New England Biolabs) in 1x T4 DNA ligase reaction buffer (50mM Tris-HCI pH 7.5, 10mM $MgCI_2$, 1mM ATP, 10mM DTT) provided by the company. The reaction was further supplemented with 10mM ATP, and incubated at 16°C for 10hours.

Transformation of competent bacteria

Transformation describes the genetic alteration of a bacterial cell resulting from the naturally or artificially introduced exogenous DNA. Bacterial cells that are in the state of being able to uptake the exogenous genetic material are called competent, and there are different ways of artifically-inducing competence. The most routinely-used method for preparation of competent bacteria utilizes $CaCI_2$, and the protocol was originally described by Morton Mandel and Akiko Higa (Mandel and Higa, 1970). For transformation, frozen aliquots of chemically competent *E.coli* cells were thawed on ice, and the plasmid DNA to be transformed was added followed by incubation on ice for 30min. Following incubation, the cells were heat-shocked at 42°C for 45-60 seconds and incubated on ice for an additional 2 minutes before LB or SOC medium was added. Subsequently, the cells were allowed to recover for 1h at 37°C by shaking before they were finally plated out or inoculated into liquid cultures supplemented with antibiotics.

2.1.4. Sequencing

All the plasmids constructed by PCR amplification during the course of this work were confirmed by DNA sequencing, which is based on the chain-termination reaction developed by Frederick Sanger (Sanger et al., 1977) (Sanger F. et al., 1977). The key principle behind this technique, also known as Sanger method, is the use of dideoxynucleotide triphosphates (ddNTPs), which can no longer be elongated due to the lack of 3'-OH group required for the formation of phosphodiester bond between two nucleotides. Currently, there are several advancements in DNA sequencing methods, and one key development which set the stage for automated, high-throughput DNA sequencing was the use of fluorescently labeled ddNTPs and primers (Smith et al., 1985; 1986) (Smith et al., 1985 & 1986). The sequencing reactions were carried out from 20μL plasmid DNA (30-100ng/μL) and 20μL custom primers (10pmol/μL) (alternatively standard primers provided by company) by GATC Biotech. The sequences obtained were analyzed by DNASTAR softwares.

2.1.5. Site-directed mutagenesis

Site-directed mutagenesis was originally described in 1978 (Hutchison et al., 1978) (Hutchison C.A. et al., 1978) and used to introduce either site-specific point mutations or a pair of mutations if the sites for mutation were close enough to each other. The protocol was based on a manual provided with the QuickChange® Site-Directed Mutagenesis Kit, Stratagene. The principle behind site-directed mutagenesis is the use of two complementary primers, each having the desired mutation, which are then used for the amplification of the whole plasmid DNA. Following amplification, the methylated/hemimethylated parental DNA template is eliminated by the endonuclease DpnI, which then selects for the mutation-containing DNA only. The reactions were set up as 50μL, and included 5-50ng template plasmid DNA, ~0.25μM of each complementary primers, 200μM of each dNTPs, and 1.25 units of PfuUltra DNA polymerase. The 50μL reaction mix was split into 10μL samples, and gradient PCR was applied for the amplification of the DNA. In general, following program was used:

Initial Denaturation	95°C	2 min	
Denaturation	95°C	30 sec	
Annealing	50 - 70°C	1 min	28 cycles
Elongation	72°C	30 sec/kb	
Final elongation	72°C	10 min	
Hold	4°C		

Following gradient PCR, each 10μL sample was digested with 5units of DpnI endonuclease at 37°C for 4-5 hours, and then transformed into DH5α *E.coli* cells.

2.1.6. Vectors and plasmids constructed in this work:

pET11d-Ran K130,132,134R: pET11d-Ran wt was subjected to site-directed mutagenesis to introduce three mutations at lysines 130,132, and 134 (with oligos #1666, 1667 in common stocks)

pEGFP-C1-Ranwt and RanK130,132,134R: Ranwt and Ran triple mutant were PCR-amplified (#2180, 2181) introducing a 5' SacI and 3' EcoRI restriction sites followed by cloning into pEGFP-C1.

pQE80-Imp13 variants: pQE80-Imp13 wt was subjected to site-directed and multi-site-directed mutagenesis to construct three plasmids: Two plasmids had single amino acid exchange at positions 856 or 553, whereas the third one had both mutations (#1670, 1671 and #1672, 1673).

pGEX-6P-1-Ubc9: Mouse Ubc9 coding sequence was PCR-amplified from pET23a-mUbc9 (Pichler et al., 2002) and cloned into BamHI and XhoI sites of pGEX-6P-1.

pET23a-Impβ: Impβ was PCR-amplified (#1493,1494) from pET30a-Impβ (kindly provided by Prof. Ralph Kehlenbach, University of Göttingen) introducing a 5' BamHI and 3' NotI restriction sites followed by cloning into pET23a.

2.2. Biochemical techniques

2.2.1. Measurement of protein concentration

Concentrations of recombinant proteins purified were usually determined by the combination of two methods. As a first choice of method, the Bradford assay was utilized to estimate the concentrations, which was followed by the direct comparison of the differing amounts of recombinant protein of interest with defined amounts of BSA (Pierce) on the same gel stained with coomassie. The Bradford protein assay was developed by Marion M.Bradford (Bradford, 1976), and it is based on the fact that the cationic free form of the dye Coomassie brilliant Blue G-250 can bind to basic amino acids (arginine, lysine, and histidine) as well as amino acids with aromatic side chains under acidic conditions, which, in turn, stabilizes the anionic form of the dye. The protein-dye complex formation results in blue color, which is due to the spectral shift of the dye that can be easily detected at 595nm. Therefore, 10-15μL of the unknown protein solutions together with a series of BSA proteins with known concentrations were mixed with 750μL of Bradford 1x dye reagent, and absorbance values at 595nm were recorded. A standard curve for BSA protein was prepared, and the concentration of the unknown samples were estimated from the standard curve.

For the quantification of total protein amounts of mammalian cell lysates, the „660nM Protein assay" from Pierce was used according to the manufacturer's instructions. This assay is based on the binding of the proteins to a proprietary dye-metal complex under acidic conditions, which results in a shift in the dye's absorption maximum. If required, this assay was used in combination with the ionic detergent compatibility reagent (IDCR) provided by the company, which tolerates high concentrations of detergents or other interfering reagents.

2.2.2. SDS-PAGE and protein detection methods

SDS-PAGE

SDS polyacrylamide gel electrophoresis was used to resolve proteins with different molecular weights and modified from the original description by Ulrich K. Laemmli (Laemmli, 1970). In most cases, continuous gradient gels (5-20%) were used, although depending on the exact need, 8% gels were also employed. The gels were prepared in a special apparatus which can accommodate eight gels simultaneously. In order to have 5-20% gels, a double cylindrical gradient mixer was filled with equal volumes of 5% and 20% polyacrylamide solutions in 400mM Tris-HCI pH 8.8, 0.1% (v/v) SDS. Immediately after the polymerization was started by adding approximately equimolar amounts of APS (final concentration of 2.2mM) and TEMED (final concentration of 3.3mM), the two

cylindrical chambers were allowed to mix, yielding a polyacrylamide gradient of 5-20% from top to the bottom of the gel. An overlay of isopropanol was applied to the top, and only removed after the completion of polymerization. After washing off isopropanol thoroughly, the stacking gel (5% (w/v) polyacrylamide, 140mM Tris-HCl pH 6.8, 0.1% (v/v) SDS, 2.5mM APS, 3.7mM TEMED, and 0.0007% (w/v) bromophenolblue) was poured. The gels were allowed to polymerize for at least 1h before running. Additional gels were stored in wet paper at 4°C. Gels with samples were run with Laemmli buffer (25mM Tris, 192mM glycine, 0.05% (w/v) SDS) at 20-30 mAmp per gel at room temperature.

Coomassie Staining

Mostly, the gels to be analyzed by coomassie staining were first fixed with a solution having 40% (v/v) ethanol and 10% (v/v) acetic acid for half an hour. Following the precipitation of proteins, the gels were rehydrated in H_2O for 5-10 minutes, and finally stained with 0.005% (w/v) coomassie R-250 in 10% acetic acid till the protein bands were clearly visible. For most purposes destaining was not required. However, if required, the gels were briefly destained in a solution with 10% (v/v) ethanol and 2% (v/v) phosphoric acid to get rid of the background staining.

In cases where higher sensitivity was required (for instance, the visualization of sumoylated proteins), colloidal coomassie staining was of choice. For this purpose, a dye stock solution (0.1% (w/v) Coomassie brilliant blue G250, 2% (w/v) ortho-phosphoric acid, 10% (w/v) ammonium sulfate) was prepared at least 24h before staining. The gel to be stained was initially fixed with 40% (v/v) ethanol and 10% (v/v) acetic acid for an hour followed by rehydration of the gel with H_2O for a total of 20 min. The gel was then stained overnight in a solution having 4 volumes of dye stock solution and 1 volume of methanol. Excess coomassie particles and background staining were subsequently removed by incubating the gel in a solution with 1% (v/v) acetic acid with frequent changes.

Immunoblotting

Immunoblotting was the method of choice when a specific protein was needed to be detected in complex mixtures. The technique, developed in the lab of George Stark, is based on the transfer of separated proteins from gels to a more stable platform such as membranes followed by detection of the protein of interest with specific antibodies (Renart et al., 1979). In general, the proteins resolved by SDS-PAGE were transferred from gels on nitrocellulose membranes. This was carried out by first placing the gel on top of nitrocellulose membrane, which was then mounted between whatman papers soaked in

western buffer. The transfer was done for 2hours with a semi-dry western blot apparatus applying 200 mAmp per gel. The efficiency of the transfer was subsequently evaluated by staining the membrane with 0.5% (w/v) Ponceau S in 1% (v/v) acetic acid for 1-2 minutes followed by the removal of the background staining by washing the membrane with 1% (v/v) acetic acid solution for a couple of times. Prior to the application of primary antibodies, unspecific binding sites were blocked by incubation of the membrane in blocking buffer (5% (w/v) skim milk prepared in PBST) for 30 minutes. Primary and horseradish peroxidase-coupled secondary antibodies were diluted in blocking buffer. Primary antibodies were applied overnight at 4°C, whereas secondary antibodies were applied for 45 minutes at room temperature. After the incubation of the membrane with primary and secondary antibodies, the membrane was washed three times with PBST for 30min. Bound antibody was detected by chemiluminescence produced by the reaction of horseradish peroxidase with its enhanced luminol-based chemiluminescent substrate provided in ECL kits from Pierce and Millipore. Afterwards, chemiluminescence-exposed X-ray films were developed using an automatic developing machine. In case the same membrane was to be used to detect another protein of interest, the primary antibody of the second protein was applied in the presence of 2mM sodium azide (NaN_3), which irreversibly blocks the horseradish peroxidase (Ortiz de Montellano et al., 1988). This, in turn, allows the detection of the signal only coming from the last antibody applied provided that the primary antibodies are from different species.

2.2.3. Sample Preparation

In most cases, protein samples were diluted 1:1 with 2x sample buffer supplemented freshly with 200mM DTT and boiled at 95°C for 5-10 min before loading on the gels. If the samples were to be to stored, they were flash-frozen in liquid nitrogen and were kept at -80°C till use.

Methanol-Chloroform Precipitation

In certain cases, the samples had more volume than could be accommodated by the gel pockets. Therefore, the proteins were concentrated by methanol-chloroform precipitation (Wessel and Flügge, 1984). The method is based on a defined mixture of methanol-chloroform-water, which is separated into organic and aqueous phases. Proteins having both hydrophilic and hydrophobic groups precipitate at the interface of the two phases, which is followed by the removal of the aqueous layer. In the final step, proteins are pelleted again. In short, 1 volume of the sample (usually ~200μL) was mixed with 3 volumes of methanol and 1 volume of chloroform followed by vortexing. After the addition of 3 volumes of H_2O, the samples were mixed thoroughly followed by

centrifugation. The aqueous layer was then carefully removed without disturbing the protein layer at the interface, and subsequently 3 volumes of methanol was added. The proteins were pelleted at the bottom of the tube by centrifugation, dried at 37°C for a few minutes, and reconstituted in 2x sample buffer prior to loading on gels.

Trichloroacetic acid (TCA) Precipitation

Methanol-chloroform precipitation was of choice when the protein solution was too dilute. However if the solutions were more concentrated, TCA precipitation was employed. It is also a very effective way of precipitating proteins. Although the underlying principle is not fully understood, it was suggested that the method is based on hydrophobic aggregation (Sivaraman et al., 1997). The method was perfomed by mixing the protein samples with TCA solution to have a final concentration of ~14% TCA, and letting them stay on ice for an hour. The samples were then centrifugued for half an hour at 4°C at 14.000g, followed by the aspiration of the supernatant. Subsequently, the pellet was washed with ice-cold 100% acetone at least twice, and the proteins were collected by a final centrifugation for 15min at 4°C at 14.000g. In the final step, the proteins were dried about half an hour, and solubilized in 2x sample buffer. Residual amounts of TCA, indicated by the yellow color of the dye at acidic pH, was neutralized by 1M Tris-HCI, pH 8 before loading on gels.

2.2.4. Immobilization of proteins to Cyanogenbromide (CNBr)-activated sepharose beads

Cyanogenbromide-activated sepharose beads (Sigma-Aldrich) are formed due to the reaction of cyanogen bromide in base with –OH groups on sepharose, which results in the formation of either cyanate esters or imidocarbonates. The coupling reaction is based on the high reactivity of such groups with primary amines, which results in covalent bond formation between proteins and the matrix. For coupling of the protein of interest to the bead material, the protein was dialyzed extensively against 0.2M Na_2CO_3 buffer, pH 8.9 to get rid of all traces of primary amines, which would otherwise be coupled to the beads. Cyanogenbromide-activated sepharose beads were swollen in 1mM HCl for 10 min, and washed with carbonate buffer once. Immediately after washing, the protein of interest was incubated with the activated bead material (at a ratio of ~1mg protein/mL beads) for 1h at room temperature, followed by overnight incubation at 4°C. The beads were washed a couple of times with carbonate buffer, and the remaining coupling sites were blocked by incubation with 100mM ethanolamine for an hour. As a final step, the beads were washed again with carbonate buffer a couple of times, reequilibrated in PBS, and stored at 4°C. For prolonged storage, 1mM sodium azide was added.

2.2.5. Generation of Crm1 antibodies

Generation of antibodies was essentially performed based on an established lab protocol. In short, for the generation of Crm1 antibodies, the goat was immunized with pure full-length hCrm1 protein which was C-terminally His-tagged. Total of four injections were performed by the personal of the animal house over a period of four months. The blood of the animal was tested 10 to 14 days post-injection for the presence of antibodies against Crm1 before the final bleed. The serum of the animal was obtained by centrifugation of the blood which was allowed to wait for 1h at room temperature followed by overnight incubation at 4°C. Subsequently, the serum was aliquoted and stored at -20°C before it was used for affinity purification.

2.2.6. Antibody purification

Affinity purification of antibodies was carried out to enrich the specific antibodies of interest from the complex milieu of serum. For this purpose, 1-2mL of affinity matrix was incubated with 20mL serum diluted 1:1 with PBS at 4°C overnight. The affinity matrix was subsequently collected in a column, and washed with 100 column volumes of PBS with 500mM NaCI. The antibodies were eluted with 10 column volumes of 0.2M acetic acid, pH 2.5. 500μL eluates were immediately neutralized by the addition of 100μL 1M Tris base. The eluates with the antibodies were pooled, dialyzed against PBS, and concentrated. The antibody concentrations were estimated by NanoDrop (OD_{280}=1 corresponds to ~0.8mg/mL of IgGs). For long-term storage, antibodies were diluted 1:1 with 87% glycerol, and kept at -20°C.

2.2.7. Recombinant protein expression and purification

In general, recombinant proteins were purified after overexpression in bacteria. Expression plasmids for recombinant proteins were transformed into *E.coli* expression strains (BL21(DE3), BL21(DE3)pLysS, or Rosetta2). Transformed bacteria were either directly inoculated into pre-culture media supplemented with antibiotics or plated out on antibiotic-containing LB plates. For the latter, a single colony was picked the next day, and inoculated into the pre-culture. Pre-cultures were grown O/N at 37°C, and diluted 1:40-1:100 the next day with fresh medium (LB or 2YT medium) supplemented with fresh antibiotics to maintain the desired expression plasmids. The bacteria were grown up to logarithmic phase (OD_{600}~ 0.6), and the protein expression was induced with 0.1-1mM IPTG for differing time periods. After induction, the bacteria were harvested, and kept at -80°C until purification. Protein purifications were carried out by utilizing different strategies such as ammonium sulfate precipitation, affinity tag pulldowns, gel filtration, and ion-exchange chromatography. If not stated otherwise, the buffers used during the

purification were supplemented with 1mM DTT, 0.1mM PMSF, 1μg/mL of leupeptin, pepstatin, and aprotinin to prevent oxidation and degradation of proteins. As a general final step, purified proteins were brought to the desired concentration, aliquoted, flash frozen in liquid nitrogen, and stored at -80°C.

Untagged Ran WT and its variants

Ran was expressed and purified essentially as described by Melchior et al. (Melchior et al., 1993). In short, Ran in pET11d was expressed in BL21(DE3) cells by 0.6mM IPTG induction for 3 hours at 37°C. Cells were harvested and resuspended in 50mM Tris-HCI/pH 8, 75mM NaCI, 1mM MgCI$_2$, 1mM DTT, 0.1mM PMSF, 1μg/mL of leupeptin, pepstatin, and aprotinin (50mL lysis buffer/2L of bacterial culture). Lysis was done by passing the cells through EmulsiFlex three times, and the cell lysate was cleared by centrifugation at 29,000rpm for 30 minutes. As the first step for purification, total cell lysate (~50mL) was passed over pre-equilibrated DEAE column (~20mL) (Sigma Aldrich). Flow through as well as 20mL of the subsequent wash was collected. Ran was precipitated from the solution by adding ammonium sulfate gradually up to ~53% saturation. The precipitate was resuspended in 4mL transport buffer (TB: 20mM HEPES pH 7.3, 110mM K-acetate, 2mM Mg-acetate and 1mM EDTA) supplemented with 2mM DTT, 1μg/mL of leupeptin, pepstatin, aprotinin, and 250μM GDP or GTP. The resuspended precipitate was resolved through a preparative Superdex200 (S200) column with a flow rate of 1mL/min, and 5mL fractions were collected. Ran containing fractions were pooled, concentrated to the final volume of ~5mL, and applied to MonoQ column. The protein was eluted with a salt gradient (up to 300mM NaCI). The elution order of proteins was RanGDP (~60mM NaCI) and RanGTP (~130mM NaCI). Excess salt was removed by another run over preparative Superdex75 column in transport buffer.

Average Yield: ~3mg RanGDP or ~1mg RanGTP/L of bacterial culture

His-Importin β

Imp β was expressed and purified essentially as described by Chi et al. (Chi et al., 1996). Briefly, Imp β in pET23a was expressed as His-tagged recombinant protein in BL21(DE3)pLysS cells by 0.5mM IPTG induction for 4h at 25°C. Cells were harvested and resuspended in 50mM Na-PO$_4$ buffer/pH 7.5 with 500mM NaCl, 2mM MgCI$_2$, 1mM β-mercaptoethanol, leupeptin, pepstatin, and aprotinin (1μg/mL of each) (70mL resuspension buffer/2L of bacterial culture). Lysis was done by passing the cells through EmulsiFlex three times, and the cell lysate was cleared by centrifugation at 29,000rpm for 30 minutes. The cell lysate (~70mL) was incubated with ~3mL Ni-NTA agarose beads (Qiagen) for an hour in the presence of 20mM imidazole to prevent unspecific binding.

The beads were centrifuged down and washed with 100 column volumes of resuspension buffer supplemented with 20mM imidazole. Elution of the His-tagged proteins was done with resuspension buffer with 300mM imidazole. Ni^{++} pulldown fractions (1mL) were collected, and the presence of proteins was checked with Ponceau stain. Protein containing fractions were pooled and resolved through a preparative S200 column in transport buffer. Finally, His-Importin β containing fractions were pooled and concentrated via 30,000da MWCO concentrators (Vivaspin) followed by flash freezing in liquid nitrogen.

Average Yield: ~10mg Impβ/L of bacterial culture

His-Impα

His-Impα was expressed and purified essentially as described by Hu et al. (Hu et al., 1996). Imp α in prSETb (kindly provided by Prof. Ralph Kehlenbach/University of Göttingen) was expressed as His-tagged recombinant protein in BL21(DE3) cells by 1mM IPTG induction for 5h at 25°C. Cells were harvested and resuspended in 50mM $Na-PO_4$ buffer/pH 7.5 with 500mM NaCI, 2mM $MgCI_2$, 1mM β-mercaptoethanol, leupeptin, pepstatin, and aprotinin (1μg/mL of each) (50mL resuspension buffer/2L of bacterial culture). Lysis was done by passing the cells through EmulsiFlex three times, and the cell lysate was cleared by centrifugation at 29,000rpm for 30 minutes. Subsequently, the Ni^{++} pulldown and gel filtration were performed as described for His-Impβ (see above). In the final step, His-Impα was concentrated, flash frozen in liquid nitrogen, and stored at -80°C.

Average Yield: ~3-4mg Impα/L of bacterial culture

His-Importin 13 and its variants

His-Imp13 was expressed and purified according to an established protocol kindly provided by Dr. Ralph Kehlenbach. Imp13 in pQE80 was expressed as His-tagged recombinant protein in JM109 cells. A single colony after transformation was picked and grown in 2YT medium supplemented with 2% (w/v) glucose, 30mM K_2HPO_4 pH 7.0, and ampicillin (100μg/mL) at 37°C overnight. Next day, the bacteria was pelleted and resuspended in fresh 2YT medium supplemented with 2% (v/v) glycerin, 30mM K_2HPO_4 pH 7.0, and ampicillin (100μg/mL). The cells were grown until OD_{600} is ~1.0 at 37°C, diluted 1:1.5 with fresh 2YT medium, and further grown until OD_{600} is ~0.75 at 16°C. The expression of the recombinant protein was induced with 0.1mM IPTG for ~18 hours at 16°C. Subsequently, cells were harvested and resuspended in 50mM Hepes buffer pH 7.5 with 500mM NaCI, 2mM $MgCI_2$, 1mM β-mercaptoethanol, leupeptin, pepstatin, and

aprotinin (1μg/mL of each) (50mL resuspension buffer/2L of bacterial culture). Lysis was carried out by passing the cells through EmulsiFlex three times, and the cell lysate was cleared by centrifugation at 29,000rpm for 1 hour. The cell lysate (~50mL) was incubated with 1.5mL Ni-NTA agarose beads to pulldown the His-tagged protein. The Ni^{++} pulldown and gel filtration were performed as described for His-Impβ (see above). In the final step, His-Imp13 was concentrated, flash frozen in liquid nitrogen, and stored at -80°C.

Average Yield: ~5-6mg Imp13/L of bacterial culture

His-Transportin

His-Transportin was expressed and purified essentially as described by Baake et al. (Matunis et al., 1996; Baake et al., 2001). Transportin in pQE32 was expressed as His-tagged recombinant protein in JM109 cells. The cells were grown until OD$_{600}$ is ~0.75, and the expression was induced by 0.5mM IPTG for 4h at 25°C. Cells were harvested and resuspended in 50mM Na-PO$_4$ buffer/pH 7.5 with 500mM NaCI, 2mM MgCI$_2$, 1mM DTT, leupeptin, pepstatin, and aprotinin (1μg/mL of each) (50mL resuspension buffer/2L of bacterial culture). Lysis was done by passing the cells through EmulsiFlex three times, and the cell lysate was cleared by centrifugation at 29,000rpm for 30 minutes. The cell lysate (~50mL) was incubated with ~1.5mL Ni-NTA agarose beads (Qiagen) for an hour in the presence of 20mM imidazole to prevent unspecific binding. The beads were centrifuged down and washed with 100 column volumes of resuspension buffer supplemented with 20mM imidazole. Elution of the His-tagged proteins was done with resuspension buffer with 300mM imidazole. Ni^{++} pulldown fractions (1mL) were collected, and the presence of proteins was checked with Ponceau stain. Protein containing fractions were pooled and resolved through a preparative S200 column in transport buffer. Finally, His-Transportin containing fractions were pooled and concentrated via 30,000da MWCO concentrators (Vivaspin) followed by flash freezing in liquid nitrogen.

Average Yield: ~5mg Transportin/L of bacterial culture

His-YFP-M9

His-YFP-M9 was expressed and purified according to an established protocol kindly provided by Prof. Ralph Kehlenbach. His- and YFP-tagged M9 in pET28a (kindly provided by Prof. Ralph Kehlenbach/Uni. of Göttingen) was expressed in BL21(DE3) cells by 0.5mM IPTG induction for 6h at 37°C. Cells were harvested and resuspended in 50mM Na-PO$_4$ buffer/pH 7.5 with 500mM NaCI, 2mM MgCI$_2$, 1mM DTT, leupeptin, pepstatin,

and aprotinin (1μg/mL of each) (70mL resuspension buffer/3L of bacterial culture). Lysis was done by passing the cells through EmulsiFlex three times, and the cell lysate was cleared by centrifugation at 29,000rpm for 30 minutes. The cell lysate (~70mL) was incubated with 2mL Ni-NTA agarose beads (Qiagen) for an hour in the presence of 20mM imidazole to prevent unspecific binding. The beads were centrifuged down and washed with 100 column volumes of resuspension buffer supplemented with 20mM imidazole. Elution of the His-tagged proteins was done with resuspension buffer with 300mM imidazole. Ni^{++} pulldown fractions (1mL) were collected, and the presence of proteins was checked with Ponceau stain. Protein containing fractions were pooled and resolved through a preparative S75 column in transport buffer. Finally, His-YFP-M9 containing fractions were pooled, concentrated via 10,000da MWCO concentrators (Vivaspin), flash frozen in liquid nitrogen, and stored at -80°C.

Average Yield: ~6mg His-YFP-M9/1L of bacterial culture

His-Crm1

His-Crm1 was expressed and purified essentially as described by Guan et al. (Guan et al., 2000). Crm1 in pQE60 was expressed as His-tagged recombinant protein from a glycerol stock of *E.coli* TG1 cells (kindly provided by Prof. Ralph Kehlenbach/Uni. of Göttingen) without IPTG induction. The bacteria were allowed to grow at 37°C overnight with constant shaking at 180rpm. Subsequently, the bacteria were harvested and resuspended in 50mM Hepes buffer pH 7.5 with 500mM NaCI, 2mM MgCI$_2$, 1mM β-mercaptoethanol, leupeptin, pepstatin, and aprotinin (1μg/mL of each) (40mL Resuspension Buffer/1.5L of bacterial culture). Lysis was carried out by passing the cells through EmulsiFlex three times, and the cell lysate was cleared by centrifugation at 29,000rpm for 1 hour. The cell lysate (~40mL) was incubated with 1mL Ni-NTA agarose beads (Qiagen) to pulldown the His-tagged protein. The Ni^{++} pulldown and gel filtration were performed as described for His-Impβ (see above). After gel filtration, another purification step was included since the purity of the protein was not sufficient. Pooled fractions containing the recombinant protein were concentrated and applied on MonoQ anion exchange column. The bound proteins were eluted with a salt gradient (up to 500mM NaCI). The fractions containing Crm1 were pooled and reapplied to gel filtration to remove the excessive salts and to change the buffer to TB supplemented with 1mM DTT, leupeptin, pepstatin, and aprotinin (1μg/mL of each). His-Crm1 fractions were concentrated, flash frozen in liquid nitrogen, and stored at -80°C.

Average Yield: ~1mg Crm1/1.5L of bacterial culture

GST-Ubc9

Ubc9 in pGEX-6P-1 was expressed as GST-tagged recombinant protein in BL21(DE3) cells by 1mM IPTG induction for 3h at 37°C. Cells were harvested and resuspended in 50mM Tris-HCl, pH 8.0, 100mM NaCl supplemented with 1mM DTT, leupeptin, pepstatin, and aprotinin ($1\mu g/mL$ of each) (40mL GST buffer/2L of bacterial culture). Lysis was done by passing the cells through EmulsiFlex two times, and the cell lysate was cleared by centrifugation at 29,000rpm for 30 min. The cell lysate (~40mL) was incubated with ~4mL pre-equilibrated glutathione-sepharose beads (Macherey-Nagel) under constant rotation for an hour at 4°C. The mixture was transferred into a column, and washed with ~50 bed volumes of GST buffer. The bound proteins were eluted with GST buffer supplemented with 10mM glutathione, pH 8.0. The fractions with the recombinant protein were pooled, concentrated, and applied to S200preparative gel filtration column equilibrated in TB supplemented with 1mM DTT, leupeptin, pepstatin, and aprotinin ($1\mu g/mL$ of each). As a final step, GST-Ubc9 was concentrated, flash frozen in liquid nitrogen, and stored at -80°C.

Average Yield: ~10mg GST-Ubc9/1L of bacterial culture

GST-Rcc1

Rcc1 in pGEX-TEV was expressed as GST-tagged recombinant protein in Rosetta2 (DE3) cells by 0.3mM IPTG induction for 4-5h at 25°C. Cells were harvested and resuspended in 50mM Tris-HCl, pH 8.0, 100mM NaCl supplemented with 1mM DTT, leupeptin, pepstatin, and aprotinin ($1\mu g/mL$ of each) (40mL GST buffer/1.5L of bacterial culture). Lysis was done by passing the cells through EmulsiFlex two times, and the cell lysate was cleared by centrifugation at 29,000rpm for 30 minutes. Subsequently, GST pulldown and S200 preparative gel filtration were performed as described for the purification of GST-Ubc9 (see above). As a final step, GST-Rcc1 was concentrated, flash frozen in liquid nitrogen, and stored at -80°C.

Untagged NTF2

NTF2 was expressed and purified essentially as described by Ribbeck et al. (Ribbeck et al., 1998). NTF2 in pET vector (kindly provided by Prof. Dirk Görlich/MPIbpc, Göttingen) was expressed in BL21(DE3) cells by 0.5mM IPTG induction for 3 hours at 37°C. Cells were harvested and resuspended in TB supplemented with 1mM DTT, 0.1mM PMSF, $1\mu g/mL$ of leupeptin, pepstatin, and aprotinin (50mL TB/2L of bacterial culture). Lysis was done by passing the cells through EmulsiFlex three times, and the cell lysate was cleared by centrifugation at 29,000rpm for 1h. As the first step for purification, NTF2 was

precipitated out of the solution by adding ammonium sulfate gradually up to ~50% saturation. The precipitate was resuspended in ~5mL transport buffer (TB: 20mM HEPES pH 7.3, 110mM K-acetate, 2mM Mg-acetate and 1mM EDTA) supplemented with 1mM DTT, 1μg/mL of leupeptin, pepstatin, and aprotinin. The resuspended precipitate was resolved through a preparative S200 column in TB, and 5mL fractions were collected. NTF2 containing fractions were pooled, concentrated, and flash-frozen in liquid nitrogen before storing at -80°C.

Average Yield: ~1mg NTF2/1L of bacterial culture

2.2.8. Labeling of GST-Ubc9 with Alexa Fluor 488

For labeling of proteins with fluorescent reactive dyes, thiol-reactive probes (Invitrogen) were chosen. 2.5mL GST-Ubc9 (~3.3mg/mL) in TB, pH 7.3 was thawed, and fresh 1mM DTT was added to reduce any oxidized thiol groups. Excess DTT was subsequently removed by PD10 column, and 1mL freshly prepared dye solution (1mg/mL in DMSO) was dropwise added to 3.5mL protein solution (~1mg/mL). The mixture was stirred for 2h at room temperature, protected from light. The molar ratio of reactive dye:protein was approximately 16:1. Upon completion of the reaction, 2mM DTT was added to consume excess thiol-reactive reagent. The unconjugated dye was removed from the protein by another run on a PD10 column. The protein labeled with the dye was concentrated, flash frozen in liquid nitrogen, and stored at -80°C.

2.2.9. Pulldown assays with immobilized Rcc1 and NTF2

For GST pulldowns, equimolar amounts of GST-Rcc1 (~12μg) and GST (~5μg) were bound to 20μL glutathione beads separately by mixing each protein together with the beads for an hour at 4°C. Afterwards, the beads were washed three times with TB and incubated with the recombinant protein (~6μg Ran wild type and the mutant) to be tested in TB on a rotating wheel for an hour at 4°C. Subsequently the beads were centrifuged, and the supernatant was discarded. After washing the beads three times with TB, bound proteins were eluted with 50μL 2x sample buffer. Subsequent analysis was performed by SDS-PAGE and colloidal coomassie staining.

Pulldowns with NTF2 coupled to CNBr-activated sepharose beads (see above) were performed in the presence of 20μL beads preequilibrated in TB (1mg NTF2/1mL beads). The beads were incubated with ~12μg Ran wild type or mutant (final concentration of 500nM) on a rotating wheel for an hour at 4°C. Following binding, the beads were centrifuged and the supernatant was discarded. After washing the beads three times with

TB, bound proteins were eluted with 40μL 2x sample buffer supplemented freshly with 200mM DTT. Subsequent analysis was performed by SDS-PAGE and colloidal coomassie staining.

2.2.10. Cultivation of hybridoma cells for SUMO1 and SUMO2/3 antibodies

Mouse-hybridoma cells (SUMO1 21C7, SUMO2 8A2) producing SUMO1 and SUMO2/3 antibodies were obtained from Developmental Studies Hybridoma Bank, University of Iowa (Matunis et al., 1996; Zhang et al., 2008b). The cultivation of the cells were performed routinely by another member of the lab, Dr. Janina Becker and described in great detail in her PhD Thesis („Endogenous sumoylation in cells and tissues", Dr. Janina Becker).

2.2.11. Crosslinking of SUMO antibodies to beads

Monoclonal SUMO1 and SUMO2/3 antibodies were incubated with Protein G agarose (Roche) equilibrated in 20mM Na-phosphate buffer, pH 7.0 for 1h at 4°C (8mg antibodies/mL Protein G agarose). Afterwards the beads were collected by centrifugation at 700g for 5min and washed with 10 volumes of 20mM Na-phosphate buffer, pH 7.0. Subsequent crosslinking of antibodies to the bead material was performed in 50mM borate buffer, pH 9.0 supplemented with 20mM DMP (Thermo Scientific) for an hour at room temperature. The beads were collected and incubated with 50mM Tris-HCl pH 8.0 for quenching. In the final step, protein G agarose coupled to antibodies were washed twice with 20mM Na-phosphate buffer, pH 7.0 and stored at 4°C in the same buffer supplemented with 5mM sodium azide.

2.2.12. SUMO Immunoprecipitations (IPs)

Prior to each IP, ~250mL HeLa suspension cells (1x10^6 cells/mL) were either incubated at 37°C or heat shocked at 43°C in a water bath for half an hour. Following heat shock, the cells were treated immediately with 20mM freshly prepared NEM and centrifuged at 200g for 5min at room temperature. Cells were subsequently washed with cold PBS supplemented with 10mM NEM, and the pellet was flash frozen in liquid nitrogen until IPs were performed.

Each IP was performed from 250mL cell pellet. Cells were lysed with lysis buffer (20mM Na$_2$HPO$_4$ pH 7.4, 150mM NaCl, 1% TritonX-100, 0.5% sodiumdeoxycholate, 1% SDS, 10mM NEM, 1mM DTT, and protease inhibtiors leupeptin, pepstatin, and aprotinin (1μg/mL of each)). The lysate obtained was sonified briefly and diluted 1:10 with dilution buffer (Lysis buffer without SDS). The diluted lysate was sonified, centrifuged, and filtered to get rid of the undissolved cellular debris and aggregates. The cleared lysate was

incubated with ~400μL Protein G beads crosslinked to monoclonal SUMO antibodies at 4°C overnight on a rotating wheel. The beads were collected by centrifugation and washed three times with washing buffer (20mM Na_2HPO_4 pH 7.4, 150mM NaCI, 1% TritonX-100, 0.5% sodiumdeoxycholate, 0.1% SDS, 10mM NEM, 1mM DTT, and protease inhibitors leupeptin, pepstatin, and aprotinin (1μg/mL of each)). Following washing, the beads were incubated with elution buffer without epitope peptide (20mM Na_2HPO_4 pH 7.4, 500mM NaCI, 1% TritonX-100, 0.5% sodiumdeoxycholate, 0.1% SDS, 10mM NEM) on ice for 15min. The beads settled down, and the supernatant was removed. The following elution step was carried out in two steps. First, the prewarmed (at 30°C) elution buffer with epitope peptide (0.5mg/mL final concentration) was added to the beads, which were then incubated at 30°C for 30min constantly shaking at 1400rpm. Afterwards, the beads were centrifuged and the supernatant (eluate) was kept on ice. The elution step was repeated once with fresh elution buffer with the epitope peptide, and the two eluates were pooled before proceeding with TCA precipitation of the samples, which were performed as described previously (Section 2.2.3.).

2.2.13. Permeabilization of HeLa suspension cells with digitonin

50mL Hela suspension cells (growing at 4-6x10^5 cells/mL) were centrifuged at 70g for 5min and washed with TB. Subsequently, the cells were resuspended in 5mL TB supplemented with 0.007% digitonin and incubated on ice for 4-6 min. The degree of cell permeabilization was controlled by staining the cells with Trypan blue. If permeabilization was sufficient (>95%), the cells were diluted 1:10 with TB and centrifuged again. The pellet was resuspended in TB (volume depending on following application). The concentration of the suspension was determined by measuring the OD_{550} values and comparison to a standard curve (OD_{550} vs cell number determined with a hemocytometer).

2.2.14. In vitro sumoylation assays with recombinant proteins

In vitro sumoylation assays were set up in 20μL reaction volumes and contained purified recombinant proteins. In general, the reaction mixtures included 69nM E1, 83nM E2, and 15μM SUMO1 or SUMO2 in sumoylation assay buffer (SAB) supplemented with 0.2 mg/mL ovalbumin or BSA. The target proteins to be tested for sumoylation were used in the range of 200-500nM, whereas the E3 ligase (RanBP2 fragment or RanBP2 complex) concentrations changed between 50-150nM. The reactions were started by adding 5mM ATP, incubated at 30°C or 37°C for a duration of 30-60 minutes, and stopped with the addition of 2x SDS sample buffer. If the samples were not analyzed immediately by SDS-PAGE and immunoblotting, they were frozen in liquid nitrogen and stored at -80°C until analysis.

2.2.15. In vitro sumoylation of Ran with semi-permeabilized cells

Sumoylation assays employing semi-permeabilized cells were set up in $60\mu L$ reaction volumes and contained recombinant Ran ($5\mu M$), ATP-regenerating system (1.3mM ATP, 3.2mM creatine phosphate, 13 U/mL creatine phosphate kinase), YFP-SUMO1 or YFP-SUMO2 ($5\mu M$ for each), and semi-permeabilized HeLa suspension cells (total of 3×10^6 cells) in SAB supplemented with BSA. Semi-permeabilized cells were prepared as described in 2.2.13. Cells were brought to a concentration of 10^5 cells/μL, and $30\mu L$ of cells were pipetted to the rest of the reaction mix to start the sumoylation. Reactions were incubated at 30°C for 30min and stopped by adding 2x SDS sample buffer. If the samples were not analyzed immediately by SDS-PAGE and immunoblotting, they were frozen in liquid nitrogen and stored at -80°C until analysis.

Where indicated, the sumoylation reaction was boosted either with the addition of 120nM E1 and 155nM E2 enzymes or by blocking isopeptidases. For the latter, suspension cells were divided into two parts after semi-permeabilization. The first half was incubated with HA-SUMO2-Vinylmethylester (Schulz et al., 2012) (0.5 μg/mL final concentration was sufficient to block isopeptidases) for half an hour on ice, whereas the second half was left on ice unperturbed prior to mixing with the rest of the reaction mix.

2.2.16. Mass spectrometry analysis of SUMOylation sites

$20\mu L$ in vitro sumoylation reactions of Imp13 and Ran were upscaled to $200\mu L$ and resolved on 5-20% gradient gels, which were then stained with colloidal coomassie. The regions corresponding to the sumoylated proteins were excised and sent for analysis by mass spectrometry (In collaboration with Prof. Henning Urlaub/ MPIbpc). In-gel digestion with trypsin, mass spectrometry, and data analysis were carried out by Dr. He-Hsuan Hsiao from the group of Prof. Henning Urlaub.

2.3. Cell biological techniques

2.3.1. Cultivation and storage of mammalian cells

Adherent HeLa cells were cultured in DMEM (Dulbecco's modified eagle medium) (including D-Glucose 4.5g/L, L-glutamine ~4mM, and sodium pyruvate 110mg/L) supplemented with 10% (v/v) fetal bovine serum (FBS), and penicillin (100units/mL)/streptomycin ($100\mu g$/mL) at 37°C and 5% CO_2. Before reaching 100% confluency, they were split at a 1:10 or 1:20 ratio. For this purpose, cells were washed once with sterile PBS, trypsinized, and diluted with fresh medium. HeLa suspension cells, on the other hand, were cultured in Jokliks medium supplemented with 5% (v/v) newborn calf serum (NCS), 5% FBS (v/v), 2mM glutamine, and penicillin

(100units/mL)/streptomycin (100μg/mL). They were continuously stirred at 100rpm in spinner flasks at 37°C. The cells were split every day and kept at a density of 3-10 x 10^5 cells/mL. For long term storage, exponentially growing cells were trypsinized, mixed with fresh medium, and centrifuged at 70g for 5min. The supernatant was removed, and the cells were resuspended in 9 volumes of FBS followed by the dropwise addition of 1 volume of DMSO. Aliquots were frozen to -80°C at a rate of ~ 1°C/minute in an isopropanol jacketed freezing box, which circumvents the negative effects of rapid freezing. Once -80°C is reached, the vials were transferred to the liquid nitrogen tanks.

2.3.2. Cell cycle arrest

Exponentially growing HeLa suspension cells were arrested in prometaphase by addition of 75ng/mL nocodazole for ~20 hours. The cells were confirmed to be arrested in prometaphase by either analyzing the DNA content by staining the cells with propidium iodide followed by flow cytometric analysis or by staining the DNA with Hoechst 33258 followed by fluorescent microscopy.

2.3.3. Transient transfection of mammalian cells

Transfection of mammalian cells with plasmids

Transient transfections were carried out with FuGENE® HD transfection reagent according to manufacturer's instructions mostly in 12-well plate format. In short, HeLa cells were seeded the day before transfection at a density of no more than 30-40% confluency in an antibiotic-free medium. Reagent and DNA (1μg/well) were mixed at a ratio of 3:1 in reduced serum medium (Opti-MEM) and incubated at room temperature for 5min to allow complex formation. The complex was subsequently applied to the cells, and the medium was changed 4-6 hours post-transfection.

Transfection of mammalian cells with siRNAs

To downregulate the levels of Uba2 enzyme, cells were transfected with siRNA oligonucleotides directed against Uba2 by using Lipofectamine RNAiMAX reagent. In short, cells were seeded the day before the transfection at a density of no more than 15-20% confluency in an antibiotic-free medium. The reagent and siRNAs were mixed in Opti-MEM to have a final concentration of 20nM or 40nM siRNAs. The mix was incubated at room temperature for 20min before being added to the cells. The knock-down was performed for 48h or 72h, followed by analysis by immunoblotting and immunofluorescence.

2.3.4. Lysate preparation from adherent HeLa cells

Adherent HeLa cells were washed once with sterile PBS and trypsinized. Following detachment of cells, they were diluted with normal growth medium and centrifuged at 200g for 5min. After washing with PBS, cells were directly lysed in 2x sample buffer (50μL sample buffer/500.000 cells) and boiled for 10min at 95°C. In order to load equal amounts of lysates, protein concentrations were determined using the Pierce 660nm assay in the presence of ionic detergent compatibility reagent according to manufacturer's instructions. For SDS-PAGE analysis, 20-30μg of total protein was loaded on gradient gels followed by immunoblotting.

2.3.5. Fluorescence-based detection of intracellular proteins

Overexpression and detection of fluorescent proteins

N-terminally GFP tagged Ran plasmids were transfected in HeLa cells on glass coverslips as described above (Methods, Section 2.3.3.). 48h post-transfection cells were analyzed by immunoblotting and immunofluorescence. For immunoblotting, cells were directly lysed in 2x SDS sample buffer and boiled for 10min at 95°C. For immunofluorescence, cells were fixed in 3.7% (w/v) formaldehyde in PBS, and the nuclei were counterstained with Hoechst (final concentration of 1μg/mL). Subsequently, coverslips were mounted in Slow Fade® gold antifade mounting reagent (Invitrogen) on glass slides. The fluorescence was detected with Leica SP2 confocal microscope using the HCX PL APO 63x/1.4 OIL BD UV objective and appropriate filter settings. The pictures were processed using Image J software.

Indirect immunofluorescence and confocal microscopy

For immunofluorescence, HeLa cells were seeded on sterile 12mm coverslips at no more than 30-40% confluency. The next day, coverslips were washed gently with PBS, and the cells were fixed with 3.7% (w/v) formaldehyde in PBS for 10min at room temperature. Following fixation, the cells were washed, permeabilized with 0.2% (v/v) TritonX-100 in PBS for 5 minutes on ice, and incubated with 2% (w/v) BSA in PBS for half an hour to block unspecific binding sites. Subsequently 50μL of primary antibody solution (diluted in 2% BSA in PBS) was applied on each coverslip for an hour in a humidified chamber. After the removal of excess unbound antibodies by dipping the coverslips several times in and out of PBS solution, the secondary antibody solution (diluted in 2% BSA in PBS) supplemented with Hoechst 33258 (final concentration of 1μg/mL) was applied on cells for 45 min at room temperature under dark. The cells were washed 3x with PBS and 1x with H_2O before mounting them in 5μL Slow Fade® gold antifade mounting reagent on glass slides. After a few minutes, the coverslips were sealed with nail polish, and kept at 4°C for short-term storage. The fluorescence was detected on a Leica SP2 confocal

microscope using the HCX PL APO 63x/1.4 OIL BD UV objective and appropriate filter settings. The pictures were processed using Image J software.

2.3.6. In vitro import assays

In vitro import assays were essentially carried out and analyzed by flow cytometry as described by Melchior F. (Melchior F., 1998). The reactions were set up in a volume of 40μL, and the assays included differing concentrations of recombinant transport factors, fluorescently labeled cargos, and semi-permeabilized cells (originally described in Adam et al., 1990). In general, for Imp13-dependent import assays, 1μM Imp13 and 60nM GST-Ubc9-Alexa488 were used whereas Ran concentrations were titrated in the range of 2-12μM. For Impα/β-dependent import, 0.5μM Impα/β and 0.5μM FITC-BSA-NLS were used together with Ran (titrated in the range of 1-8μM). For the import assay, a premix of transport factors, cargos, and Ran was prepared in TB on ice. The mix was supplemented with ATP-regenerating system (1mM ATP, 2.5mM creatine phosphate, 10 U/mL creatine phosphate kinase). Separately, semi-permeabilized HeLa suspension cells were prepared as described above (see section 2.2.13.) and 3 x 10^5 cells/assay were pipetted onto the premix to start import reactions. The whole mixture in 5mL FACS tubes was incubated at 30°C for 30min in water bath, and the import reactions were stopped by the addition of 4mL ice-cold TB. The cells were collected at 200g for 5min followed by the aspiration of the supernatant except for 300μL. Subsequently, the fluorescence was detected with BD FACSCanto™ II with appropriate filter settings. The mean fluorescence values from a population of 10.000 cells were used for the data analysis.

RESULTS

Chapter I: RanBP2-dependent sumoylation in nuclear transport

Considering the domain structure of RanBP2 as well as the intriguing molecular architecture of the RanBP2 complex, which brings the RanGTPase activity in close proximity to the E3 ligase region, nuclear transport receptors and the small GTPase Ran are the obvious candidates for RanBP2-dependent sumoylation during interphase. In line with this idea, several nuclear transport receptors including Crm1, Impβ, CAS, Impα, and Imp5 as well as Ran were identified as potential SUMO targets in mass-spectrometry based screens (Rosas-Acosta et al., 2005; Golebiowski et al., 2009; Kaminsky et al., 2009; Nie et al., 2009; Bruderer et al., 2011), yet none of them were confirmed in vitro and in vivo. Therefore, I aimed to test whether NTRs and/or Ran are endogenously sumoylated, and if the RanBP2 complex can serve as their E3 ligase.

1. The nuclear transport receptors Crm1, Imp β, and Imp5 are endogenously sumoylated in HeLa cells

For this purpose, I turned to denaturing SUMO IP experiments, and the protocol I used was optimized by another lab member Dr. Janina Becker (refer to her PhD Thesis, "Endogenous sumoylation in cells and tissues"). It allowed us to enrich endogenously sumoylated proteins with monoclonal SUMO antibodies and elute the bound proteins specifically with epitope peptides. In two of the above mentioned screens (Golebiowski et al., 2009; Bruderer et al., 2011), heat shock was utilized to induce SUMO2/3 conjugation. Therefore, in a similar approach, I used HeLa suspension cells which were either kept at 37°C or heat-shocked for 30 min at 43°C. Following heat shock, cells were lysed under denaturing conditions with lysis buffer supplemented with 1% SDS, and subsequently the lysate was diluted to RIPA buffer conditons to perform the immunoprecipitations (IPs). SUMO IPs to enrich the sumoylated proteins from interphase cells were carried out by using monoclonal SUMO2/3 antibodies, and the bound proteins were specifically eluted with epitope peptides (Fig. 6A). To determine the efficiency of the IP protocol as well as to control for heat shock, eluates were first analyzed by immunoblotting with α-SUMO2/3 antibodies. Fig. 6B clearly showed that heat shock rapidly decreased the free SUMO2/3 levels which was accompanied by the appearance of higher molecular weight species (compare lanes 1 and 5), and the IP protocol was very efficient in enriching the sumoylated species (compare lanes 1&4 and lanes 5&8). As a positive control for the protocol, the eluates were also probed for two known SUMO targets; TRIM28 (Lee et al., 2007) and PARP1 (Blomster et al., 2009; Martin et al., 2009), for which induction of sumoylation upon heat shock was previously described (Golebiowski et al., 2009; Martin et al., 2009). The control experiments could confirm the endogenous sumoylation of both
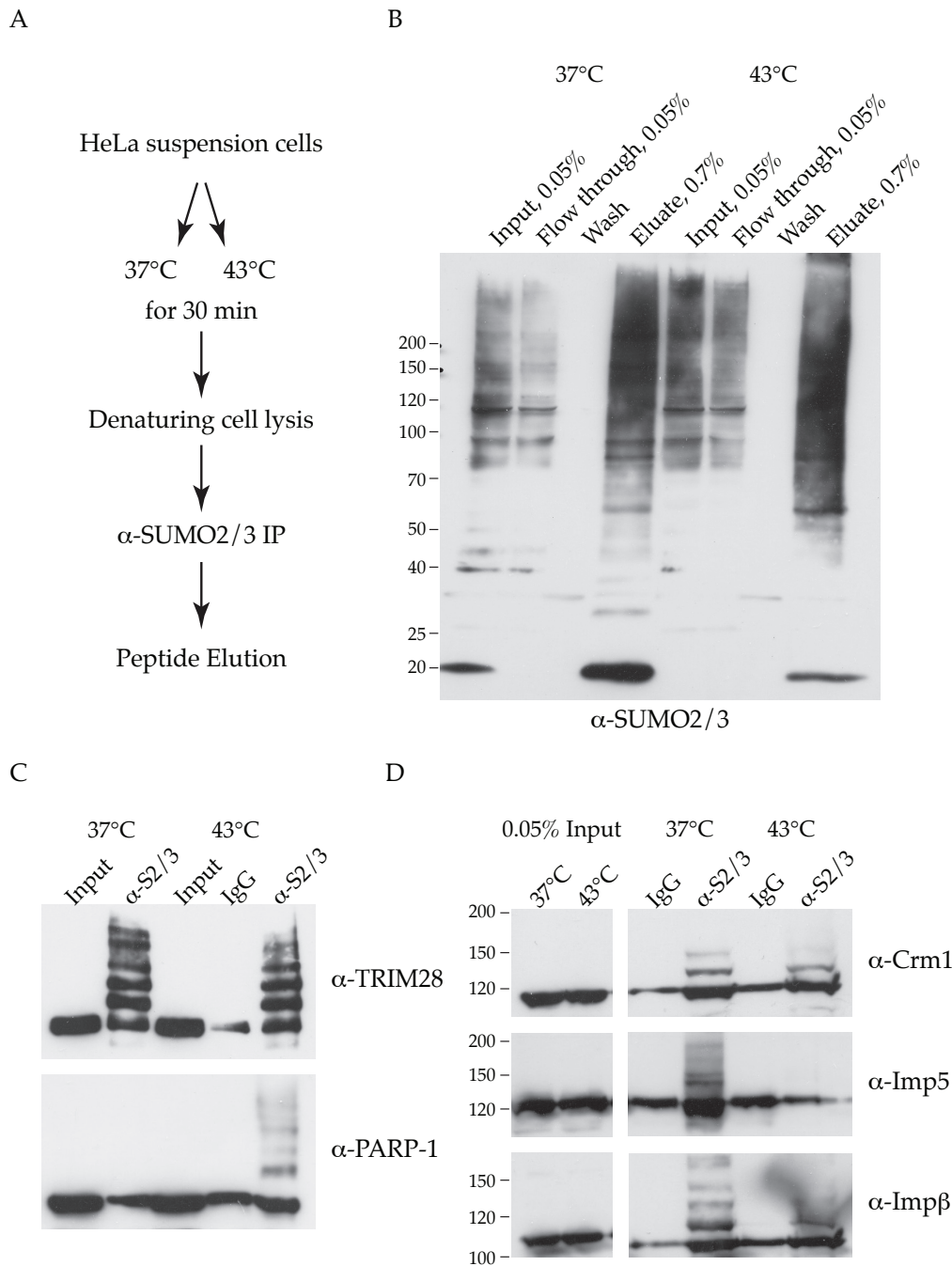
Fig. 6: Crm1, Imp β and Imp5 are endogenously sumoylated with SUMO2/3. (A) General experimental setup for denaturing SUMO2/3 immunoprecipitation. For each IP experiment, 250mL HeLa cells (1.0 x 10⁶ cells/mL) were kept either at 37°C or at 43°C for 30min. Afterwards, the cells were harvested by centrifugating in the presence of 20nM NEM at 200g for 5min and washed twice with PBS having 10mM NEM. Cells were lysed under denaturing conditions (1%SDS), and the SUMO2/3 IP was carried out in RIPA buffer conditions (0.1% SDS). Sumoylated proteins were eluted with epitope peptide. (B,C and D) Eluted proteins were analyzed with SDS-PAGE followed by western blot analysis using antibodies specific for SUMO2/3 (B), TRIM28 and PARP1 (C), and several nuclear transport receptors as indicated (D). Protein markers are shown as kDa.

TRIM28 and PARP1 as well as the induction of PARP1 sumoylation upon heat shock (Fig. 6C). Following establishment of the IP protocol as well as heat shock conditions, another IP experiment with SUMO2/3 antibodies was performed, and the samples were probed for several nuclear transport receptors. Indeed, three transport receptors, namely the main export receptor Crm1 and two import receptors, Imp5 and Impβ, turned out to be endogenously sumoylated (Fig. 6D). Surprisingly, the sumoylation pattern for Crm1 and Impβ looked comparable for 37°C and 43°C samples indicating that heat shock was not necessary for modification. Imp5, on the other hand, appeared even less sumoylated at 43°C (Fig. 6D). Of note, similar experiments with SUMO1 antibodies indicated that all three transport receptors are also sumoylated with SUMO1 although to a much less extent (data not shown and personal communication, Dr.Janina Becker). The sumoylation of several other transport receptors (Importin 13, CAS, importin α2) as well as the GTPase Ran could not be detected under the same experimental conditions tested (data not shown).

2. A catalytic fragment of RanBP2 can stimulate transport receptor sumoylation in vitro
After confirming the endogenous sumoylation of three nuclear transport receptors, the next question I asked was whether RanBP2 could stimulate the sumoylation of transport receptors as an E3 ligase. To adress this question, I turned to in vitro sumoylation assays. Since RanBP2 is a relatively huge protein (~358kDa) (Fig. 5), an 80kDa RanBP2 fragment with two Ran binding domains, E3 ligase region as well as FG and FxFG repeats was produced (provided by Dr. Andreas Werner) (Fig. 7A). This fragment is able to interact with RanGTP and transport receptors and has the E3 ligase region required for sumoylation activity. Therefore, it was used as the source of E3 ligase activity in in vitro sumoylation assays for the initial screening of nuclear transport receptors. As described in the introduction, all transport receptors belonging to the Imp β superfamily interact with RanGTP via their N-terminus (Fried and Kutay, 2003) and RanBP2 has RanGTP binding sites. In vitro sumoylation assays were therefore done in the presence and absence of RanGDP and RanGTP.

Strikingly, modification of Imp13 was strongly enhanced by the presence of RanGTP but not RanGDP (Fig. 7B, compare lanes 2 and 3 for Imp13). Although not as striking, Imp5 sumoylation was also stimulated by RanGTP (Fig. 7B, compare lanes 3 and 4 for Imp5). For Impβ, slight sumoylation was already observed in the presence of RanGDP, and exchanging RanGDP to RanGTP further stimulated the reaction (Fig. 7B). Although Crm was sumoylated without Ran, the addition of RanGTP also stimulated the modification (Fig. 7B, top left panel). Importantly, in vitro sumoylation pattern for Crm1 seemed to be

A

~80kDa RanBP2 fragment

B

α-Crm1

α-Imp 13

α-Imp β

α-Imp 5

α-Imp 9
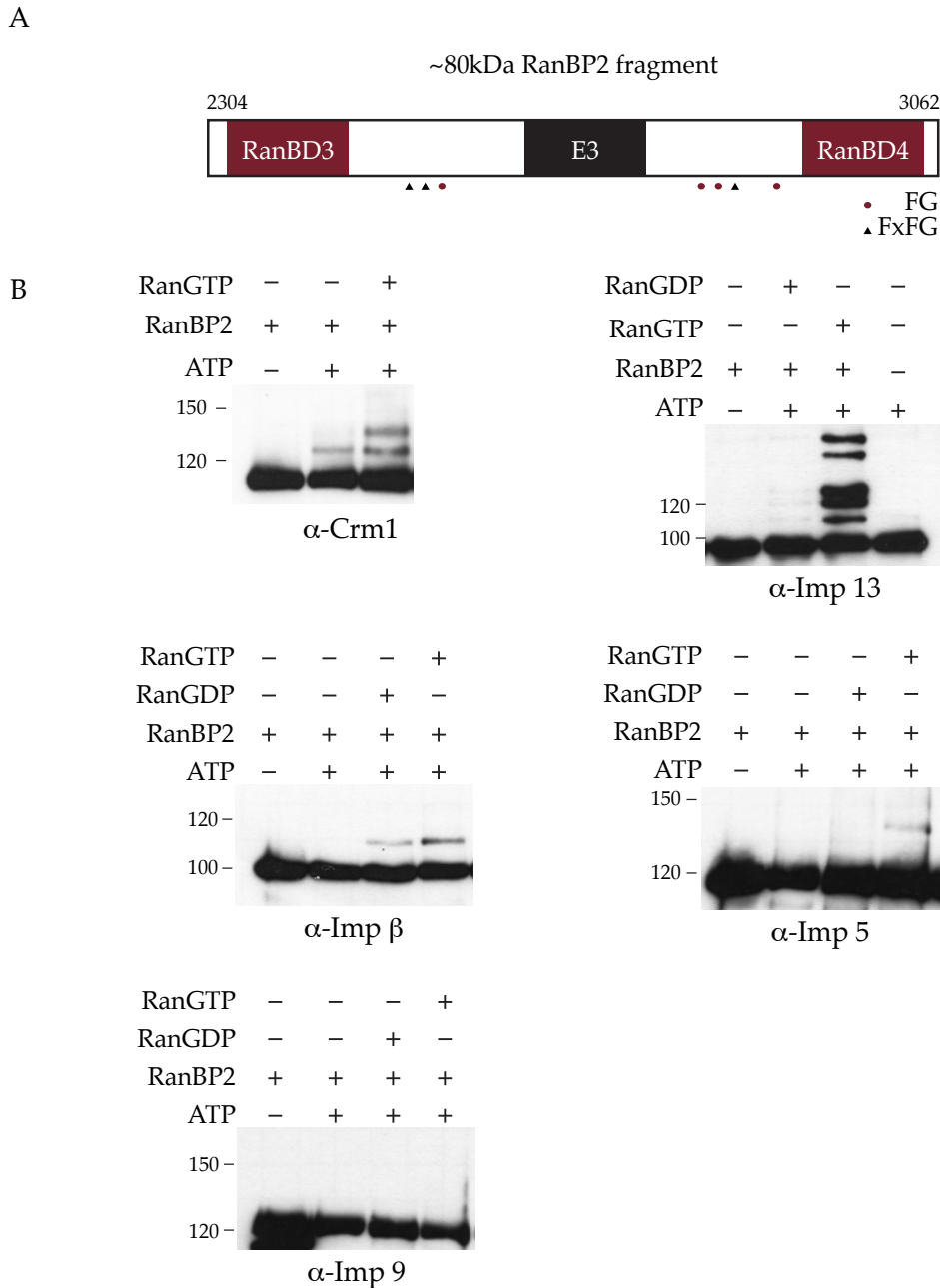
Fig. 7 : In the presence of RanBP2 and RanGTP several nuclear transport receptors can be sumoylated in vitro. (A) The domain structure of the recombinant 80kDa His-RanBP2 fragment used for the in vitro experiments. The E3 ligase region is flanked N- and C-terminally by Ran binding domains (RanBD3 and RanBD4) and FG/FxFG repeats. The numbers indicate amino acid positions. (B) In vitro sumoylation assays were performed in the presence of 69nM E1, 83nM E2, 15μM SUMO1 with or without 5mM ATP at 30°C for 30min. Where indicated, RanBP2 was added as E3 ligase (55nM for Crm1 sumoylation and 148nM for other substrates). Recombinant Crm1 was used at ~200nM whereas other NTRs were used at ~160nM concentrations. Where indicated, 1μM RanGDP or RanGTP was added to the reaction. The reactions were stopped with 2X SDS sample buffer and separated by SDS PAGE followed by western blot analysis. Crm1, Imp13, and Imp β blots were probed with antibodies directed against proteins themselves whereas Imp5 and Imp9 were visualized by anti-His antibody. Protein markers are indicated as kDa.

very similar to the pattern observed for the endogenous sumoylation (Compare Fig 6D and Fig 7B). Such similarity was, however, not observed for the other transport receptors shown to be endogenously sumoylated. Imp9 was not sumoylated under all conditions tested (Fig. 7B). Overall, the results indicated that several nuclear transport receptors can be sumoylated in the presence of RanBP2 fragment and RanGTP.

3. RanBP2 complex poorly stimulates transport receptor sumoylation in vitro

During the course of this work, Dr. Andreas Werner (currently a post-doc in Melchior lab) established a protocol to reconstitute the RanBP2 complex (Werner et al., 2012). This allowed me to test whether the physiologically relevant E3 ligase rather than the free RanBP2 fragment could stimulate transport receptor sumoylation. Therefore, I carried out in vitro sumoylation assays with Crm1, Imp13, and Impβ in the presence of SUMO1 or SUMO2/3. For Imp13 and Impβ, RanGTP is required for efficient sumoylation by RanBP2 fragment. However, sumoylation assays with RanBP2 complex includes RanGAP1, which hydrolyzes RanGTP rapidly and does not allow sumoylation. In order to circumvent this problem, I preformed complexes between Imp13 or Impβ and a non-hydrolyzable form of RanQ69L loaded with GTP over gel filtration and used them in in vitro sumoylation assays with RanBP2 complex. The results showed that Crm1 was in vitro sumoylated with RanBP2 complex with SUMO1 but not with SUMO2/3 (Fig. 8A). Imp13 in complex with RanQ69L was not sumoylated with neither SUMO1 nor SUMO2/3 (Fig. 8A). Overexposure of the blot indicated minor levels of sumoylation with SUMO1, however, the reactions were very inefficient. Impβ, on the other hand, was not sumoylated with RanBP2 complex neither in the presence of SUMO1 nor SUMO2/3. It was only with Impβ* RanQ69L complex that slight sumoylation of Impβ could be observed in the presence of SUMO1, but not SUMO2/3 (Fig. 8B, compare the two panels). Overall, although the physiologically relevant E3 ligase RanBP2 complex showed activity towards Impβ (only in complex with RanQ69L) and Crm1, the sumoylation reactions were rather inefficient and not even detectable for Imp13.

4. Recombinant Ran is sumoylated with YFP-SUMO1 in semi-permeabilized cells

Next, I turned to the GTPase Ran and wanted to test endogenous sumoylation of Ran by performing denaturing SUMO1 and SUMO2/3 IPs as described for the identification of sumoylated transport receptors (Fig. 6). Several trials to detect sumoylated Ran in non-stressed and heat shock-treated HeLa cells or interphase and nocodazole-arrested mitotic cells, however, failed (data not shown). There are a number of simple explanations why it might be challenging to detect Ran sumoylation: As with many other proteins only a minor pool of Ran might be sumoylated in cells, and this pool can simply be difficult to be

A

B
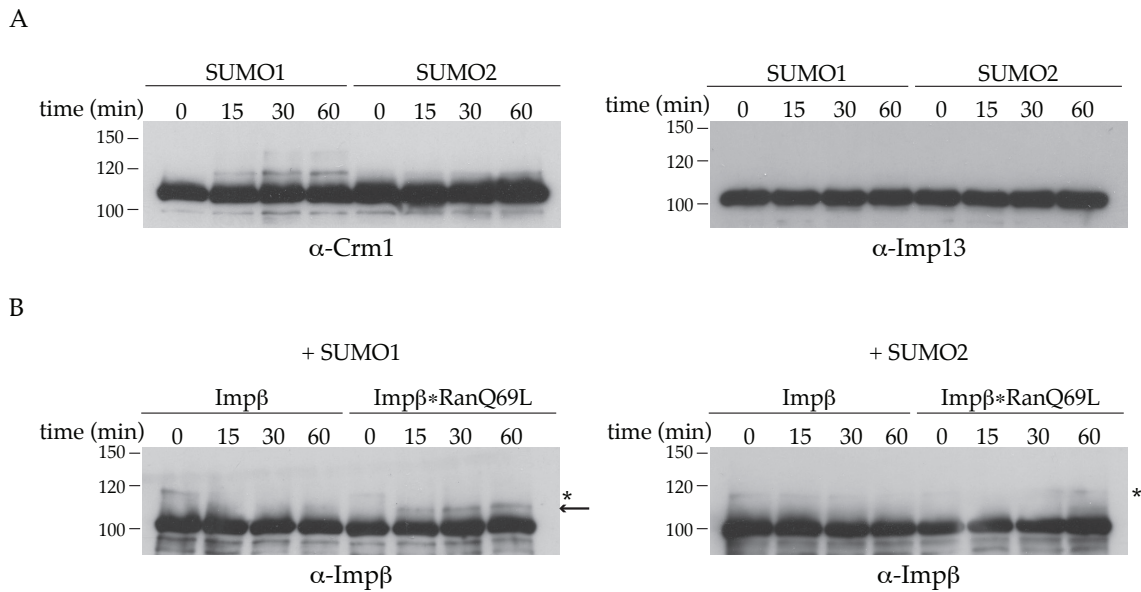
Fig. 8: In vitro sumoylation of Crm1, Imp13, and Impβ with the RanBP2 complex. (A,B) In vitro sumoylation assays were performed in the presence of 69nM E1, 56nM E2, 15µM SUMO1 or SUMO2, 5mM ATP, and 72nM RanBP2 complex (in vitro reconstituted). Where indicated 435nM Crm1, 400nM Impβ or Impβ∗RanQ69L (GTP loaded) complex or 400nM Imp13*RanQ69L (GTP loaded) complex were added. The reactions were incubated at 30°C and stopped at indicated time points with 2X SDS sample buffer. The proteins were resolved on 5-20% gradient gels followed by immunoblot analysis with anti-Crm1, anti-Imp13, and anti-Impβ antibodies. Protein markers are indicated as kDa. Arrow and * indicate the sumoylated Impβ and unspecific band recognized by Impβ antibody, respectively.

detected within the technical limits of the experiment (e.g. due to poor antibody sensitivity). Another explanation would be that sumoylation might require certain stimuli, such as a specific cell cycle stage or DNA damage, etc., which might be missing in the experimental set-up. In conclusion, we decided to take another approach to test the sumoylation of Ran, and we switched to semi-permeabilized cells. Here, cells are treated with low concentrations of digitonin which selectively permeabilizes the plasma membrane leaving nuclear envelope intact (Adam et al., 1990). This allows to specifically inhibit SUMO isopeptidases with the help of SUMO-Vme, which is a recombinant SUMO protein modified with vinylmethylester at its C-terminus (Hemelaar et al., 2004; Schulz et al., 2012). Due to this modification, which mimics the peptide bond, the attacking SUMO isopeptidases form a covalent bond with SUMO-Vme and thereby are inactivated. If reversible sumoylation of Ran takes place in semi-permeabilized cells that are fully competent to transport proteins into the nucleus, addition of the SUMO-Vme should increase the amounts of modified Ran.

To ensure that my conditions of digitonin permeabilization retain enough SUMO E1 and E2 enzymes in the cells, I determined the levels of cell-associated SUMO E1 and E2 enzymes after semi-permeabilization. For this, HeLa suspension cells were treated with 0.007% digitonin and separated from the leaking cytosol by centrifugation (Fig. 9A). Both cellular and cytosolic fractions were lysed in sample buffer, resolved by SDS PAGE, and probed with Ran, Ubc9, Aos1, Uba2, SUMO1, and SUMO2 antibodies (Fig. 9B) The results showed that a large proportion of Ran was found in the cytosolic fraction as expected, which indicates that permeabilization of the cells worked properly (Fig. 9B). Concerning the SUMO enzymes, Ubc9 was found in both cellular and cytosolic fractions at significant levels, whereas Aos1 and Uba2 were mostly cellular. SUMO1 and SUMO2, on the other hand, seemed to remain in the cells although minor levels of free SUMO2 as well as several SUMO2-modified species were found in the cytosolic fraction (Fig. 9B, top panels). Taken together, the results showed that HeLa cells permeabilized with digitonin still have significant amounts of E1 and E2 enzymes whereas free SUMO1 and SUMO2 levels could potentially be limiting. To adress the question whether this system is sufficient to sumoylate Ran, semi-permeabilized cells were incubated with recombinant Ran and YFP-SUMO1 in the presence of ATP (Fig. 10A). Where indicated, cells were pretreated with SUMO-Vme in order to block isopeptidases. The samples were resolved by SDS PAGE and immunoblotted with antibodies against Ran, GFP (to detect YFP-SUMO), and SENP1. SENP1 was used as a positive control to test whether the SUMO-Vme was efficient to block isopeptidases. Active SUMO-Vme should form an adduct with SENP1, which can easily be visualized by immunoblotting. Analysis of these sumoylation experiments clearly showed that semi-permeabilized cells have sufficient sumoylation machinery to covalently link YFP-SUMO1 to unknown targets in the system in an ATP-dependent manner (Fig. 10B, left panel, lanes 1&2). Pre-treatment of cells with SUMO-Vme blocked the isopeptidases as can be clearly seen by the shift of SENP1 (Fig. 10B, right panel), and this was accompanied by a clear increase in the overall sumoylation levels (Fig. 10B, compare lane 3 and 4). Addition of 120nM E1 and 155nM E2 together or separately slightly boosted the sumoylation reaction. When the same samples were probed with Ran antibody, Ran sumoylation was clearly observed even under core reaction conditions (Cells + Ran, YFP-SUMO1, ATP) (Fig. 10C, lane 3). However, it was a very small proportion of the Ran population. Blocking isopeptidases with SUMO-Vme or adding E1 and E2 enzymes clearly increased the sumoylation of Ran (Fig. 10C, compare lane 3 with lanes 4, 5, and 6). In summary, these results not only demonstrated that recombinant Ran is sumoylated in semi-permeabilized cells in the presence of YFP-SUMO1 but also showed that endogenous isopeptidases contribute to the low steady state levels of Ran sumoylation.

A

HeLa suspension cells, 70g 5min

↓

Wash 1X, 200g 5min

↓

0.007% digitonin, 5min on ice

↓

200g, 5min

↓ ↘

cytosol   cells

↓

Lysed in 2X Sample buffer

B

α-SUMO1   α-SUMO2

α-Ran
α-Ubc9
α-Uba2
α-Aos1
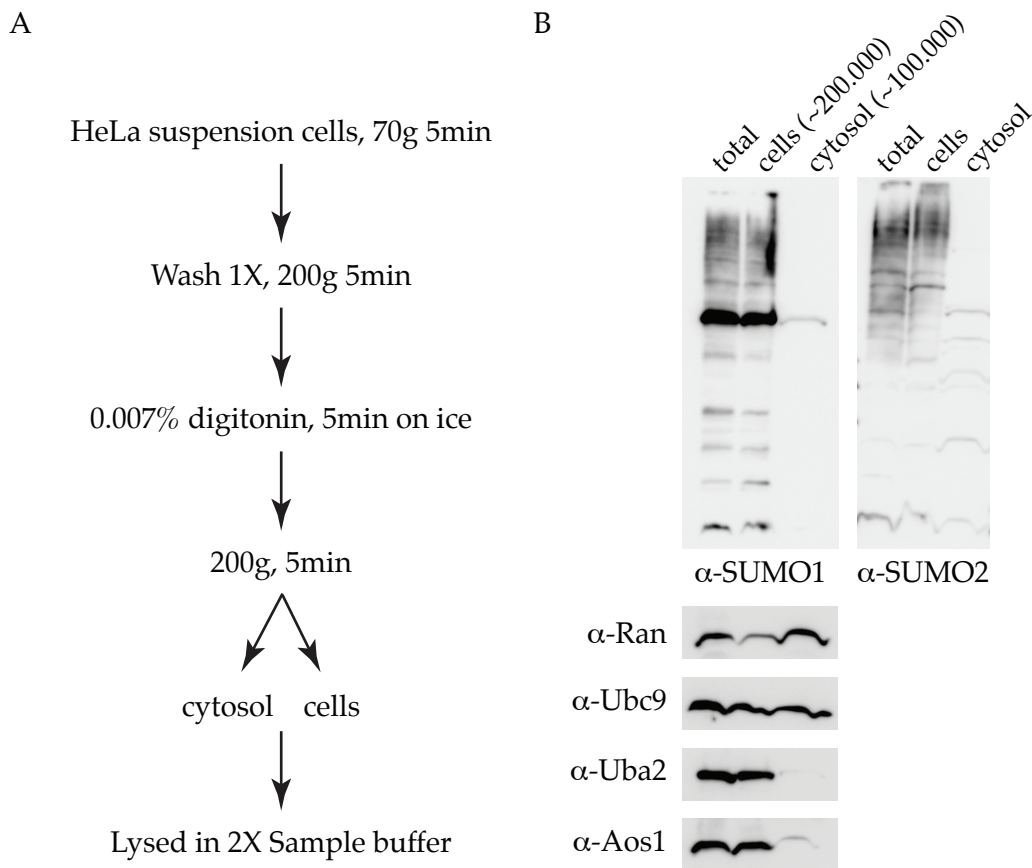
Fig. 9: Digitonin permeabilization of HeLa cells leads to rapid leakage of Ubc9 and Ran, whereas Aos1/Uba2 heterodimer mainly remains in the cells. (A) Experimental setup for the permeabilization of HeLa cells. HeLa suspension cells were briefly centrifuged and washed with transport buffer followed by 0.007% digitonin treatment on ice for 5min. After permeabilization, cellular and cytosolic fractions were separated by centrifugation and lysed with 2X SDS sample buffer. (B) Lysed cells prior to permeabilization were separated by SDS PAGE together with permeabilized cells and the leaked cytosol. Approximately 200.000 intact and permeabilized cells were loaded whereas cytosol corresponded to ~100.000 cells. Following SDS PAGE, the samples were analyzed by western blot with αSUMO1, αSUMO2, αRan, αUbc9, αUba2, and αAos1 antibodies as indicated.

5. Analysis of Ran Sumoylation in vitro

5.1. Ran sumoylation is inefficient with SUMO E1 and E2 For some SUMO targets such as RanGAP1, catalytic amounts of E1 and E2 are sufficient for efficient sumoylation whereas for most targets low amounts of E1 and E2 are not enough, and E3 ligase activity is required. In some cases, very high amounts of E1/E2 can compensate for the lack of E3. In order to test whether the sumoylation activity observed for Ran is E3 ligase-dependent

A

+ Ran

+ YFP-SUMO1   + ATP

semi-permeabilized cells   30°C, 30min

Lysed with 2X sample buffer

B

α-GFP

α-SENP1

C

α-Ran
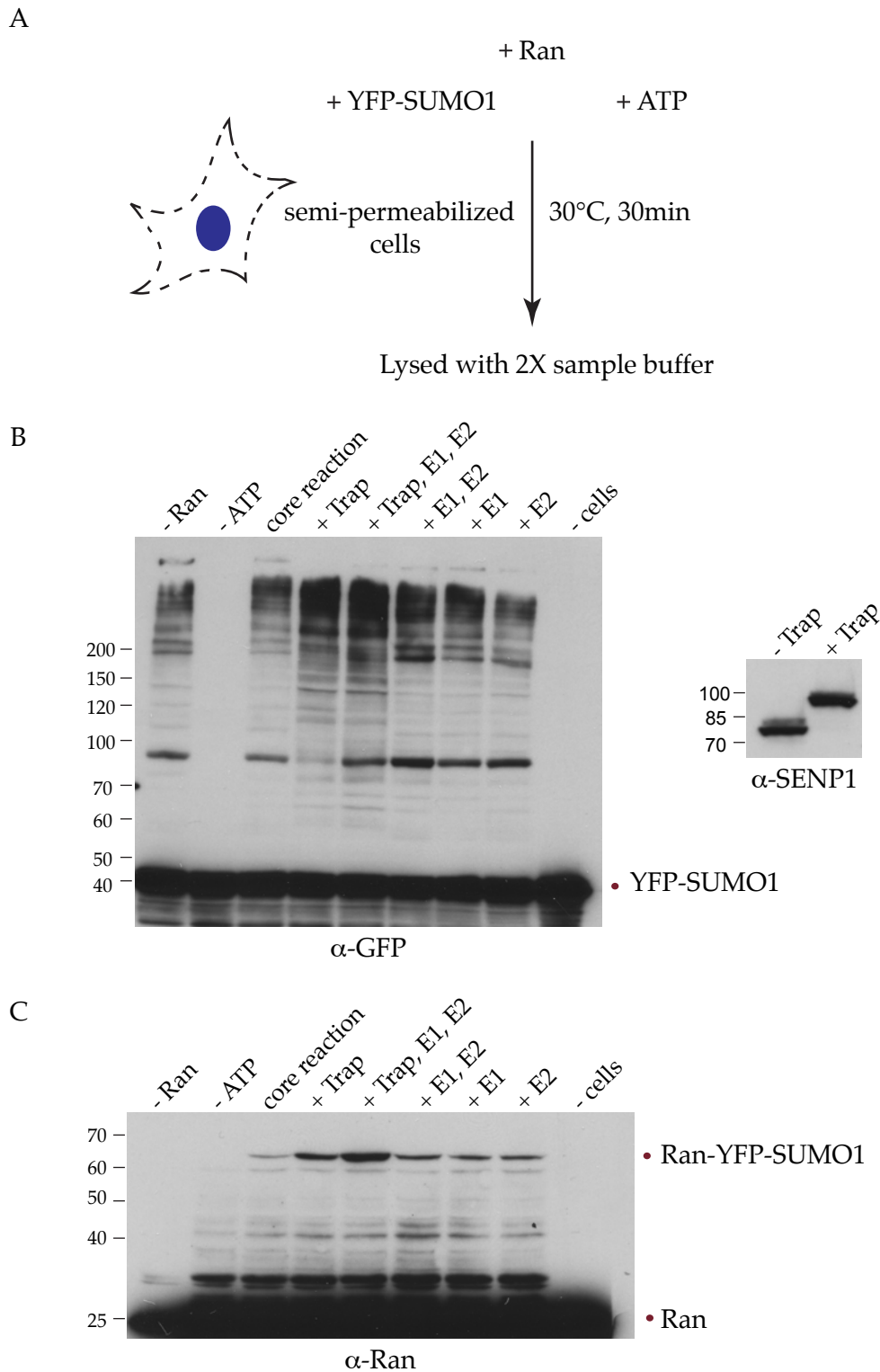
Fig 10: Ran is sumoylated with YFP-SUMO1 in semi-permeabilized cells supplemented with ATP. (A) General experimental setup for in vitro sumoylation with semi-permeabilized cells. Cells were treated with 0.007% digitonin on ice for 5min, and incubated with $5\mu M$ Ran and $35\mu M$ YFP-SUMO1 at 30°C for 30min in the presence of an ATP-regenerating system (final concentrations 1.3mM ATP, 3.7mM creatine phosphate, and 13U/mL creatine phosphate kinase) (core reaction).

(B,C) In vitro sumoylation assays with semi-permeabilized cells were done as described in A, and modifications to the core reaction were shown above the gels. Where indicated, cells were preincubated with SUMO-Vme (Trap) for 30min on ice prior to the sumoylation assay in order to block isopeptidase activity. For lanes 5, 6, 7, and 8, the sumoylation reaction was stimulated with the addition of 120nM E1 and/or 155nM E2. The reactions were stopped by 2X SDS sample buffer, and the proteins were resolved by SDS PAGE. Western blot analysis was done with αGFP (for YFP-SUMO1), αRan, and αSENP1 antibodies.

or not, in vitro sumoylation assays with recombinant Ran in the presence of E1 and E2 were performed. The reactions were pushed with 400nM E1 and 500nM E2 at 37°C for a time course of maximum 2 hours. The results showed that Ran can be sumoylated in the presence of high E1 and E2 concentrations, with both SUMO1 and SUMO2 (Fig. 11A and 11B). However, this reaction is very inefficient, and a small fraction of sumoylated Ran could be observed only after 1h at 37°C. Of note, sumoylation assays with SUMO1 and YFP-SUMO1 seemed more efficient compared to SUMO2 and YFP-SUMO2, respectively (Fig. 11A and 11B), which might be a hint for paralog specificity.

5.2. The RanBP2/ Ubc9/ RanGAP1-SUMO1 complex stimulates Ran sumoylation whereas PIAS proteins do not

The low efficiency of in vitro sumoylation of Ran with E1 and E2 suggests that Ran sumoylation is E3 ligase-dependent. In order to test this idea, RanGDP and RanGTP were purified and incubated with different E3 ligases (RanBP2 fragment or PIAS E3 ligases) in an in vitro sumoylation assay. The results were striking. Ran was efficiently sumoylated with SUMO1 and SUMO2/3 in either conformation by RanBP2 fragment (Fig. 12A and 12B). RanGDP sumoylation resulted in one distinct band, whereas RanGTP was heavily sumoylated resulting in a smear in addition to the monosumoylated Ran (Fig. 12). PIAS E3 ligases, on the other hand, did not stimulate RanGDP sumoylation in the presence of SUMO1 or SUMO2/3 although all of them except for PIASxβ stimulated p53 sumoylation (Fig. 13, lower panel). In the same reactions, RanBP2 fragment was sufficient to sumoylate Ran. For RanGTP, preliminary experiments suggested that it is not sumoylated by PIAS proteins neither with SUMO1 nor with SUMO2/3 although the experiments need to be repeated (data not shown). Overall, the results suggested that RanBP2 is likely to be the relevant E3 ligase. Therefore, I repeated the sumoylation reaction in the presence of the RanBP2 complex. Indeed, Ran could again be sumoylated. RanGDP and RanGTP sumoylation had identical patterns over 30min reaction time (Fig. 14, upper panel). This was surprising considering that Ran-binding domains of RanBP2 recognize RanGTP with a much higher affinity. One explanation for this observation was that all RanGTP was quickly hydrolyzed to RanGDP by RanGAP1 present in RanBP2 complex. In order to

A
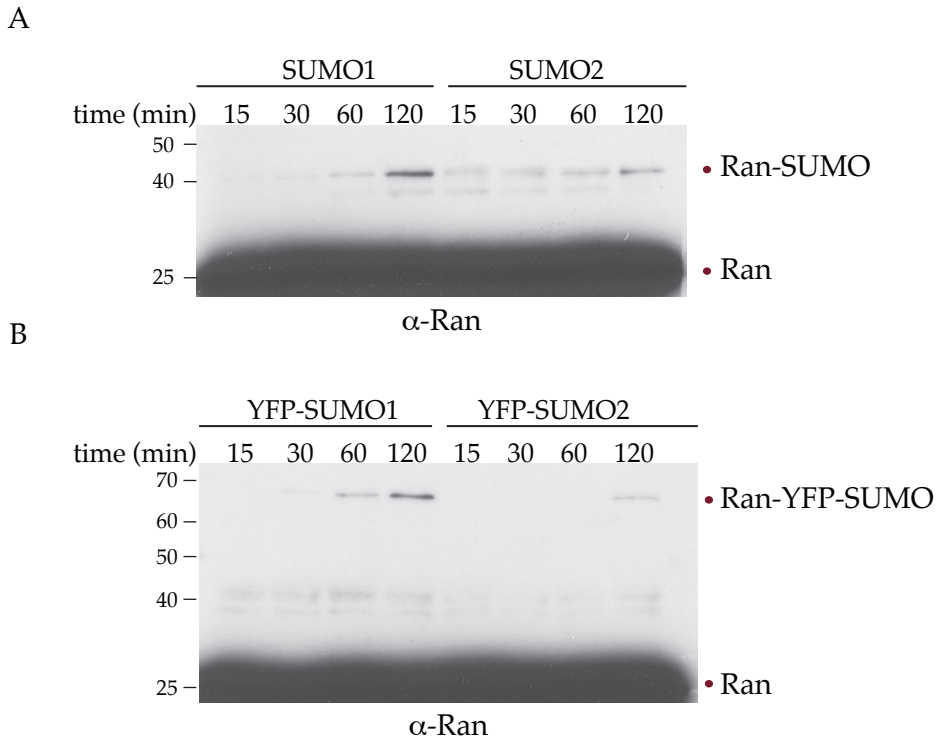
Fig. 11: High concentrations of E1 and E2 are required for sumoylation of Ran in vitro (A,B) In vitro sumoylation assays were performed with 2µM Ran, 400nM E1, 500nM E2, and 5mM ATP at 37°C. Where indicated 3µM SUMO1, SUMO2, YFP-SUMO1, or YFP-SUMO2 were added. The reactions were stopped at indicated time points with 2X sample buffer. The samples were resolved by SDS PAGE followed by immunoblotting with Ran antibodies. Protein markers are indicated as kDa.
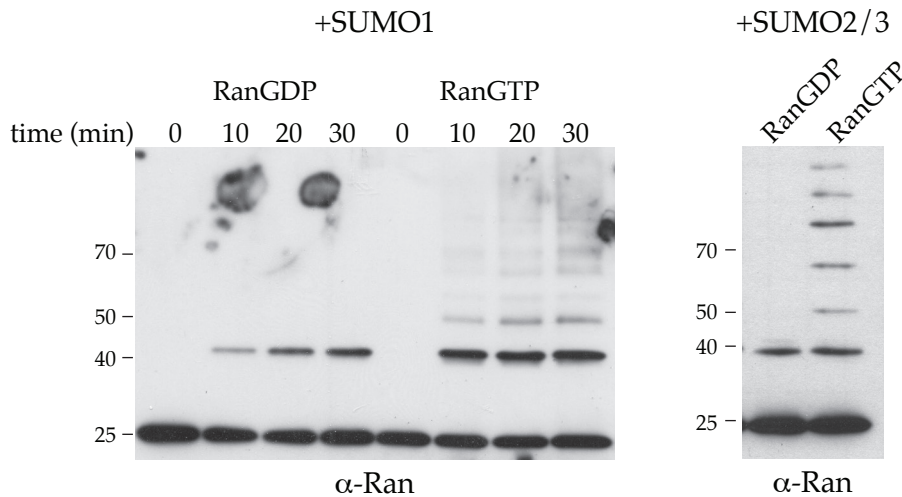
Fig. 12: RanBP2 fragment stimulates sumoylation of Ran in GDP- and GTP-bound conformations. In vitro sumoylation of Ran was performed with 400nM RanGDP or RanGTP, 68nM E1, 56nM E2, 72nM RanBP2 fragment, 15µM SUMO1 or SUMO2/3, and 5mM ATP at 30°C. Reactions were stopped with 2X SDS sample buffer at indicated time points for SUMO1, and after one hour for SUMO2/3. The samples were resolved by SDS PAGE followed by immunoblotting with Ran antibodies. Protein markers are indicated as kDa.

circumvent this problem, the RanBP2 complex was reconstituted using a truncated version of RanGAP1 (lacking the N-terminal catalytic domain), which can no longer catalyze the hydrolysis of RanGTP to RanGDP (provided by Dr. Andreas Werner). When in vitro sumoylation of RanGDP and RanGTP was performed with this RanBP2 complex variant, RanGTP sumoylation was more efficient compared to RanGDP sumoylation (Fig. 14, lower panel). Interestingly, the sumoylation pattern was quite different compared to Ran sumoylation with the RanBP2 fragment: Rather than the high molecular weight smear, only one distinct band corresponding to the monosumoylated Ran was visible indicating different behaviour of the RanBP2 fragment and the RanBP2 complex. The RanBP2 complex seemed to be restrained in its activity, which possibly brings along specificity.
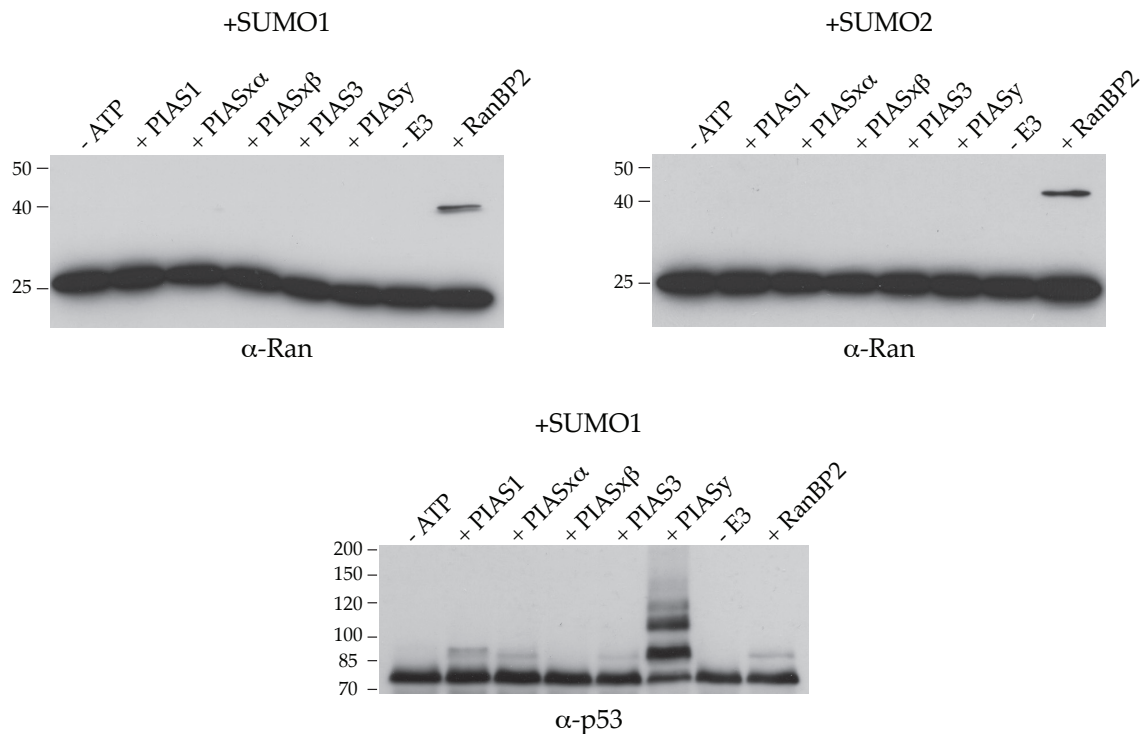
Fig. 13: Ran is not sumoylated by PIAS E3 ligases. In vitro sumoylation assays were performed in the presence of 400 nM RanGDP or 460nM GST-p53, 68nM E1, 56nM E2, 15μM SUMO1 or SUMO2, 5mM ATP, and 72nM RanBP2 fragment or ~50nM PIAS proteins (GST-PIAS1, GST-PIASxα, PIAS-xβ, PIAS3 and GST-PIASy). The reactions were incubated at 30°C for an hour and stopped with 2X SDS sample buffer. The proteins were resolved on 5-20% gradient gels followed by immunoblot analysis with anti-Ran or anti-p53 antibodies. Protein markers are indicated as kDa.
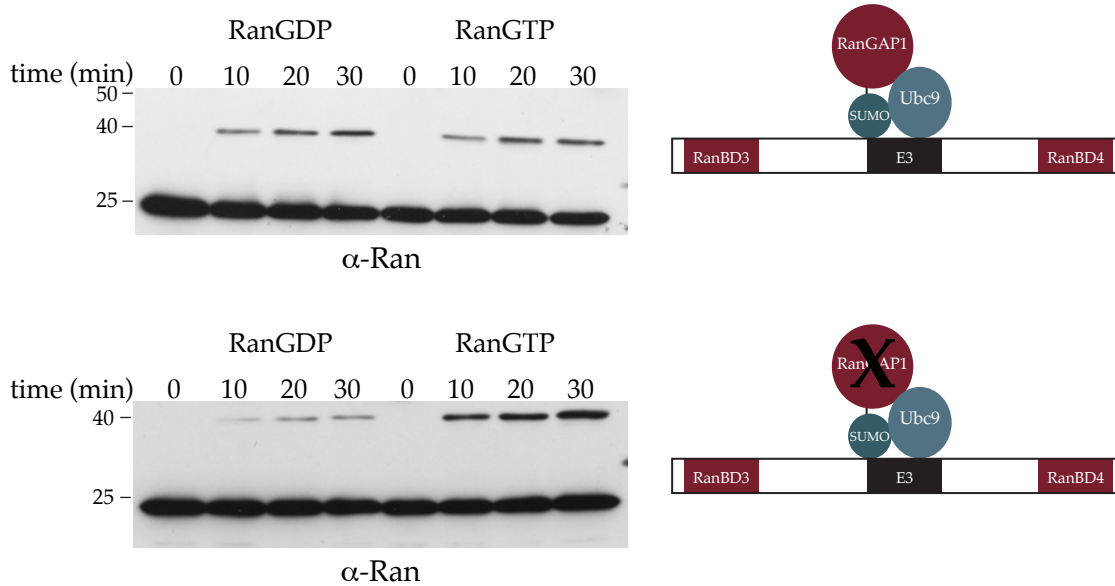
Fig. 14: In vitro reconstituted RanBP2 complex stimulates Ran sumoylation with a preference for RanGTP. In vitro sumoylation of Ran was performed at 30°C with 400nM RanGDP or RanGTP, 68nM E1, 56nM E2, 15μM SUMO1, 5mM ATP, and 72nM of either RanBP2 complex (upper panel) or a variant containing a RanGAP1 that lacks the N-terminal catalytic domain (lower panel). The reactions were stopped at indicated time points with 2X SDS sample buffer. The samples were resolved by SDS PAGE followed by immunoblotting with Ran antibodies. Protein markers are indicated as kDa.

5.3. Transport receptors prevent poly- or multi-mono-sumoylation of Ran but still allow mono- sumoylation

During interphase, Ran shuttles continuously between nucleus and cytoplasm and interacts with RanBP2 complex largely in association with nuclear transport receptors (NTRs). There are 21 NTRs belonging to Impβ-superfamily members (Görlich and Kutay, 1999) in humans, and all of them interact with RanGTP in order to release or recognize their respective cargos in the nucleoplasm. Therefore, at any given time, a significant portion of Ran is bound to transport receptors. In fact, it has been estimated that there is only a three fold excess of Gsp1 (Ran homologue in *S.cerevisiae*) over all Impβ family members in the nucleus (Hahn and Schlenstedt, 2011). Since a significant portion of Ran is in complex with NTRs, which then encounter RanBP2 complex, I wanted to test whether transport receptors have an influence on Ran sumoylation. For this, different concentrations of the main import and export receptor, Impβ and Crm1, respectively were added to in vitro sumoylation reactions of RanGTP with RanBP2 fragment. The concentrations of transport receptors varied from ~100nM to ~800nM whereas Ran concentrations were kept constant at ~200nM. The results clearly showed that in the presence of both transport receptors higher molecular weight species, which are either poly- or multi-sumoylated forms of Ran, disappeared. However, mono-sumoylation of

A
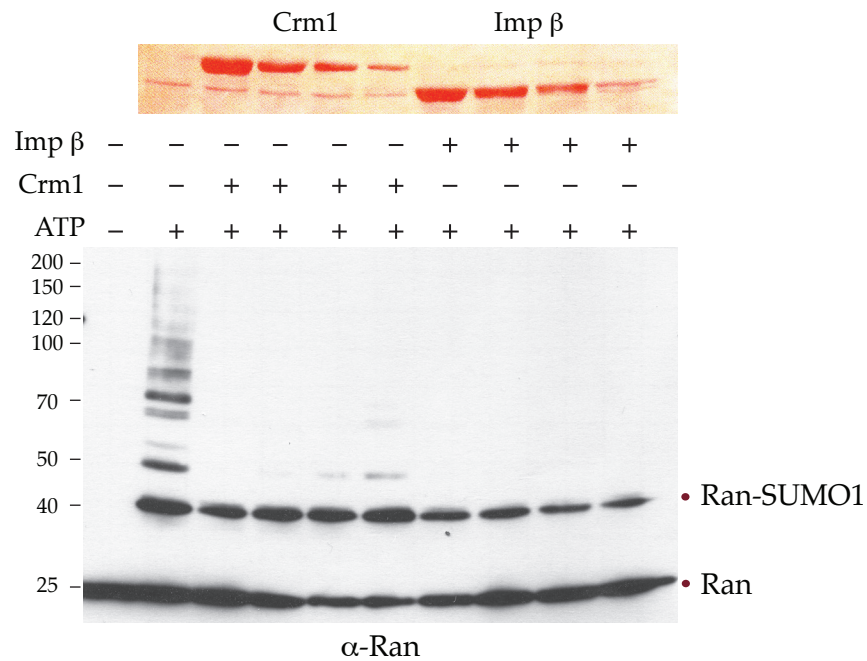
B
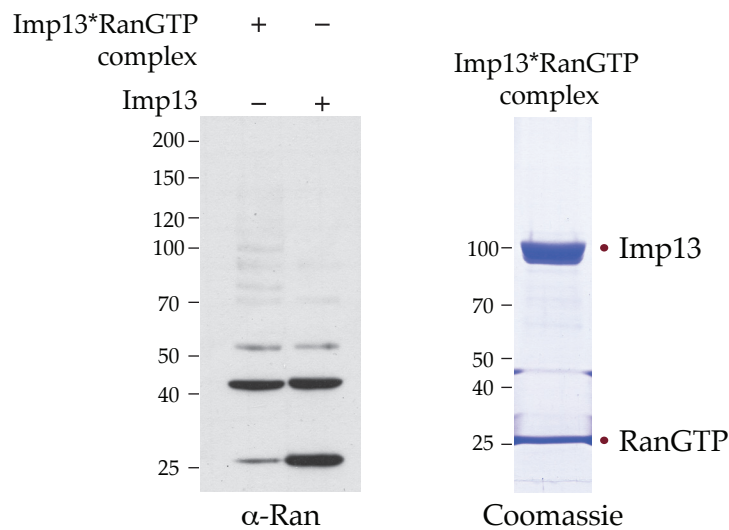
Fig. 15: Ran can be sumoylated in the presence of nuclear transport receptors. (A,B) In vitro sumoylation reactions were performed at 30°C for 30min in the presence of 68nM E1, 56nM E2, 15μM SUMO1, 148nM RanBP2 fragment, and 5mM ATP (except for the first lane, top panel). The reactions were stopped with 2X SDS sample buffer. The samples were resolved by SDS PAGE followed by immunoblotting with Ran antibodies. For (A), 210nM RanGTP was used. Where indicated, Crm1 or Impβ was titrated into the reaction at 836-418-209-104nM concentrations. For (B), either 205nM RanGTP*Imp13 complex (purified over gel filtration, right panel) or 205nM Ran in the presence of 203nM Imp13 was used. Protein markers are indicated as kDa.

Ran was detected even with the highest concentrations of transport receptors (Fig. 15A). Importantly, the results are consistent with the crystal structures of Impβ*RanGTP (Vetter et al., 1999) or Crm1*RanGTP*Snurportin (Monecke et al., 2009) complexes in that some of the surface area of RanGTP is no longer accessible when it is in complex with either of the transport receptors. After testing one prototype for import and export receptors, I also wanted to test the effect of Imp13 since it is a unique, bidirectional transport receptor which can work both as an importin and exportin. Therefore, I compared sumoylation of RanGTP when Imp13 was added separately or allowed to form a proper complex run over gel filtration (Fig. 15B). Surprisingly, Imp13 did not have a dramatic effect on Ran sumoylation by RanBP2 fragment. Monosumoylated Ran as well as the higher molecular weight smear were visible (Fig. 15B). Interestingly Ran in Imp13*RanGTP preformed complex was sumoylated more efficiently compared to when Imp13 was added separately to the reaction. The depletion of unmodified Ran was discernible when Ran was in complex with Imp13 (Fig. 15B, lane 1), which was not the case when the components were pipetted separately. Imp13 seems to have a slight stimulatory effect on the reaction. One explanation for the slight differences observed concerning Ran sumoylation in the presence of different transport receptors might be the different affinities between Ran and transport receptors. To give an example, the Kd value determined for Impβ and RanGTP is ~140pM with a very low dissociation rate (Villa Braslavsky et al., 2000), whereas it is likely to be much higher for Crm1 and Imp13, since export factors' interactions with RanGTP is not very stable, and cargo associations increase the affinity.

6. Identification of Ran sumoylation sites

Next, I wanted to determine the target lysines for sumoylation in Ran. For this purpose, the in vitro sumoylation of RanGTP in the presence of RanBP2 fragment was upscaled, and the proteins were methanol-chloroform precipitated. Precipitated samples were separated on SDS PAGE followed by colloidal coomassie staining to visualize nanogram quantities of proteins. With this method, it was possible to visualize the sumoylated Ran in the presence of RanBP2 and SUMO1 (Fig. 16, Lanes 1 and 2). The regions shown with red boxes in Fig. 16 were cut and subjected to mass spectromety (In collaboration with Prof. Henning Urlaub, MPIbpc, Götingen), which in turn identified three consecutive lysines, K130, K132, and K134, as the acceptor sites for SUMO.
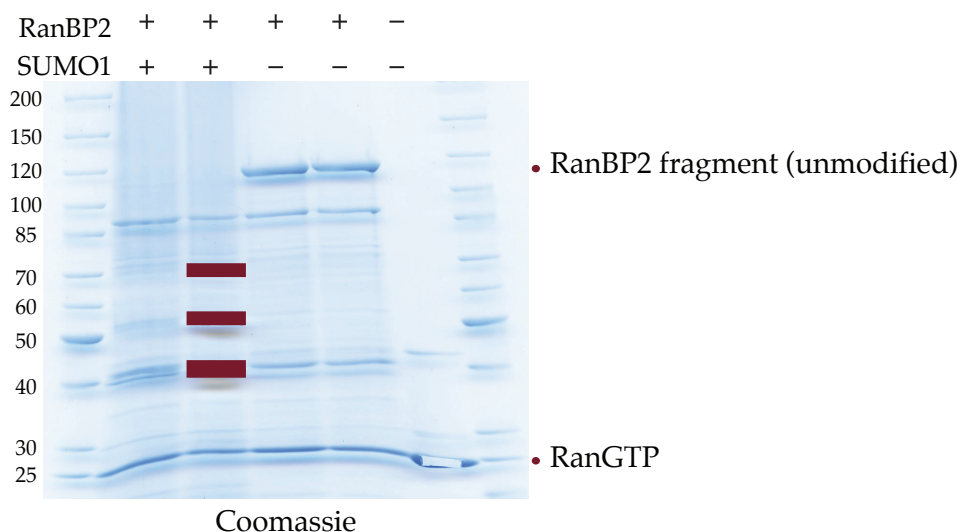
Fig. 16: Mass spectrometry analysis of Ran sumoylation identified three lysines: K130, K132, and K134. In vitro sumoylation reactions of 1μM RanGTP in the presence of 69nM E1, 83nM E2, 148nM RanBP2 fragment (except for last lane), 15μM SUMO1 (Lanes 1&2), and 5mM ATP were performed in 200μL reaction volumes. The whole reaction was precipitated by methanol-chloroform, and proteins were seperated by SDS PAGE. Subsequent staining with colloidal coomassie visualized distinct bands. Indicated areas with red boxes were cut, and sent for mass spectrometry. Protein markers are indicated as kDa. Of note, RanBP2 fragment undergoes massive autosumoylation. Therefore, it is not visible in the presence of ATP and SUMO1.

In order to test whether these lysines are the main acceptor sites, all three lysine residues were mutated to arginine in a site-directed mutagenesis reaction followed by the purification of the mutant protein. The Ran K130,132,134R variant (Ran triple mutant) behaved exactly like the wild type in terms of elution volume from gel filtration and ion exchange columns during purification, which indicated that the mutant was folded properly. To confirm the sumoylation sites, I applied the Ran triple mutant (Ran tm) to sumoylation assays with semi-permeabilized cells. The core reaction and the modifications were carried out as described for Fig. 10. As already seen earlier, Ran wild type was sumoylated in the presence of semi-permeabilized cells, YFP-SUMO1, and ATP, and the sumoylation was stimulated in the presence of SUMO-Vme and/or E1 and E2 (Fig. 17, lanes 1-4). Of note, E1 and E2 enzymes were not sufficient to sumoylate recombinant Ran in the absence of cells (Fig. 17, lane 5). Sumoylation of Ran triple mutant, on the other hand, was not detected at all with the core reaction components alone (Fig. 17, lane 6). Upon stimulation of sumoylation by either blocking isopeptidases or by adding E1 and E2 enzymes, minor amounts of sumoylated Ran triple mutant could be observed, but much less compared to wild type (Fig. 17, compare lanes 3 and 8). As the sumoylation was not completely abolished in the reaction with Ran triple mutant, it is
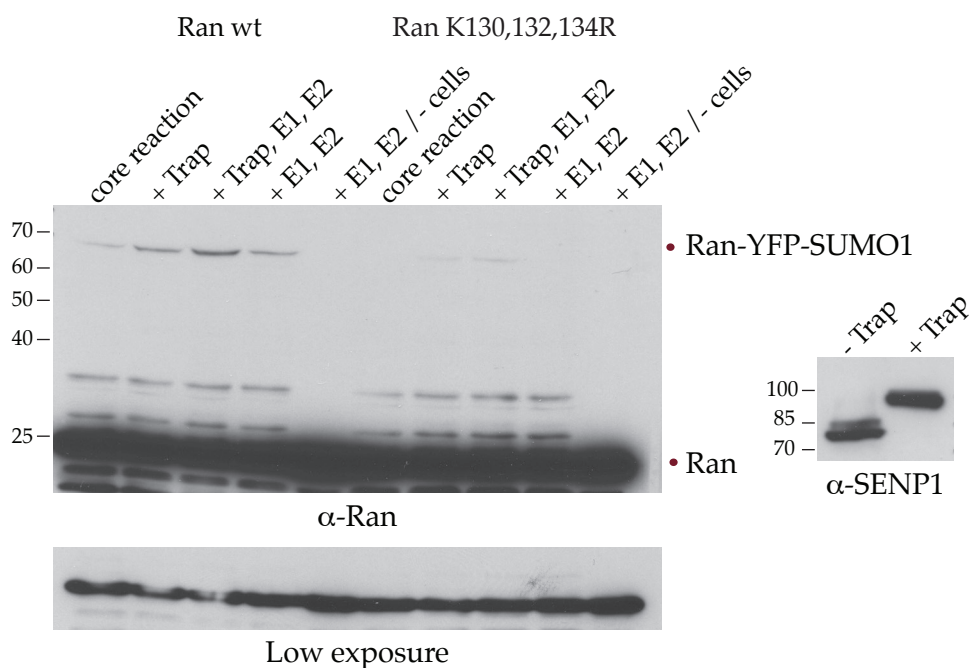
Fig. 17: Ran K130,132,134R sumoylation is strongly reduced compared to Ran wild type in semi-permeabilized cells. Cells were semi-permeabilized with 0.007% digitonin on ice for 5min, and incubated with 5μM Ran (wild type or K130,132,134R mutant) and 35μM YFP-SUMO1 at 30°C for 30min in the presence of ATP regenerating system (final concentrations 1.3mM ATP, 3.7mM creatine phosphate, and 13U/mL creatine phosphate kinase) (Core reaction) for sumoylation assays. Modifications to the core rx were shown above the gels. Where indicated, cells were preincubated with SUMO-Vme (Trap) for 30min on ice before sumoylation in order to block isopeptidase activity. For lanes 3-5 and 8-10, the sumoylation reaction was stimulated with the addition of 120nM E1 and 155nM E2. The reactions were stopped by 2X SDS sample buffer, and the proteins were resolved by SDS PAGE. Western blot analysis was done with αRan and αSENP1 antibodies. Protein marker is shown in kDa.

important to note that there is still residual endogenous Ran present in the system even though digitonin permeabilization causes a rapid loss of Ran from cells (Fig. 9B).

Next, I wanted to test whether Ran triple mutant can be in vitro sumoylated with RanBP2 or not. For this purpose, Ran variants were preloaded with GTP or GMP-PNP, a GTP analog which locks Ran in GTP bound conformation since it can not be hydrolyzed by RanGAP1 in the RanBP2 complex. Both RanGTP and RanGMP-PNP were then subjected to in vitro sumoylation assays with RanBP2 fragment and the RanBP2 complex, respectively. The sumoylation assays over a period of 30 min indicated that Ran triple mutant in GTP-bound conformation was sumoylated with equal efficiency compared to Ran wild type by both RanBP2 fragment and the RanBP2 complex (Fig. 18). Overall, the results demonstrated that K130, 132, and K134 identified by mass spectrometry are

relevant sumoylation sites for Ran. However, whether RanBP2 complex is the relevant E3 ligase or not still remains elusive.
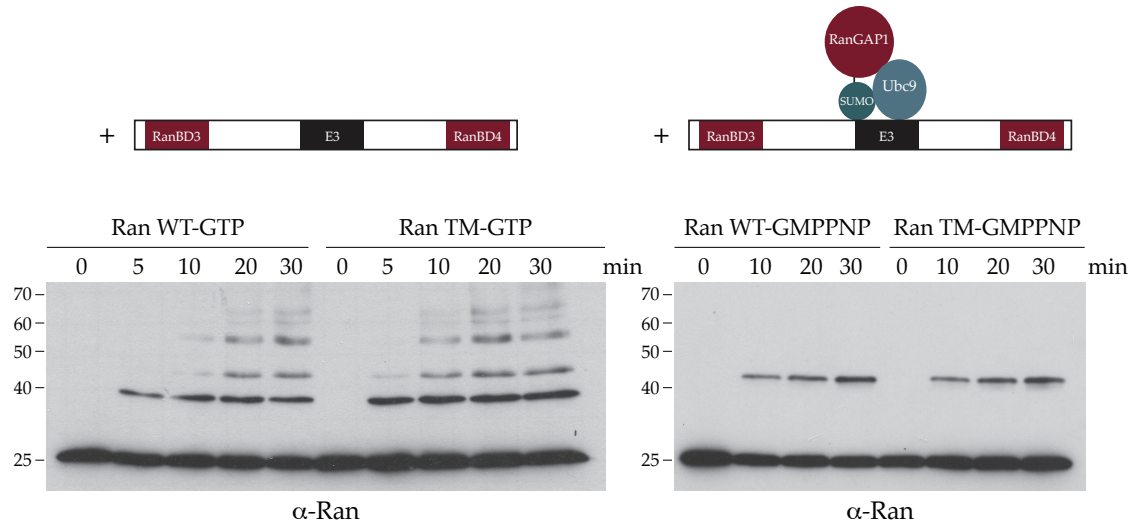
Fig. 18: Ran K130,132,134R and Ran wild type in GTP-bound conformation are equally well sumoylated by RanBP2 fragment and the RanBP2 complex. In vitro sumoylation of 200nM Ran wild type or 500nM Ran triple mutant (TM) was performed at 30°C in the presence of 69nM E1, 56nM E2, 15μM SUMO1, 5mM ATP, and 148nM RanBP2 fragment or the RanBP2 complex. Ran variants were preloaded with GTP and GMP-PNP (a non-hydrolyzable analog of GTP) for in vitro sumoylation assays with RanBP2 fragment and the RanBP2 complex, respectively. The reactions were stopped at indicated time points with 2X SDS sample buffer. The proteins were resolved on 5-20% gradient gels followed by immunoblot analysis with anti-Ran antibodies. Protein markers are indicated as kDa.

7. Functional Analysis of Ran sumoylation

Showing that Ran is sumoylated via K130, 132, and 134, we next wanted to investigate the functional outcomes of the sumoylation of Ran with a main focus on nucleocytoplasmic transport.

7.1. Does sumoylation of Ran affect its nuclear localization?

Considering Ran function in nucleocytoplasmic transport, an obvious question was whether sumoylation alters its intranuclear localization. To test whether sumoylation of Ran contributes to its correct nuclear localization, two different approaches were taken: In the first approach, Ran wild type and Ran triple mutant were cloned with an N-terminal GFP fusion in an eukaryotic expression vector. GFP-Ran fusion proteins were expressed for 48hours in HeLa cells seeded on cover slips followed by formaldehyde fixation. The localizations of GFP-tagged Ran proteins was subsequently analyzed by confocal

microscopy. As shown in Fig. 19A, both variants were observed to localize mainly to the nucleus. To ensure that both variants were expressed as full-length proteins, a fraction of the cells were lysed with 2X SDS sample buffer followed by immunoblotting with anti-Ran antibodies. Importantly, both Ran wild type and the triple mutant were expressed at full length with comparable expression levels (Fig. 19B). These observations allowed to conclude that sumoylation is not essential for intranuclear localization of Ran.
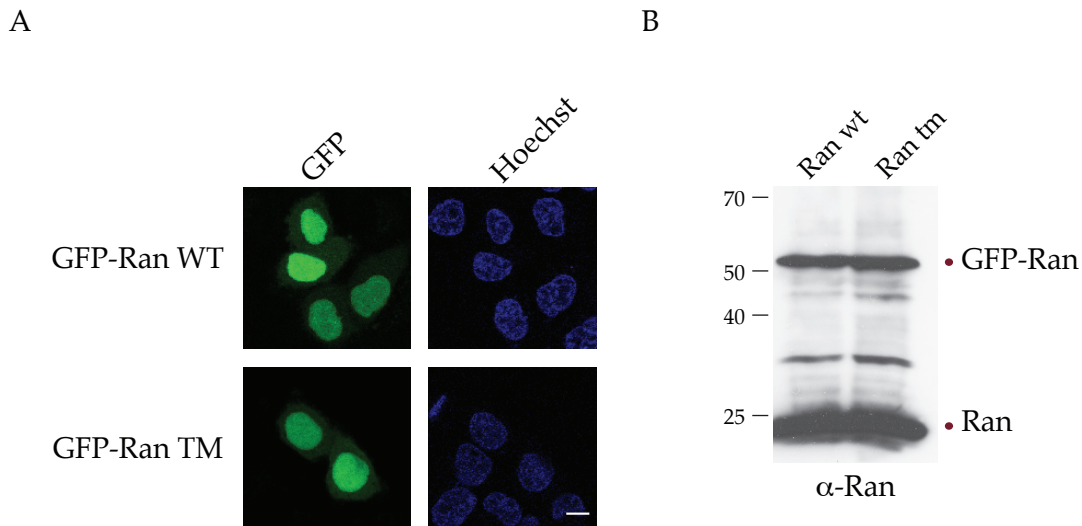
Fig. 19: GFP-Ran K130,132,134R localizes to nucleus as Ran wild type. (A) HeLa cells seeded on coverslips were transiently transfected with pEGFP-Ran wild type (WT) and pEGFP-RanK130,132,134R (Triple mutant-TM). 48h post transfection, cells were fixed, and the nuclei were counterstained with Hoechst. The images were taken by confocal microscopy. Scale bar, 10μM. (B) 48h post transfection, cells were lysed with 2X SDS sample buffer. The samples were resolved on SDS PAGE, and the expression of full length Ran wild type and the mutant was verified by immunoblotting using anti-Ran antibodies. Protein markers are indicated as kDa.

In an alternative approach, the catalytic subunit of the E1 heterodimer, Uba2, was knocked down in HeLa cells, and the localization of endogenous Ran was analyzed by indirect immunofluorescence by using monoclonal Ran antibodies. HeLa cells were transfected with either non-targeting control siRNAs or siRNAs against Uba2 for 48 and 72 hours at two different concentrations (20nM and 40nM). Post 48h and 72h transfections, the cells were lysed with 2X SDS sample buffer, and the efficiency of the knockdown was evaluated by immunoblotting with anti-Uba2, anti-α-tubulin, and anti-SUMO1 antibodies. The results clearly showed that Uba2 knockdown was very efficient after 72hours, and the loss of Uba2 was accompanied by an overall decrease in sumoylation and a slight increase in free SUMO1 levels (Fig. 20A, top and bottom panels). Quantification of the Uba2 knockdown demonstrated that almost 90% knockdown efficiency was accomplished after 48h, whereas after 72h Uba2 signals disappeared with
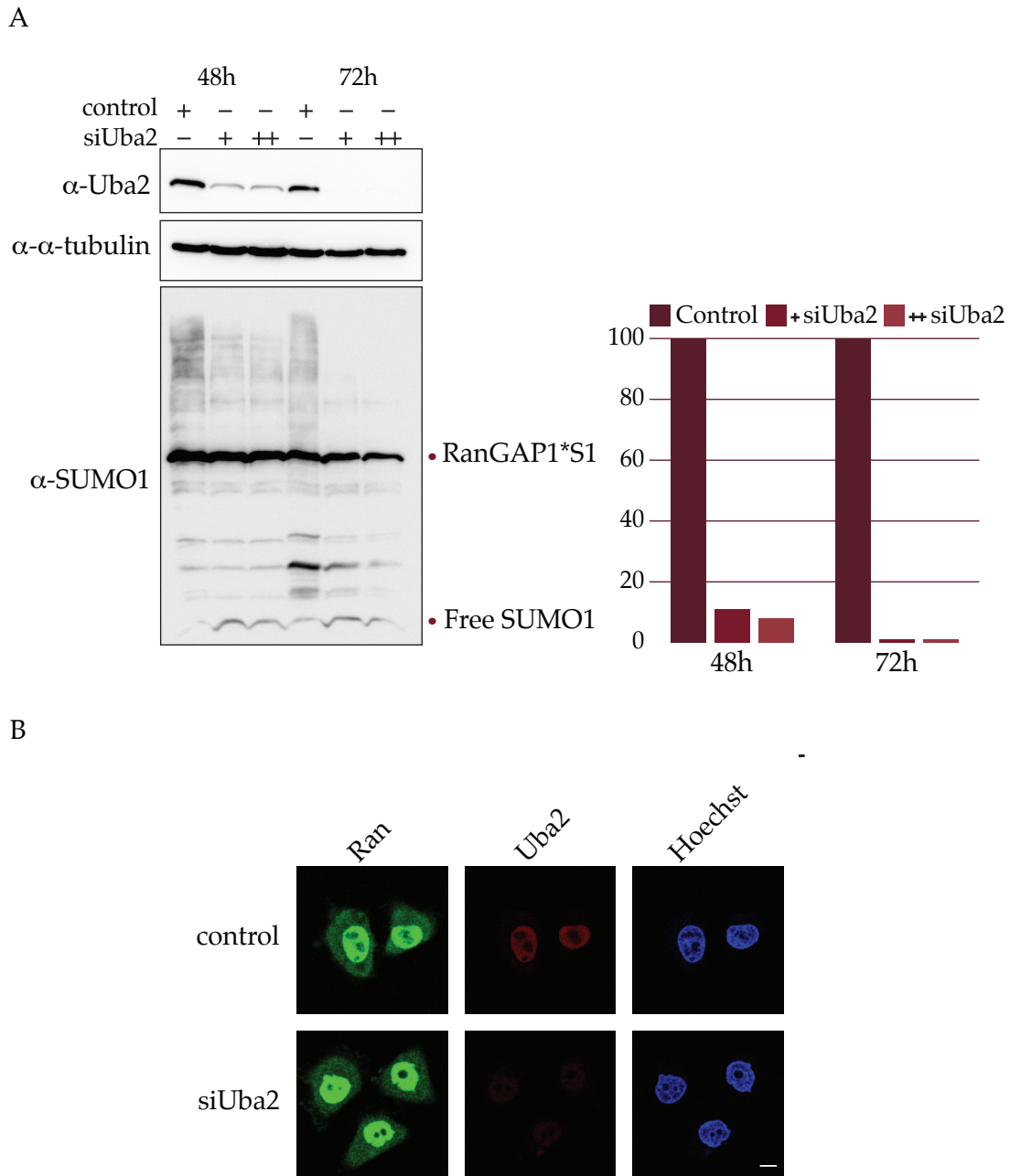
Fig. 20: Endogenous Ran localization does not change upon knockdown of Uba2. (A) HeLa cells were either transfected with control siRNA (+: 20nM) or siRNA directed against Uba2 (+: 20nM and ++: 40nM) for 48h and 72h. The efficiency of the knockdown was monitored by immunoblotting using anti-Uba2, anti-α-tubulin, and anti-SUMO1 antibodies for indicated time points (left panel). Quantification and normalization of Uba2 levels with respect to α-tubulin is shown in the right panel. Y-axis represents the ratio of Uba2/α-tubulin, which is set to 100 for control samples (B) 72h post transfection, the localization of endogenous Ran and the knockdown were monitored by indirect immunofluorescence using anti-Ran and anti-Uba2 antibodies. The nuclei were counterstained with Hoechst, and the images were taken by confocal microscopy. Scale bar, 10μM.

more than 95% knockdown efficiency (Fig. 20A, right panel). Subsequently, the localization of endogenous Ran was determined by indirect immunofluorescence, and no difference could be observed between control and siRNA samples (Fig. 20B). Ran seemed to be mostly nuclear with a slight cytoplasmic signal in each case. This result strongly suggested that Ran localization to the nucleus is not linked to the sumoylation status of the protein.

7.2. Does sumoylation of Ran play a role in regulation of nucleocytoplasmic transport?
Since the primary function of the small GTPase Ran during interphase is to regulate the directionality of nucleocytoplasmic transport, I wanted to investigate Ran sumoylation in the context of transport. Ran can interact with all members of the Impβ superfamily, albeit with differing affinities, and it regulates their cargo release or association. Therefore, it could be envisioned that any transport event that is dependent on Ran could in principle be regulated by sumoylation of this small GTPase. In order to test the effects of Ran variants on transport, I turned to in vitro import assays with semi-permeabilized HeLa suspension cells (Melchior et al., 1995). A brief summary of the experimental setup is shown in Fig. 21. In this system, semi-permeabilization of cells leads to the leakage of cytosolic nuclear transport receptors as well as Ran. Therefore, the cells can no longer support import or export unless they are provided with exogenous transport receptors and Ran as well as an ATP-regenerating system. Ran is an indispensible component of the system and required for transport cycles. Therefore, I aimed to compare the effects of Ran wild type and the sumoylation-deficient mutant on transport cycles without saturating the system. Among different transport pathways, I decided to start with the canonical Impα/β-dependent import.

7.2.1. Ran triple mutant can bind to its interactors NTF2 and RCC1 with comparable affinities to Ran wt

Although in vitro import assays provide an easy way of testing import or export, the system is still complicated in that for one round of recycling of import receptors, series of biochemical reactions have to take place as described in detail in introduction. In such a complicated series of protein-protein interactions, any kinetic advantage that RanK130,132,134R gained for one of its interactors could lead to an increased import rate. In order to test whether the Ran mutant has altered affinity towards any of its interactors and to make sure that Ran variants behave similarly except for their sumoylation potential in import assays, I started to characterize the interaction between Ran variants and their known interactors before in vitro import assays. Although the list is not complete, the interactions of Ran wild type or mutant with NTF2 and RCC1 could be
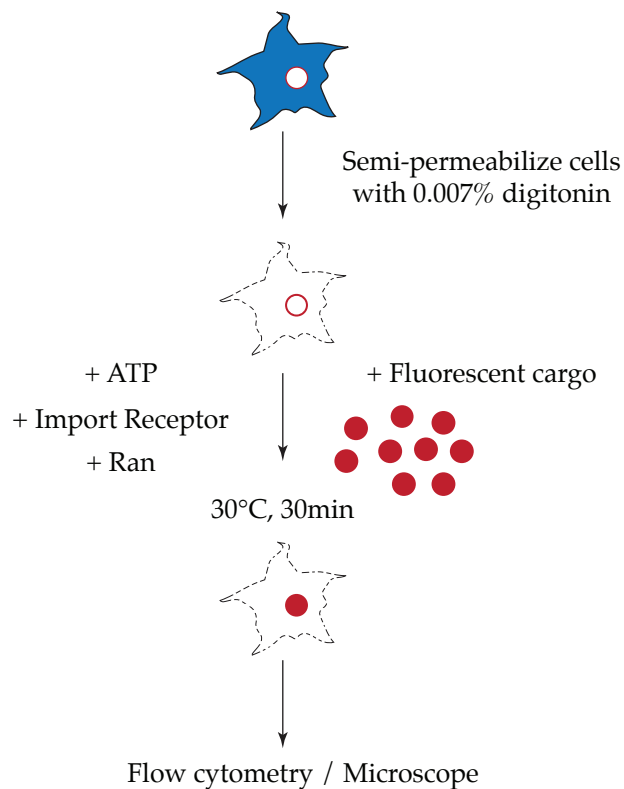
Fig. 21: In vitro transport assay experimental setup. HeLa cells were semi-permeabilized with 0.007% digitonin for 5min on ice. Semi-permeabilized cells were incubated with selected import receptor, recombinant Ran, and fluorescently labeled cargo in the presence of ATP-regenerating system at 30°C for 30min. The reactions were stopped with excess transport buffer, and the cells were spun down at 200g for 5min. The supernatant was removed except for ~300μL buffer. The fluorescence was measured by flow cytometry and where indicated by microscopy.

tested by pulldown assays, and other Ran effectors still require further investigation. The results of the pulldown experiments with immobilized NTF2 and GST-RCC1 indicated that Ran wt and the triple mutant bind to either NTF2 or GST-RCC1 comparably under the experimental conditions tested (Fig. 22A & 22B).

7.2.2. RanK130,132,134R behaves as RanWT in Impα/β-dependent import

Next, I wanted to adress the question whether Ran variants have any effect on Impα/β-dependent import. For this purpose, I performed in vitro import assays in the presence of 0.5μM Impα/β and 0.5μM transport cargo (FITC-BSA-NLS). The recycling of Imp β was stimulated with the addition of differing concentrations of Ran wt or Ran triple mutant (1μM-6μM). The reactions were allowed for a period of 30 min, stopped by the addition of excess buffer, and analyzed by flow cytometry for cell-associated fluorescence. The experiments showed that the stimulatory effects of Ran variants for Imp α/β-dependent import turned out to be very comparable (Fig. 23) at non-saturating Ran concentrations. The results also indicated that Ran mutant is fully functional and the mutations did not cause major problems.

A
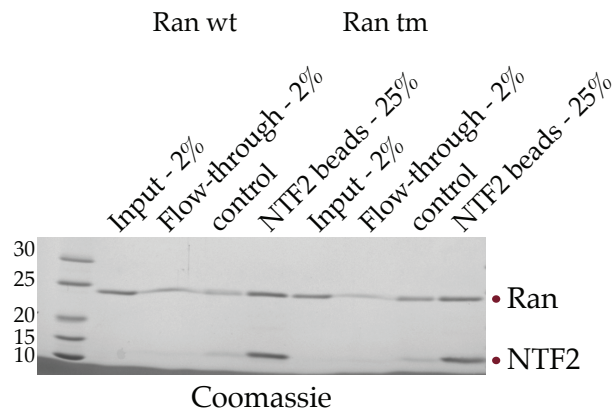
B
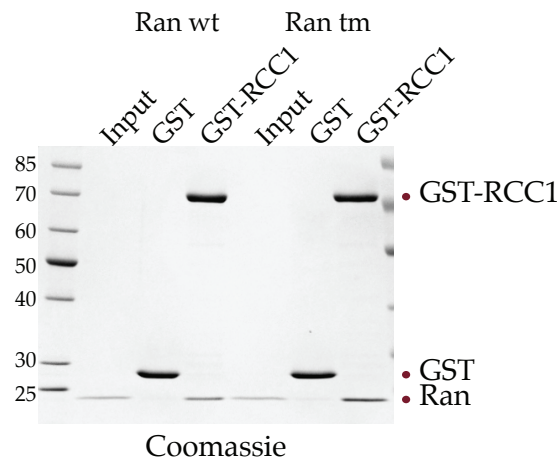
Fig. 22: Comparable interaction of Ran wild type and sumoylation-deficient mutant with NTF2 and RCC1. (A) NTF2 was coupled to CNBr-activated sepharose beads ($20\mu L$), which were equilibrated in transport buffer and incubated with ~$12\mu g$ Ran wt or RanK130,132,134R at 4°C for 1h. The beads were washed three times followed by elution with 2X SDS sample buffer. Samples were boiled at 95°C for 5min and resolved by SDS PAGE. The gel was stained with colloidal coomassie. For negative control, empty sepharose beads were used. Of note, NTF2 forms a dimer and therefore is detected in the eluate fraction. (B) GST-Pulldown assays. GST-RCC1 and GST (negative control) were immobilized to glutathione-sepharose beads prior to pulldowns. GST-RCC1 and GST (170nM each) were incubated with either Ran wt or RanK130,132,134R (260nM, each) at 4°C for 1h. The beads were washed three times followed by elution with 2X SDS sample buffer. Samples were boiled at 95°C for 5min and resolved by SDS PAGE. The gel was stained with colloidal coomassie. Input (4%), eluates for GST and GST-RCC1 (40%).

Imp α/β-dependent import
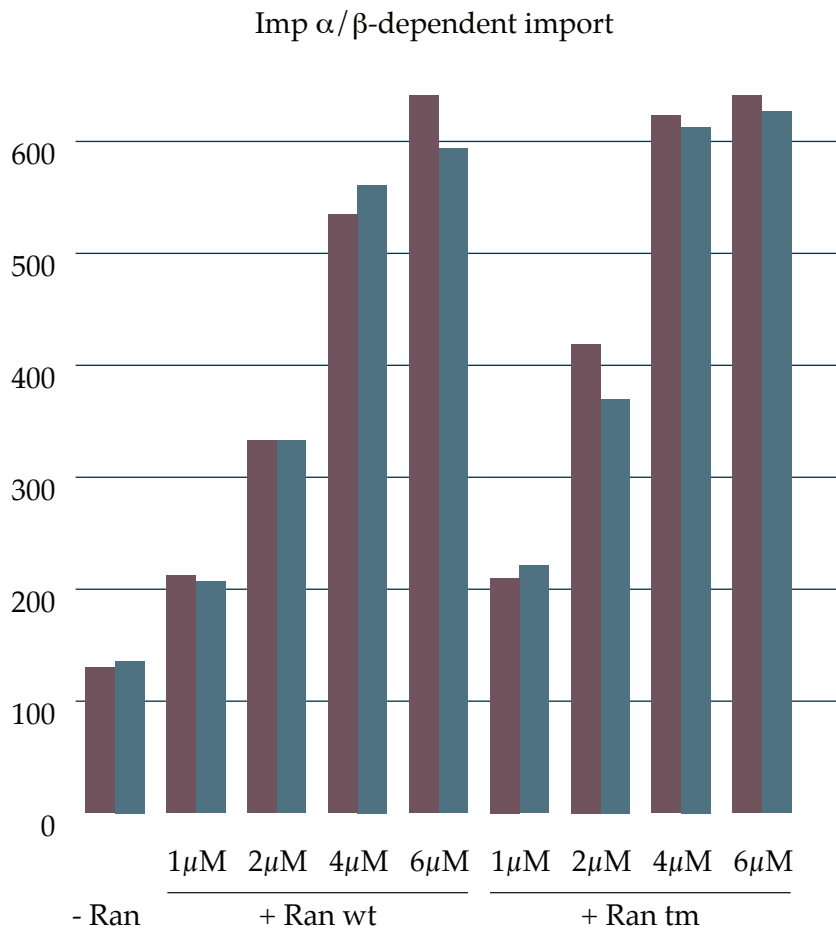
Fig. 23: The RanK130,132,134R behaves like Ran wild type in Imp α/β-dependent import. Imp13-dependent import assays were carried out in duplicates with 1μM Imp13, 60nM GST-Ubc9-Alexa488, and increasing concentrations of either RanWT or RanK130,132,134R (4μM-8μM) as indicated. Imp α/β-dependent import assays were perfomed with 0.5μM Impα and Impβ, 0.5μM FITC-BSA-NLS, and increasing concentrations of either RanWT or RanK130,132,134R (1μM-6μM) as indicated. For each type of tranport assays, Ran was omitted from the first sample as a control for background levels of import. Transport reactions were incubated at 30°C for 30min, and were stopped by the addition of excess transport buffer. The fluorescence was quantified by flow cytometry and represented as the mean value calculated from 10,000 cells. The two concentration values where the effect was observed were highlighted with dark blue.

7.2.3. RanK130,132,134R is more efficient than wild type in in vitro import reactions involving GST-Ubc9-Alexa488 and Imp13

Next, I turned to Imp13-dependent transport pathway due to mainly two reasons: First of all, Imp13-dependent import is intriguing since it is the import receptor for Ubc9 (Mingot et al., 2001) and therefore is required itself for nuclear sumoylation. Secondly, it is a unique bidirectional transport receptor (Mingot et al., 2001) which might be exposed to

additional regulation. In order to compare the effects of Ran variants on Imp13-dependent import, we decided to use Ubc9 as a model substrate in in vitro transport assays. However, Ubc9 is a small protein which also leaks into the nucleus by diffusion. In order to circumvent this problem, previous studies used GST-tagged Ubc9 labeled with the fluorophore Alexa488 as a cargo in their in vitro transport assays, and it was efficiently imported by Imp13 (Mingot et al., 2001). Therefore, Ubc9 was cloned as a GST-fusion protein followed by purification. It was subsequently labeled with Alexa488 to have a read out for flow cytometry or microscopy. First, control experiments were performed to optimize the cargo/transport receptor ratio for maximal dependence on Ran, and it turned out that in the presence of 60nM cargo and 1μM Imp13, import was stimulated maximally when 10μM Ran wild type was used (data not shown). GST-Ubc9 was completely inactive in sumoylation assays (data not shown), and in order to prevent a dominant-negative effect of GST-Ubc9, the concentration was kept slightly lower than typical cargo concentrations in in vitro import assays. Next, the import assays were performed at constant cargo/Imp13 and increasing Ran concentrations (in a range where it is rate-limiting). Since the import levels are highly dependent on the amounts of Ran present in the system, recombinant Ran variants added to the cells were controlled tightly. This was done by directly comparing the concentrations of Ran preparations (Fig. 24B, left panel) as well as the total amounts of Ran in the actual experiment (Fig 24B, right panel). Of note, recombinant Imp13 amounts added were very comparable as well between the two samples tested (Fig 24B, right panel). Intriguingly, the results of the experiment showed that Ran mutant seemed more efficient to stimulate import than wild type Ran (Fig. 24A, dark blue columns).

7.2.4. The Ran triple mutant seems independent of NTF2 in Imp13-dependent import

To understand if Ran import itself is the reason for the different effects observed, I decided to add NTF2, the import receptor of Ran, to the in vitro import assays. NTF2 should accelerate the nuclear accumulation of Ran, which in turn increases the rates of recycling of import receptors leading to an increase in overall import levels. Therefore, it was interesting to see whether NTF2 would increase the import levels for both Ran wild type and the mutant. To answer this question, I performed in vitro import assays with Imp13, GST-Ubc9-Alexa, 12μM Ran variants in the presence and absence of 1.2μM NTF2 over a period of 30min. At different time points (10, 20, 30min) the reactions were stopped and analyzed by flow cytometry. Interestingly, the results showed that NTF2 stimulated Imp13-dependent import in the presence of 12μM Ran wt but not in the presence of Ran triple mutant (Fig. 25). It seemed that the kinetic advantage that was observed with Ran mutant could be leveled out for Ran wt by adding NTF2. It is surprising to observe that t
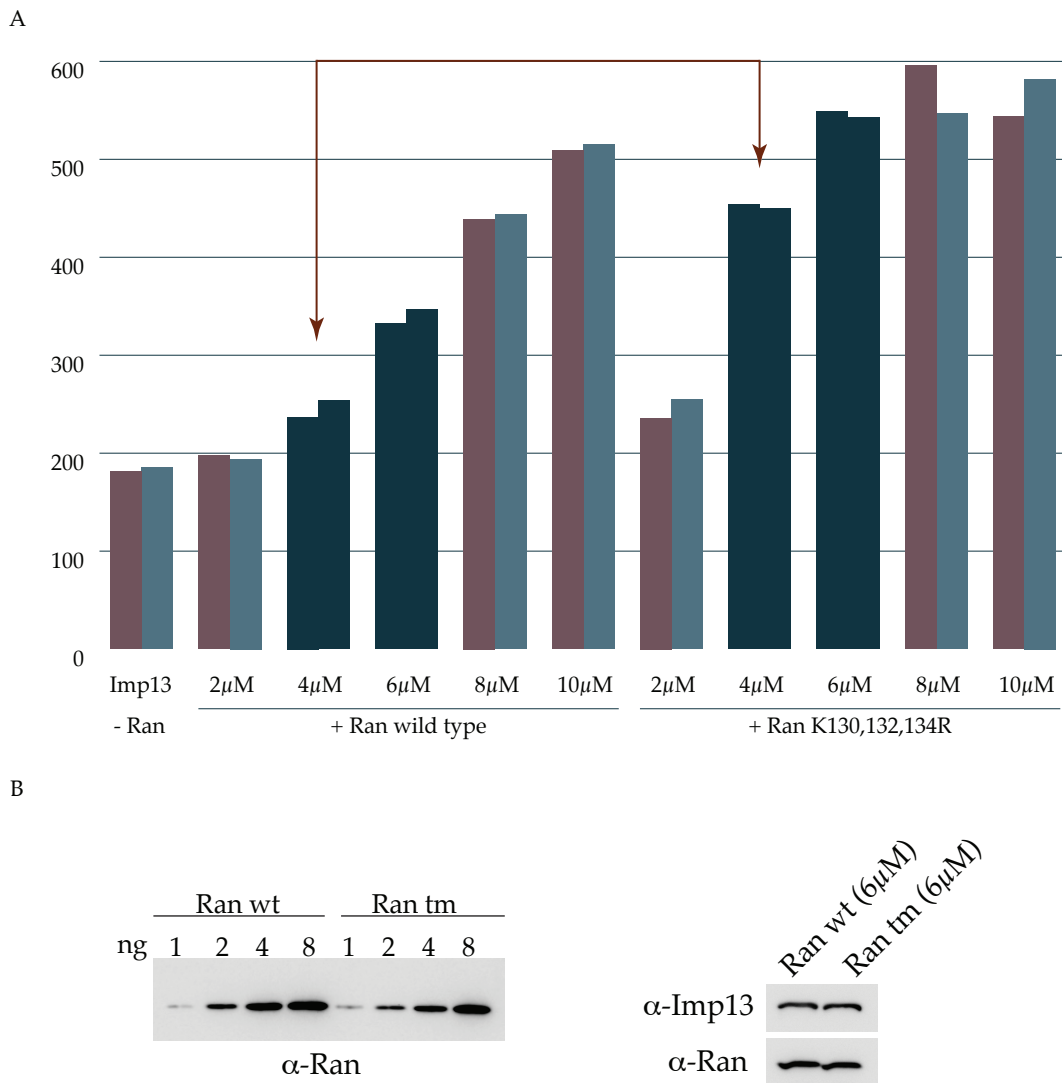
Fig. 24: The RanK130,132,134R is more efficient than wild type to stimulate Imp13-dependent import. In vitro import assays were carried out in duplicates with 1μM Imp13, 60nM GST-Ubc9-Alexa488, and differing concentrations of either RanWT or RanK130,132,134R (2μM-10μM) as indicated. Ran was omitted from the first sample as a control for background import. Transport reactions were incubated at 30°C for 30min, and were stopped by addition of 4mL transport buffer. The fluorescence was quantified by flow cytometry and represented as the mean value calculated from 10,000 cells. The two concentrations where the effect was the most prominent are highlighted with dark blue, and one of them is indicated by arrows. (B) Recombinant Ran wt and RanK130,132,134R protein stocks were titrated (1ng-8ng), and the signal intensities were compared after immunoblotting with anti-Ran antibodies (left panel). Transport mixes with 6μM Ran wt or Ran K130,132,134R were analyzed by immunoblotting with anti-Imp13 and anti-Ran antibodies to compare the total amounts of proteins present in both samples.

he import levels stimulated by Ran mutant were not further stimulated when NTF2 was present. The residues mutated (K130, 132, and 134) were not reported to be critical for RanGDP interaction with NTF2 as deduced from the crystal structure of the Ran*NTF2 complex (Stewart et al., 1998), which makes it unlikely that the interaction of Ran with NTF2 is changed due to the mutations. Therefore, the lack of stimulation of the import for Ran mutant must be due to another rate limiting event.
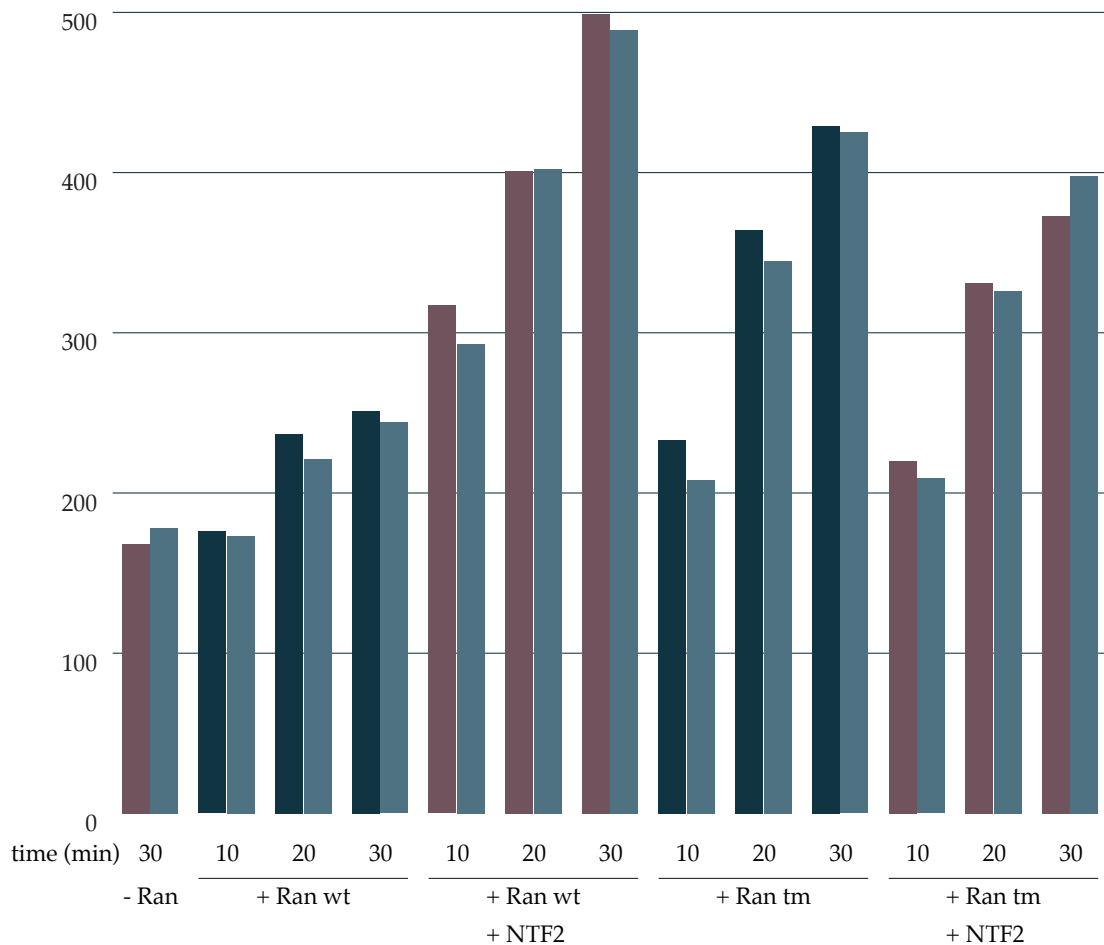
Fig. 25: NTF2 stimulates the in vitro import of GST-Ubc9-Alexa488 in the presence of RanWT but not RanK130,132,134R. Imp13-dependent import assays were carried out in duplicates with 1μM Imp13, 60nM GST-Ubc9-Alexa488, 12μM either RanWT or RanK130,132,134R. Where indicated, 1.2μM NTF2 was added to the reaction mix. Ran was omitted from the first sample as a control for background levels of import. Transport reactions were incubated at 30°C, and were stopped at indicated time points by addition of excess transport buffer. The fluorescence was quantified by flow cytometry and represented as the mean value calculated from 10,000 cells.

Chapter II: The mechanisms of intranuclear localization of SUMO E1 activating enzyme, Aos1/Uba2 heterodimer

A former PhD student in our lab, Marie Christine Moutty, investigated the mechanisms that cause the intranuclear localization of SUMO E1 activating enzyme, Aos1/Uba2 heterodimer. She discovered that both subunits of this enzyme have nuclear localization signals (NLSs), interact with Impα/β, and can be separately imported into the nucleus by the Impα/β heterodimer. By microinjecting the pre-assembled E1 complexes from the individual subunits (wild type or NLS-mutant) into HeLa cells, she also demonstrated that Impα/β can import the assembled E1 complex as well and recognizes the NLS of Uba2 in the context of the holo-enzyme.

Although the basic mechanism underlying the transport of the E1 heterodimer was resolved by Marie, several questions remained unanswered that needed to be addressed for revision of her manuscript. The first question was related to the role of transportin and Imp13 in Aos1 import since she observed that they interact with the immobilized Aos1 in a RanGTP-sensitive manner. The second question was whether recombinant Impα/β heterodimer recognizes the NLS of Uba2 in the context of the recombinant preassembled holo-enzyme. In an attempt to answer these two questions, I was able to show that Imp13 and transportin do not support the nuclear import of Aos1 alone. I was also able to show that recombinant Impα/β heterodimer interacts with the Aos1/Uba2 complex, and this interaction is mainly via the NLS of Uba2 rather than the NLS of Aos1 by gel filtration experiments. Together with my contribution, this study led to the publication "Impα/β mediates nuclear import of individual SUMO E1 subunits and of the holo-enzyme" (Moutty M.C., Sakin V., Melchior F., 2011 MBoC). A short summary of the biochemical analysis performed by me will be given in the following sections.

1. Generation of tools for in vitro import assays
In order to carry out import assays with Impα/β, Imp13, and transportin, the nuclear transport receptors and their respective model cargos were purified. For Imp13-dependent import assays, an expression plasmid for GST-Ubc9 was newly constructed followed by purification of the protein and labeling with Alexa488. For other import assays, Impα/β, Imp13, transportin, and YFP-M9 were purified and used in the following assays.

2. Neither transportin nor Importin 13 support the import of Aos1
In vitro transport assays clearly showed that neither transportin nor Imp13 was able to import CFP-Aos1 into the nucleus (Fig. 26 & Fig. 27A). However, it is known from the

literature that some transport receptors synergize to carry out the import of specific cargos. One example is the import of histone H1, which is carried out by the heterodimer of Imp β and Importin 7 (Jäkel et al., 1999). In line with this idea, I also tested whether Imp13 can synergize with Imp α/β for the import of CFP-Aos1. The results showed that Imp13 did not stimulate the import of CFP-Aos1 under rate-limiting concentrations of Impα/β, on the contrary, it inhibited the import (Fig 27B).
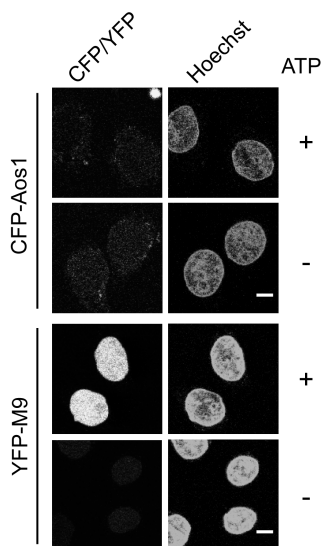
Fig. 26: Transportin does not mediate import of CFP-Aos1 in vitro. In vitro import of CFP-Aos1 (1µM) in semi-permeabilized HeLa cells was tested in the presence of Transportin (1µM) and 12 µM Ran with or without ATP. The transportin dependent cargo YFP-M9 (1µM) (Siomi and Dreyfuss, 1995; Nakielny et al., 1996) was included as a positive control. Nuclear accumulation of fluorescently labeled cargo proteins was analyzed by confocal microscopy. Bar, 10 µm.

3. Importin α/β binds to the Uba2 NLS of the SUMO E1 holo-enzyme

After showing that both subunits of the E1 heterodimer can separately be imported by the Impα/β heterodimer, Marie wanted to know whether the assembled dimeric E1 complex can be imported by Importin α/β as well. Microinjection of pre-assembled E1 complexes from the individual subunits (wild type or NLS-mutant) into HeLa cells demonstrated that Impα/β recognizes the NLS of Uba2 in the context of the holo-enzyme (Moutty et al., 2011). This finding suggested that in the assembled E1 heterodimer, the NLS of Aos1 is no longer accessible for complex formation with Imp α/β. In order to test this idea, I preformed E1 complexes with different variants of Aos1 and Uba2 (wt and NLS-mutants) and incubated them with 2-fold molar excess of Imp α/β. The formation of tetrameric complexes was then analyzed by analytical gel filtration. The results showed that when the NLS of Uba2 was intact, the tetrameric complex between E1 heterodimer and Imp α/β could form (Fig. 28B, compare panel 3 and 5). However, when the Uba2 NLS was mutated, complexes were no longer stable, although some residual interactions were still observed (Fig. 28B, compare panel 4 and 6). This is likely due to the high protein concentrations used in the experimental set-up. Overall, the results clearly demonstrated that in the stable E1 heterodimer, the Uba2 NLS is important and should be intact for the dimer to be recognized by Imp α/β. When the NLS is mutated, the interaction is mostly

lost, and the dimer is no longer imported by Imp α/β in vivo (Fig. 28B and Moutty et al., 2011)
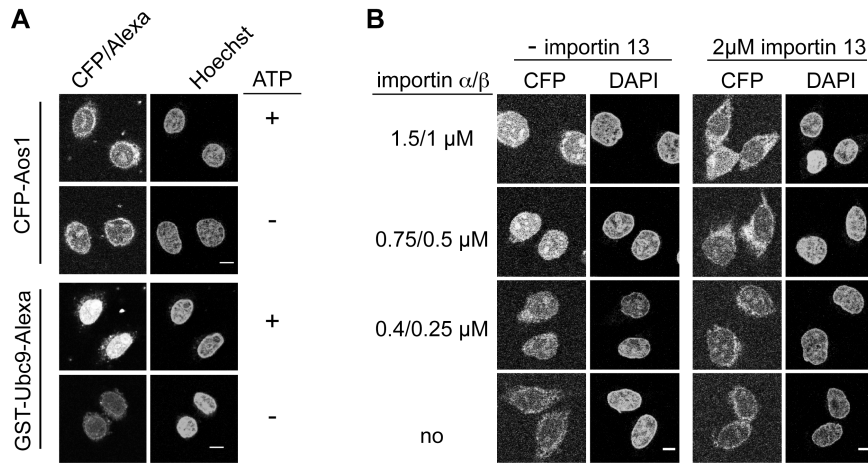
Fig. 27: Importin 13 does not support the import of CFP-Aos1 in vitro. (A) CFP-Aos1 (5 μM) import was tested in semi-permeabilized HeLa cells in the presence of importin 13 (1 μM) and Ran (12 μM) with or without ATP. Alexa488 labeled GST-Ubc9 (Mingot et al., 2001) served as a positive control. Nuclear accumulation of CFP-Aos1 and GST-Ubc9-Alexa488 was analyzed by fluorescence microscopy. Bar, 10 μm. (B) Importin 13 does not synergize with importin α/β for the import of CFP-Aos1. In vitro import of CFP-Aos1 (1μM) using semipermeabilized HeLa cells was performed with the indicated concentrations of Importin α and importin β in the presence of Ran (12μM), with or without addition of 2 μM importin13. Nuclear accumulation of CFP-Aos1 was analysed by confocal microscopy. Bar, 10μm.
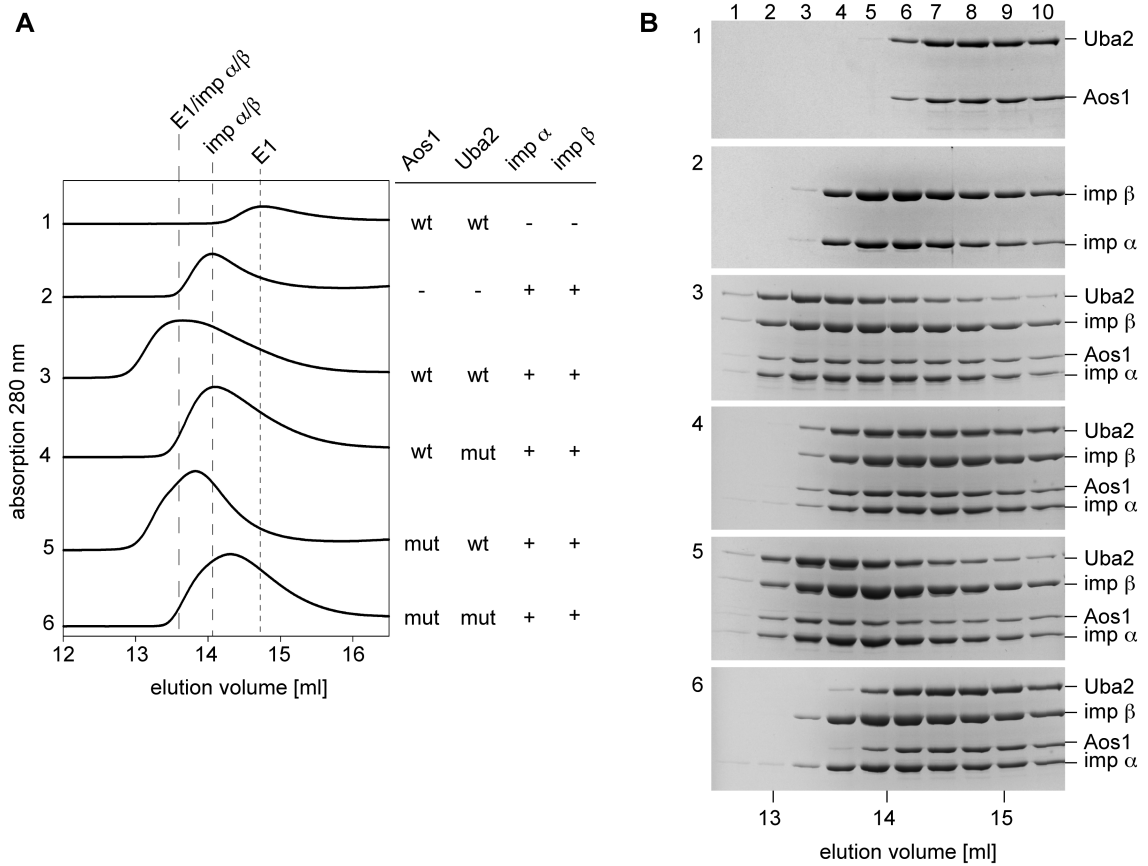
Fig. 28: Importin α/β binds to the Uba2 NLS of the SUMO E1 holo-enzyme. Wild-type and mutant CFP-Aos1/Uba2-YFP complexes (5 μM) were incubated with a twofold molar excess of importins α and β (10 μM each), and subjected to gel filtration. Aos1 mut, Aos1-KR195,196A2; Uba2 mut, Uba2-KR623,624A2. (A) Elution profies from the Superose 6-HR10/30 column were recorded by the Äkta purifier system (GE Healthcare), and processed with sigma plot 8.02 (SystatSoftware). (B) Fractions were analyzed by SDS–PAGE and Coomassie staining.

DISCUSSION

The aim of this thesis was to test whether nuclear transport receptors and Ran are subject to sumoylation, to test whether RanBP2 is the responsible E3 ligase, and to further investigate the mechanisms as well as the functional consequences of this modification. In this work, I could confirm the endogenous sumoylation of several nuclear transport receptors and provide evidence that Ran can be sumoylated in the context of semi-permeabilized cells. I went on to map the SUMO acceptor sites, and discovered that mutation of these sites results in stimulation of a specific transport pathway, which is Imp13-dependent. Intriguingly, the sumoylation deficient mutant loses dependency on the transport factor NTF2, suggesting that it may enrich in the nucleus by other means.

In addition to the main course of my PhD work, I could also show that the import of the SUMO E1 enzyme subunit, Aos1, is not supported by transportin or Imp13, and could demostrate that Imp α/β interacts mainly via the NLS of Uba2 in the context of the E1 heterodimer. These findings complemented the work by Dr. Marie Christine Moutty and were included in the publication "Imp α/β mediates nuclear import of individual SUMO E1 subunits and of the holo-enzyme" (Moutty M.C., Sakin V., Melchior F., 2011 MBoC).

The findings presented in this work open up interesting aspects concerning the regulation of nucleocytoplasmic transport, some of which will be discussed in detail in the following sections.

1. Heat shock and transport receptor sumoylation

As mentioned earlier, heat shock increases globally the sumoylation of proteins especially with SUMO2/3 (Saitoh and Hinchey, 2000). A couple of proteomic screens utilized this fact to identify sumoylated proteins that are heat shock-dependent. In two of these screens, several nuclear transport receptors (Impβ, Imp5, Crm1, Impα, Imp4, CAS, and Imp7) were identified as putative SUMO substrates (Golebiowski et al., 2009; Bruderer et al., 2011). Here, endogenous sumoylation could be confirmed for three nuclear transport receptors: Impβ, Imp5, and Crm1. Impα, CAS, and Imp7 could not be confirmed whereas Imp4 could not be tested due to lack of good antibodies. There might be several explanations for this: First, these proteins may not be sumoylated in vivo. In this work, cells were lysed under denaturing conditions in the presence of 1% SDS, and the SUMO IPs were performed under RIPA buffer conditions. However, it was still possible to observe the unmodified nuclear transport receptors in the eluates although they were much less compared to the input samples (see Fig. 6D). Since the IP or the pulldown conditions in the above-mentioned studies were not more stringent than the conditions

used in this work, unmodified transport receptors could have been sticking to the bead materials as is the case in my own work. Another explanation might be that although it takes 1-2 hours for the cells to recover completely after heat shock as judged by the the general sumoylation pattern for SUMO2/3 (Golebiowski et al., 2009), the recovery period might differ among different proteins. It might be that for certain nuclear transport receptors the sumoylation period is very brief, and therefore the protein is rapidly desumoylated as soon as heat shock stress is removed, which makes sumoylated receptors difficult to capture. Last but not least, the antibodies used for Impα, CAS, and Imp7 might be not sensitive enough to detect the sumoylated transport receptors. Although I could confirm the sumoylation of Impβ, Imp5, and Crm1, none of the receptors seemed to be dependent on heat shock to be sumoylated. On the contrary, all three receptors were found to be better mono- or multi-sumoylated at 37°C. One explanation for the lack of signal for the sumoylated transport receptors might be SUMO2/3 chain formation on receptors, which may lead to high molecular weight species get stuck in the stacking gels. Since the stacking gels were not probed with the antibodies in this work, the signal was simply not detected.

Although it is well-documented in the field that heat shock increases SUMO2/3 conjugation globally, functional consequences of this modification remained elusive. One possible outcome of heat shock-dependent polysumoylation might be the degradation of proteins that are denatured due to heat shock. In this likely scenario, the dimeric RING ubiquitin E3 ligase RNF4, which recognizes polysumoylated targets and ubiquitinates them for proteasomal degradation (Tatham et al., 2008; Plechanovova et al., 2011), might play a role for the ubiquitination of proteins to be degraded. In order to adress the role of heat shock-dependent sumoylation, more careful analysis is needed. SUMO IPs from cells either treated with proteasome inhibitors such as MG132 or knocked down for RNF4 might be useful to adress the question of whether several proteins are also ubiquitinated following heat shock. Simultaneous ubiquitination and sumoylation of transport receptors would result in very high molecular weight species, which should be taken into consideration during analysis.

2. Functional consequences of nuclear transport receptor sumoylation

In this work, three important transport receptors, Impβ, Imp5, and Crm1, are confirmed to be endogenously sumoylated in HeLa cells. However, the functional consequences of this modifications currently remain a mystery. Interestingly, towards the end of this work the first example of nuclear transport receptor regulation by sumoylation was shown in yeast (Rothenbusch et al., 2012). Rothenbusch and her colleagues discovered that Kap114p (Imp9 homolog in yeast), is sumoylated in Mms21-dependent manner in the nucleus. This

modification synergizes with RanGTP to dislocate the cargo from Kap114p (Pemberton et al., 1999; Greiner et al., 2004; Caesar et al., 2006) (see also the model in Fig. 29B). Another mechanism of regulation of cargo release was shown previously for TATA-binding protein (TBP), which is taken to the nucleus by Kap114p-mediated import. In this case, TATA-containing DNA, which is the target binding partner of TBP protein, stimulated the Gsp1-mediated dissociation of TBP from Kap114p (Pemberton et al., 1999). Such examples clearly showed that for some transport pathways, additional factors such as intranuclear interaction partners, or PTMs are required for efficient cargo release from import receptors. Rothenbusch and her colleagues also suggested that such a regulatory mechanism would serve to function as an intranuclear targeting of the cargos carried by Kap114p if sumoylation occurs at a distinct site in the nucleus where the cargo protein is spatially required. In this likely scenario, transport receptor Kap114p would function as a nuclear chaperone, which prevents the immediate unselective dissociation of the cargo protein upon nuclear entry. In fact, the idea that nuclear transport receptors might function as chaperones was previously suggested especially for the cargo proteins having exposed basic domains such as histone or ribosomal proteins which tend to aggregate or stick to other anionic proteins when not escorted by chaperones (Jäkel et al., 2002). In analogy to Kap114p regulation by sumoylation, it is intriguing to speculate that Impβ and Imp5 that were shown to be sumoylated in this work, are regulated in a similar manner. Interestingly, the two import receptors as well as Imp9 (Kap114p homolog in mammals) function in the nuclear import of core histones during the S-phase of the cell cycle, when the cell produces and imports vast amounts of histone proteins for the replicating DNA (Mühlhäusser et al., 2001). Therefore, it is very tempting to speculate that sumoylation of nuclear import receptors might be a general mechanism that is required for the controlled release of cargo proteins, which otherwise tend to interact with the proteins of the nuclear compartment in an unspecific manner, or with each other leading to aggregation. If this is the case, it is likely that Impβ and Imp 5 are sumoylated during S-phase, when their import activity is required most. Given that very low steady state sumoylation can be observed for Impβ and Imp5, it would be interesting to test whether sumoylation of transport receptors is stimulated during S-phase. This idea can be tested by synchronizing HeLa cells e.g., by double thymidine block and 2 hour release in S-phase followed by SUMO IPs. If sumoylation is S-phase dependent, the sumoylated import receptors should be readily captured. Overall, it seems to be a likely mechanism to sumoylate certain import receptors to have a controlled release of some cargos depending on the needs of the cell at a specific cell cycle stage.

A

B
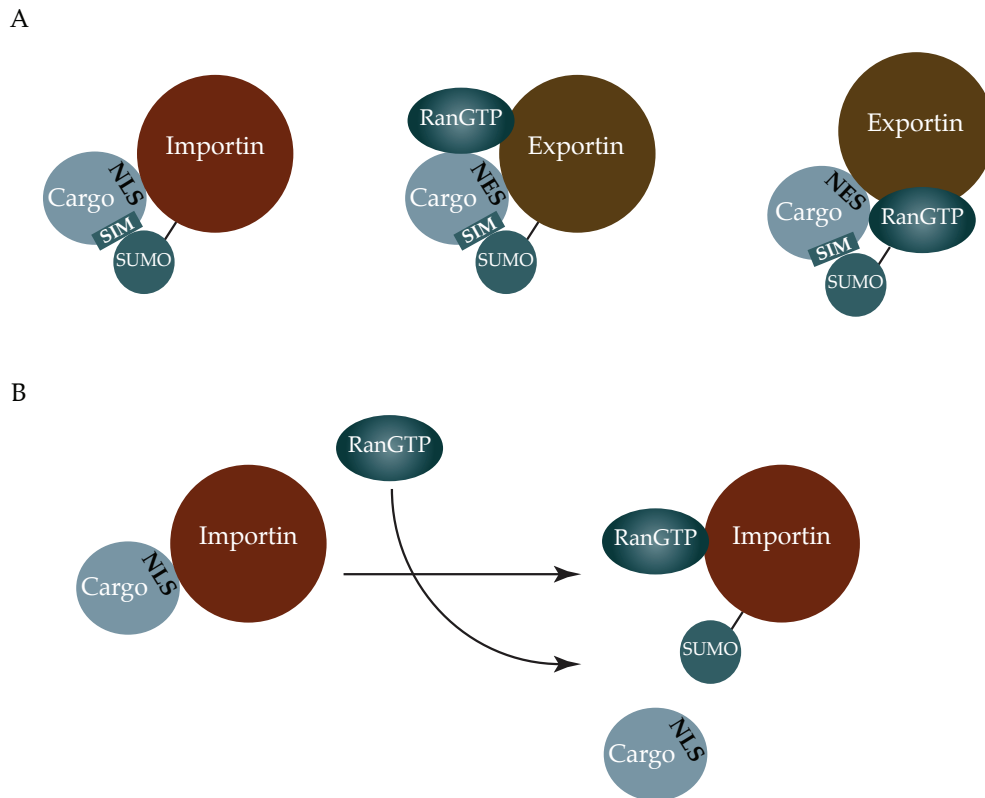
Fig. 29: Possible molecular consequences of sumoylation of nuclear transport receptors and the small GTPase Ran. (A) Sumoylation of transport receptors or Ran might be a mechanism to promote the assembly of import or export complexes by selecting certain cargos with SUMO-interaction motifs (SIMs) for transport. (B) Sumoylation of import receptors in concert with RanGTP might be a mechanism to distrupt the import complexes. The first example for such mechanism was documented by Rothenbusch and her colleagues (Rothenbusch U. et al., 2012).

Another possible function for import receptor sumoylation would be to promote the assembly of certain cargos with SUMO interactions motifs (SIMs) into import complexes (see Fig. 29A). In this scenario, the cargo NLS-import receptor interaction is not sufficient to form stable import complex, and sumoylation of the import receptor increases the stability by introducing another interaction surface via SUMO-SIM interactions. This mechanism would provide a reversible way of controlling the import of SIM-bearing cargos if the import is required only under certain circumstances.

Crm1, on the other hand, is an export receptor, and the proposed model for the regulation of Impβ and Imp5 by sumoylation would not directly apply for it since RanGTP stimulates the interaction of Crm1 with its NES substrates. However, mechanistically, it would be possible to imagine that the dissociation of certain Crm1 substrates in the cytoplasmic compartment is regulated by Crm1 sumoylation. In order for such a scenario to happen, RanGTP hydrolysis by itself should not suffice for the trimeric export complex to fall apart, which in turn requires a strong Crm1-cargo interaction even in the absence of

RanGTP. However, most NES-cargos have relatively weak affinities towards Crm1, and in the absence of RanGTP they do not bind stably. So far, only two cargos with an unusual strong affinity towards Crm1 were identified: Snurportin and Nmd3. Both proteins bind to Crm1 with affinities that are 100-fold higher than the typical cargo such as the Rev protein (Paraskeva et al., 1999; Thomas and Kutay, 2003). However, they can still be dissociated from Crm1 by RanGTP hydrolysis. A cargo with even stronger affinity towards Crm1 was described in an artificial NES peptide. This peptide was named „supraphysiological NES" since it did not require RanGTP for Crm1 association (Engelsma et al., 2004). However, this peptide accumulated at nuclear envelopes in vivo, arguing that such a strong interaction between NES cargoes and Crm1 would be physiologically irrelevant. Interestingly, the first example of a protein that has a very strong affinity towards Crm1 was recently identified in parvovirus minute virus of mice (MVM) (Engelsma et al., 2008), which proved the existence of supraphysiological NESs in nature. In line with this finding, it is possible to imagine that sumoylation of Crm1 by the RanBP2 complex at NPCs might act in concert with RanGTP hydrolysis to stimulate the dissociation of certain cargo proteins having a higher affinity for the receptor. Moreover, there is an usually strong affinity between Crm1 and RanBP2, and the two proteins co-IP from mitotic HeLa cell extracts (personal communication, Dr. Annette Flotho). However, whether RanBP2 complex is the relevant E3 ligase for Crm1 and whether the strong interaction between these two proteins contribute to the sumoylation of Crm1 by the RanBP2 complex requires further investigations.

Crm1 is responsible for the export of a great variety of proteins and ribonucleoprotein particles (Hutten and Kehlenbach, 2007). Considering the relatively simple nature of the NESs that can be recognized by Crm1, it is difficult to explain the wide plethora of cargos that Crm1 can interact with. It has been shown that modifications of several cargo proteins regulate the Crm1-dependent export events. For example, phosphorylation of cyclin D1 stimulates Crm1-dependent export, whereas phosphorylaton of c-Fos inhibits the export of this transcription factor (Benzeno et al., 2006; Sasaki et al., 2006). Besides the regulation at cargo level, there are also examples for the regulation at the transport receptor level. For example, Impα is known to be phosphorylated and acetylated, which might regulate the interactions with its respective cargos (Azuma et al., 1997; Zou et al., 2008). In a similar manner, sumoylation of Crm1 might be yet another regulation that is important for cargo selection. One intriguing idea is that cargo proteins with SUMO interaction motifs (SIMs), which are short stretches of hydrophobic amino acids, might be selected specifically by sumoylation of Crm1 (see the Fig. 29A, middle panel). This way,

upon specific stimuli, the export of certain cargoes can be selected for Crm1-dependent export via the sumoylation of Crm1 itself.

3. Mechanistic aspects of Ran sumoylation

3.1. Where does Ran sumoylation occur? Is it dependent on the RanBP2 complex?

In this work, we showed that Ran is sumoylated in semi-permeabilized cells on one or several of the three lysine residues that could be mapped. However, where modification happens and the physiologically relevant E3 ligase still remain unknown. Recombinant Ran in semi-permeabilized cells can diffuse or be actively imported into the nucleus by residual NTF2, which makes both the cytoplasm and the nucleus likely locations where sumoylation might occur. Moreover, E3 ligases are known in both compartments. Given the fact that stimulation of the active import of Ran by adding NTF2 in semi-permeabilized cells did not result in any increased levels of Ran sumoylation (data not shown), both locations remain equally likely. Ran is either sumoylated in the cytoplasm or it goes through the nuclear pores and get sumoylated in the nucleus, more likely in GTP-bound conformation. In vitro sumoylation reactions with semi-permeabilized cells in the presence of fusion proteins of Ran, which can no longer passively diffuse through the nuclear pores in combination with wheat germ agglutinin (WGA) treatment of cells to block the active import, would be helpful to adress this question.

Current evidence obtained in this work strongly suggests that sumoylation of Ran in semi-permeabilized cells is an E3-ligase dependent reaction due to the inefficient sumoylation of Ran with E1 and E2 only. There are mainly two possible candidates for SUMO E3 ligase activity: RanBP2 complex and PIAS E3 ligases. The RanBP2 complex as well as an isolated fragment of it stimulated the in vitro sumoylation of Ran very efficiently. Since RanBP2 protein is cytoplasmic, there are two possible scenarios how Ran can interact with it: Either on its way to the nucleus when it is in complex with NTF2 or on its way to cytoplasm in complex with different transport receptors. Neither complex formation with NTF2 (data not shown) nor with transport receptors prevent the sumoylation of Ran, which makes both scenarios equally likely. PIAS proteins, on the other hand, are mostly nuclear (Liu et al., 2001; Sachdev et al., 2001; Kotaja et al., 2002; Miyauchi et al., 2002), and several of them tested did not stimulate the sumoylation of Ran in vitro. Taken together, although we can not formally exclude the PIAS proteins, the RanBP2 complex seems to be the most likely E3 ligase for the sumoylation of Ran. For the clarification of this issue, it would be helpful to identify the localization of Ran sumoylation in semi-permeabilized cells which would provide indirect evidence concerning the relevant E3 ligase. Ultimate proof would require in vitro sumoylation assays with semi-permeabilized cells knocked down for RanBP2.

3.2. Sumoylation sites in Ran: K130,132, and 134

For the identification of sumoylation sites in Ran, the in vitro sumoylation of RanGTP with RanBP2 fragment was carried out at large scale and subjected to mass spectrometry, which revealed three critical lysine residues as SUMO target sites. Mutation of all three sites resulted in clear reduction in sumoylation of Ran in semi-permeabilized cells. However, it is currently not clear whether all three lysines contribute equally to the sumoylation of Ran since single mutants were not tested in this system. In vitro sumoylation of Ran triple mutant in GTP-bound conformation with RanBP2 fragment and the RanBP2 complex, on the other hand, did not abolish or diminish sumoylation (Fig. 18). This observation can be explained by the presence of many surrounding lysines in Ran and the strong interaction between RanGTP and Ran-binding domains of RanBP2 fragment. In cells, the residence time of RanGTP on RanBP2 complex is limited by RanGAP1, which hydrolyzes RanGTP. Our in vitro sumoylation system with recombinant proteins, however, lacked RanGAP1. This, in turn, increases the residence time of Ran on RanBP2 dramatically, and under such circumstances it seems that RanBP2 starts unspecifically sumoylating surrounding lysine residues available.

Recently, another member of our lab Tobias Winter in collaboration with Dr. Thomas Ruppert could repeat the identification of sumoylation sites in Ran by mass spectrometry following in vitro sumoylation of RanQ69L by the physiologically relevant RanBP2 complex. Interestingly, the analysis revealed two lysine residues this time: K134 and K159. K134 had a higher peptide score in the mass spectrometric analysis compared to K159 and was also found in the previous analysis. Therefore, it is very likely that the major sumoylation site in Ran is K134. In light of the current findings, it would be now interesting to test the single and double mutants for K134/K159 in semi-permeabilized cells for sumoylation.

4. Functional Aspects of Ran sumoylation

4.1. Ran sumoylation in mammals

In this work, we showed that the sumoylation-deficient Ran triple mutant stimulated Imp13-dependent import more efficiently compared to wild type, and the effect was not observed with Imp α/β-dependent import. Currently, it is unclear why the Ran triple mutant is more efficient to stimulate Imp13-dependent import. Is it the lack of sumoylation of Ran, or is it the K-to-R mutations per se which can change the interactions of Ran or other PTMs that might be involved? There are several effectors of Ran, which are critical for the nucleocytoplasmic transport cycle. Although not fully covered, pulldown assays suggested that there is no change in the interaction of Ran and NTF2 or

RCC1 due to three mutations introduced (Fig. 21). Concerning other interactors of Ran, even though the experimental data is currently missing, a rational guess can be made from all the crystal structures available such as Ran in complex with Ran-binding proteins, nuclear transport receptors, or nucleoporins. None of the three lysines identified belong to the switch I, switch II, or the C-terminal acidic tail region or were reported to play a significant role in the interaction of Ran with NTF2, Imp13 or RanBD (Stewart et al., 1998; Seewald et al., 2002; Grünwald and Bono, 2010). On the other hand, RCC1 and RanGAP1 seem to interact with one of the three lysines identified by mass spectrometry: the Ran-RCC1 interaction is mediated via several aminoacid contacts (24 aa.), among which is K134 of Ran (Renault et al., 2001). This residue may contribute to the interaction by salt bridges, which should not be abolished with the arginine mutations if the atomic distances are comparable. Interestingly, one of the lysine residues identified, K130, seems to be clashing with RCC1 in the complex. Upon RCC1 binding, due to this steric clash, the residues between 129-142 are repositioned resulting in the release of the acidic tail of Ran from the G domain (Renault et al., 2001). The very same residue, on the other hand, was reported to be involved in ionic interactions with Asp225 of RanGAP1, which was shown to contribute to the overall reactivity of RanGAP1 (Seewald et al., 2002). Overall, although it seems unlikely that the affinities between Ran and its effectors including RCC1 and RanGAP1 are affected dramatically by three arginine mutations considering the experiments with Impα/β and the structural information available, it would still be very useful to determine the Kd values of the interaction of the Ran mutant with RCC1 and RanGAP1. Moreover, determination of the rate of nucleotide-exchange by RCC1 and GTP hydrolysis by RanGAP1 in the presence of Ran mutant would be extremely helpful to understand the contribution of the three lysines to Ran biology. Although the structural data suggested that the three lysines do not play a major role in Ran-Imp13 interaction, it is still worthwhile to determine the affinities between Ran variants and Imp13 quantitatively, since this is the major difference between two transport pathways tested.

In order to test whether it is the lack of sumoylation that results in the stimulation of Imp13-dependent pathway, I tried to manipulate in vitro import assays by adding the components of sumoylation machinery or by blocking isopeptidases. However, import levels were not affected by such modifications to the system (data not shown), which argues against the role of sumoylation in this particular pathway. If sumoylation plays a role, it must slow down the recycling of Imp13 by any means. Although we have no evidence, one explanation might be related to the unique feature of Imp13. As mentioned previously, it works as a bidirectional transport receptor. While it imports Ubc9, as an export receptor, it carries the translation initiation factor, eIF1A, to the cytoplasm (Mingot et al., 2001). Currently it is not known whether Imp13 exits the nucleus as a dimeric

complex with RanGTP or as a trimeric complex with eIF1A in addition. Of note, it would be extremely useful to determine the association/dissociation constants for the interaction of RanGTP with Imp13 in the presence and absence of an export cargo, eIF1A, to adress the question. Although unlikely, if trimeric complex formation is an absolute requirement for Imp13 to leave the nucleus, sumoylation of Ran might interfere with it whereas sumoylation-deficient Ran would stimulate it. Since for nuclear export, formation of the export compex is the rate limiting step (Kehlenbach et al., 2001), sumoylation of Ran would decelerate the recycling of Imp13. This scenario might be a way of keeping Imp13 nuclear and blocking its export pathway by Ran sumoylation. Overall, how and why should Ran sumoylation slow down or block Imp13-dependent export remains as a challenge to explain.

Another interesting observation in this work was that Ran triple mutant was not responsive to the presence of NTF2 in terms of stimulating the Imp13-dependent import whereas Ran wild type-dependent stimulation was increased in the presence of NTF2 (Fig. 25). One possible explanation could be that nuclear accumulation of Ran triple mutant by simple or facilitated diffusion is faster or more effective than the Ran wild type. The Ran triple mutant would thus reach nuclear concentrations required to stimulate the Imp13-dependent in the absence of NTF2. Why Ran mutant may diffuse more effectively than the wild type remains elusive. One reason might be that the mutant is more effective due to the lack of PTMs such as sumoylation or acetylation via one of the three lysines mutated if these PTMs play a role in slowing down the diffusion of Ran wild type. It is possible that post-translationally modified Ran has different affinities towards its interactors, which might slow down its diffusion. Although theoretically it is possible, it is not known whether the semi-permeabilized cell system supplemented only with ATP is able to provide acetylation or sumoylation. Another possibility is that due to the three mutations introduced to Ran, the mutant might be kept in nucleus more efficiently. This can be achieved by increased interactions between Ran mutant and Imp13 or Rcc1 or any other Ran interactors in the nucleus, which in turn help Ran mutant accumulate in the nucleus faster. In order to shed some light to this issue, Ran import by NTF2 should be analyzed by in vitro import assays with fluorescently-labeled Ran to see if NTF2 can import both proteins comparably. The effect of NTF2 also needs to be tested in another import pathway such as Imp α/β- or transportin-dependent import to see if the effect is similar. As mentioned previously, quantitative data concerning the interaction between Ran and certain transport receptors including Imp13 and Impβ would also be very helpful to figure out the underlying mechanism for the differential effects of Ran wild type and the mutant.

Another intriguing idea concerning the function of Ran sumoylation would be that sumoylation of Ran might be used as a mechanism to promote the export complex assembly in a model similar to transport receptors sumoylation (see Fig. 29A) . In this model (Fig. 29A, right scheme), the interaction between export receptor and cargo is too low to stimulate stable export complex formation, and Ran sumoylation is used to select cargos with SIMs, which in turn contributes to the stability via SUMO-SIM interactions. As suggested for transport receptor sumoylation, this mechanism would provide a reversible way of controlling the export of SIM-bearing cargos if the export is required only under certain circumstances.

Although not investigated during the course of this work, Ran sumoylation might be involved in regulating mitosis-specific interactions since RanGTP is a key player of mitotic spindle formation as well as nuclear envelope reassembly (Kalab and Heald, 2008). Spindle formation is regulated in a mechanistically similar way to nucleocytoplasmic transport. RanGTP releases microtubule regulators such as TPX2 and NuMA from the inhibitory effect of Impβ by interacting with the transport receptor in the vicinity of chromosomes, thereby leading to the formation of microtubules in a spatially-regulated manner (Kalab and Heald, 2008). Ran sumoylation can be envisioned to play a role for certain cargo release or assembly processes, which might be otherwise inefficient. Although the molecular mechanisms how Ran is involved in nuclear envelope reassembly is not well-understood, since sumoylation changes molecular interactions, it would not be so surprising to see if such a regulation is involved for the fusion of nuclear membranes to reform the nuclear envelopes.

4.2. Ran sumoylation in *A.nidulans*

Ran as well as all three lysines are conserved throughout evolution from yeast to mammals. In order to understand the importance of these lysines, we turned to a lower organism, namely *A.nidulans*, where the wild type protein can be replaced with the triple mutant to see the effects on cell growth. For this purpose, a collaboration with Prof. Gerhard Braus (Institute of Microbiology & Genetics, University of Göttingen), who is working with the model organism *A.nidulans*, has been initiated. The preliminary experiments with *A.nidulans* strains which are replaced with the mutant variant of Ran, showed a drastic phenotype with respect to asexual development, whereas sexual development was not effected (personal communication, Rebekka Harting/Prof.Gerhard Braus's lab). In short, the number of asexual spores formed with the mutant strain was significantly lower compared to the wild type strain, and interestingly, similar results were observed with SUMO-knock-out strains. The preliminary results suggest that the

identified lysines are important for the biology of Ran, although not essential since all the strains with the mutant variant were viable. Whether the observed phenotype is linked to the sumoylation or other lysine modifications such as acetylation needs to be further investigated.

5. Outlook

The results of the present work opened up two interesting research areas: The sumoylation of nuclear transport receptors and the small GTPase Ran in mammals & *A.nidulans*. Endogenous sumoylation of nuclear transport receptors shown in this work provides the first clear demonstration of nuclear transport receptor sumoylation in mammals. It was previously shown in yeast that Kap114p (yeast homolog of Imp9) is regulated by sumoylation (Rothenbusch et al., 2012). However, it remains an open question whether sumoylation of nuclear transport receptors serve a similar function in higher organisms or whether it has different functional consequences. Therefore, additional work is required to pinpoint the E3 ligase(s) responsible for this modification as well as to understand the mechanisms, localization, and the outcome of nuclear transport receptor sumoylation.

Similarly, Ran sumoylation presented in this work is at its infancy. Despite the fact that the SUMO sites in Ran were mapped and an interesting transport-related phenotype was observed with the triple mutant of Ran that can no longer be sumoylated, detailed analysis is still required to understand why the mutant Ran is more active than the wild type for Imp13-dependent import. Whether the differential behaviour of Ran is due to the lack of sumoylation or due to the K-to-R mutations remains elusive. Together, these investigations will help us gain important insights concerning the novel regulation of the small GTPase Ran by sumoylation.

REFERENCES

Adam, S.A. (2001). The nuclear pore complex. Genome Biol *2*, REVIEWS0007.

Adam, S.A., Marr, R.S., and Gerace, L. (1990). Nuclear protein import in permeabilized mammalian cells requires soluble cytoplasmic factors. J Cell Biol *111*, 807–816.

Alkuraya, F.S., Saadi, I., Lund, J.J., Turbe-Doan, A., Morton, C.C., and Maas, R.L. (2006). SUMO1 haploinsufficiency leads to cleft lip and palate. Science *313*, 1751.

Andrade, M.A., Petosa, C., O'Donoghue, S.I., Müller, C.W., and Bork, P. (2001). Comparison of ARM and HEAT protein repeats. J Mol Biol *309*, 1–18.

Azuma, Y., Takio, K., Tabb, M.M., Vu, L., and Nomura, M. (1997). Phosphorylation of Srp1p, the yeast nuclear localization signal receptor, in vitro and in vivo. Biochimie *79*, 247–259.

Baake, M., Bäuerle, M., Doenecke, D., and Albig, W. (2001). Core histones and linker histones are imported into the nucleus by different pathways. Eur. J. Cell Biol. *80*, 669–677.

Baba, D., Maita, N., Jee, J.-G., Uchimura, Y., Saitoh, H., Sugasawa, K., Hanaoka, F., Tochio, H., Hiroaki, H., and Shirakawa, M. (2005). Crystal structure of thymine DNA glycosylase conjugated to SUMO-1. Nature *435*, 979–982.

Bayer, P., Arndt, A., Metzger, S., Mahajan, R., Melchior, F., Jaenicke, R., and Becker, J. (1998). Structure determination of the small ubiquitin-related modifier SUMO-1. J Mol Biol *280*, 275–286.

Bayliss, R., Leung, S.W., Baker, R.P., Quimby, B.B., Corbett, A.H., and Stewart, M. (2002). Structural basis for the interaction between NTF2 and nucleoporin FxFG repeats. Embo J *21*, 2843–2853.

Beck, M., Förster, F., Ecke, M., Plitzko, J.M., Melchior, F., Gerisch, G., Baumeister, W., and Medalia, O. (2004). Nuclear pore complex structure and dynamics revealed by cryoelectron tomography. Science *306*, 1387–1390.

Beck, M., Lucić, V., Förster, F., Baumeister, W., and Medalia, O. (2007). Snapshots of nuclear pore complexes in action captured by cryo-electron tomography. Nature *449*, 611–615.

Benzeno, S., Lu, F., Guo, M., Barbash, O., Zhang, F., Herman, J.G., Klein, P.S., Rustgi, A., and Diehl, J.A. (2006). Identification of mutations that disrupt phosphorylation-dependent nuclear export of cyclin D1. Oncogene *25*, 6291–6303.

Bernier-Villamor, V., Sampson, D.A., Matunis, M.J., and Lima, C.D. (2002). Structural basis for E2-mediated SUMO conjugation revealed by a complex between ubiquitin-conjugating enzyme Ubc9 and RanGAP1. Cell *108*, 345–356.

Birnboim, H.C., and Doly, J. (1979). A rapid alkaline extraction procedure for screening recombinant plasmid DNA. Nucleic Acids Res. *7*, 1513–1523.

Bischoff, F.R., and Ponstingl, H. (1991). Catalysis of guanine nucleotide exchange on Ran by the mitotic regulator RCC1. Nature *354*, 80–82.

Bischoff, F.R., Klebe, C., Kretschmer, J., Wittinghofer, A., and Ponstingl, H. (1994). RanGAP1 induces GTPase activity of nuclear Ras-related Ran. Proc Natl Acad Sci USA *91*, 2587–2591.

Blomster, H.A., Hietakangas, V., Wu, J., Kouvonen, P., Hautaniemi, S., and Sistonen, L. (2009). Novel proteomics strategy brings insight into the prevalence of SUMO-2 target sites. Mol Cell Proteomics *8*, 1382–1390.

Bohren, K.M., Nadkarni, V., Song, J.H., Gabbay, K.H., and Owerbach, D. (2004). A M55V polymorphism in a novel SUMO gene (SUMO-4) differentially activates heat shock transcription factors and is associated with susceptibility to type I diabetes mellitus. J Biol Chem *279*, 27233–27238.

Bonner W.M. (1978). Protein migration and accumulation in nuclei. In Busch,H. (ed.), The Cell Nucleus. Vol. 6, Part C. Academic Press, New York, NY, pp. 97–148.

Bourne, H. R., D. A. Sanders, and F. McCormick. (1991). The GTPase superfamily: conserved structure and molecular mechanism. Nature (Lond.). 349:117-127.

Bradford M.M. (1976). A rapid and sensitive method for the quantitation of microgram quantities of protein utilizing the principle of protein-dye binding Anal Biochem. 1976 May 7;72:248-54.

Braschi, E., Zunino, R., and McBride, H.M. (2009). MAPL is a new mitochondrial SUMO E3 ligase that regulates mitochondrial fission. EMBO Rep *10*, 748–754.

Bruderer, R., Tatham, M.H., Plechanovova, A., Matic, I., Garg, A.K., and Hay, R.T. (2011). Purification and identification of endogenous polySUMO conjugates. EMBO Reports.

Caesar, S., Greiner, M., and Schlenstedt, G. (2006). Kap120 functions as a nuclear import receptor for ribosome assembly factor Rpf1 in yeast. Mol Cell Biol *26*, 3170–3180.

Cheng, C.-H., Lo, Y.-H., Liang, S.-S., Ti, S.-C., Lin, F.-M., Yeh, C.-H., Huang, H.-Y., and Wang, T.-F. (2006). SUMO modifications control assembly of synaptonemal complex and polycomplex in meiosis of Saccharomyces cerevisiae. Genes Dev *20*, 2067–2081.

Chi, N.C., Adam, E.J., Visser, G.D., and Adam, S.A. (1996). RanBP1 stabilizes the interaction of Ran with p97 nuclear protein import. J Cell Biol *135*, 559–569.

Conti, E., Müller, C.W., and Stewart, M. (2006). Karyopherin flexibility in nucleocytoplasmic transport. Curr Opin Struct Biol *16*, 237–244.

Cook, A., Bono, F., Jinek, M., and Conti, E. (2007). Structural biology of nucleocytoplasmic transport. Annu Rev Biochem *76*, 647–671.

Damelin, M., and Silver, P.A. (2000). Mapping interactions between nuclear transport factors in living cells reveals pathways through the nuclear pore complex. Mol Cell *5*, 133–140.

Dawlaty, M.M., Malureanu, L., Jeganathan, K.B., Kao, E., Sustmann, C., Tahk, S., Shuai, K., Grosschedl, R., and van Deursen, J.M. (2008). Resolution of sister centromeres requires RanBP2-mediated SUMOylation of topoisomerase IIalpha. Cell *133*, 103–115.

Desterro, J.M., Rodriguez, M.S., and Hay, R.T. (1998). SUMO-1 modification of IkappaBalpha inhibits NF-kappaB activation. Mol Cell *2*, 233–239.

Desterro, J.M., Rodriguez, M.S., Kemp, G.D., and Hay, R.T. (1999). Identification of the enzyme required for activation of the small ubiquitin-like protein SUMO-1. J Biol Chem *274*, 10618–10624.

Duprez, E., Saurin, A.J., Desterro, J.M., Lallemand-Breitenbach, V., Howe, K., Boddy, M.N., Solomon, E., de Thé, H., Hay, R.T., and Freemont, P.S. (1999). SUMO-1 modification of the acute promyelocytic leukaemia protein PML: implications for nuclear localisation. J Cell Sci *112 (Pt 3)*, 381–393.

Endter, C., Kzhyshkowska, J., Stauber, R., and Dobner, T. (2001). SUMO-1 modification required for transformation by adenovirus type 5 early region 1B 55-kDa oncoprotein. Proc Natl Acad Sci USA *98*, 11312–11317.

Enenkel, C., Blobel, G., and Rexach, M. (1995). Identification of a yeast karyopherin heterodimer that targets import substrate to mammalian nuclear pore complexes. J Biol Chem *270*, 16499–16502.

Engelsma, D., Bernad, R., Calafat, J., and Fornerod, M. (2004). Supraphysiological nuclear export signals bind CRM1 independently of RanGTP and arrest at Nup358. Embo J *23*, 3643–3652.

Engelsma, D., Valle, N., Fish, A., Salomé, N., Almendral, J.M., and Fornerod, M. (2008). A supraphysiological nuclear export signal is required for parvovirus nuclear export. Mol Biol Cell *19*, 2544–2552.

Englmeier, L., Olivo, J.C., and Mattaj, I.W. (1999). Receptor-mediated substrate translocation through the nuclear pore complex without nucleotide triphosphate hydrolysis. Curr Biol *9*, 30–41.

Epps, J.L., and Tanda, S. (1998). The Drosophila semushi mutation blocks nuclear import of bicoid during embryogenesis. Curr Biol *8*, 1277–1280.

Evdokimov, E., Sharma, P., Lockett, S.J., Lualdi, M., and Kuehn, M.R. (2008). Loss of SUMO1 in mice affects RanGAP1 localization and formation of PML nuclear bodies, but is not lethal as it can be compensated by SUMO2 or SUMO3. J Cell Sci *121*, 4106–4113.

Fischer, U., Huber, J., Boelens, W.C., Mattaj, I.W., and Lührmann, R. (1995). The HIV-1 Rev activation domain is a nuclear export signal that accesses an export pathway used by specific cellular RNAs. Cell *82*, 475–483.

Floer, M., and Blobel, G. (1996). The nuclear transport factor karyopherin beta binds stoichiometrically to Ran-GTP and inhibits the Ran GTPase activating protein. J Biol Chem *271*, 5313–5316.

Fornerod, M., van Deursen, J., van Baal, S., Reynolds, A., Davis, D., Murti, K.G., Fransen, J., and Grosveld, G. (1997). The human homologue of yeast CRM1 is in a dynamic subcomplex with CAN/Nup214 and a novel nuclear pore component Nup88. Embo J *16*, 807–816.

Fried, H., and Kutay, U. (2003). Nucleocytoplasmic transport: taking an inventory. Cell Mol Life Sci *60*, 1659–1688.

Gan-Erdene, T., Nagamalleswari, K., Yin, L., Wu, K., Pan, Z.-Q., and Wilkinson, K.D. (2003). Identification and characterization of DEN1, a deneddylase of the ULP family. J Biol Chem *278*, 28892–28900.

Geiss-Friedlander, R., and Melchior, F. (2007). Concepts in sumoylation: a decade on. Nat Rev Mol Cell Biol *8*, 947–956.

Giaever, G., Chu, A.M., Ni, L., Connelly, C., Riles, L., Véronneau, S., Dow, S., Lucau-Danila, A., Anderson, K., André, B., et al. (2002). Functional profiling of the

Saccharomyces cerevisiae genome. Nature *418*, 387–391.

Golebiowski, F., Matic, I., Tatham, M.H., Cole, C., Yin, Y., Nakamura, A., Cox, J., Barton, G.J., Mann, M., and Hay, R.T. (2009). System-Wide Changes to SUMO Modifications in Response to Heat Shock. Sci Signal *2*, ra24–ra24.

Gong, L., Kamitani, T., Fujise, K., Caskey, L.S., and Yeh, E.T. (1997). Preferential interaction of sentrin with a ubiquitin-conjugating enzyme, Ubc9. J Biol Chem *272*, 28198–28201.

Görlich, D., and Kutay, U. (1999). Transport between the cell nucleus and the cytoplasm. Annu Rev Cell Dev Biol *15*, 607–660.

Görlich, D., Dabrowski, M., Bischoff, F.R., Kutay, U., Bork, P., Hartmann, E., Prehn, S., and Izaurralde, E. (1997). A novel class of RanGTP binding proteins. J Cell Biol *138*, 65–80.

Görlich, D., Seewald, M.J., and Ribbeck, K. (2003). Characterization of Ran-driven cargo transport and the RanGTPase system by kinetic measurements and computer simulation. Embo J *22*, 1088–1100.

Görlich, D., Vogel, F., Mills, A.D., Hartmann, E., and Laskey, R.A. (1995). Distinct functions for the two importin subunits in nuclear protein import. Nature *377*, 246–248.

Greiner, M., Caesar, S., and Schlenstedt, G. (2004). The histones H2A/H2B and H3/H4 are imported into the yeast nucleus by different mechanisms. Eur. J. Cell Biol. *83*, 511–520.

Grégoire, S., and Yang, X.-J. (2005). Association with class IIa histone deacetylases upregulates the sumoylation of MEF2 transcription factors. Mol Cell Biol *25*, 2273–2287.

Gruss, O.J., Wittmann, M., Yokoyama, H., Pepperkok, R., Kufer, T., Silljé, H., Karsenti, E., Mattaj, I.W., and Vernos, I. (2002). Chromosome-induced microtubule assembly mediated by TPX2 is required for spindle formation in HeLa cells. Nat Cell Biol *4*, 871–879.

Grünwald, M., and Bono, F. (2010). Structure of Importin13-Ubc9 complex: nuclear import and release of a key regulator of sumoylation. Embo J.

Guan, T., Kehlenbach, R.H., Schirmer, E.C., Kehlenbach, A., Fan, F., Clurman, B.E., Arnheim, N., and Gerace, L. (2000). Nup50, a nucleoplasmically oriented nucleoporin with a role in nuclear protein export. Mol Cell Biol *20*, 5619–5630.

Hahn, S., and Schlenstedt, G. (2011). Importin β-type nuclear transport receptors have distinct binding affinities for Ran-GTP. Biochem Biophys Res Commun *406*, 383–388.

Hamada, M., Haeger, A., Jeganathan, K.B., van Ree, J.H., Malureanu, L., Wälde, S., Joseph, J., Kehlenbach, R.H., and van Deursen, J.M. (2011). Ran-dependent docking of importin-beta to RanBP2/Nup358 filaments is essential for protein import and cell viability. J Cell Biol *194*, 597–612.

Hang, J., and Dasso, M. (2002). Association of the human SUMO-1 protease SENP2 with the nuclear pore. J Biol Chem *277*, 19961–19966.

Hannich, J.T., Lewis, A., Kroetz, M.B., Li, S.-J., Heide, H., Emili, A., and Hochstrasser, M. (2005). Defining the SUMO-modified proteome by multiple approaches in Saccharomyces cerevisiae. J Biol Chem *280*, 4102–4110.

Hardeland, U., Steinacher, R., Jiricny, J., and Schär, P. (2002). Modification of the human

thymine-DNA glycosylase by ubiquitin-like proteins facilitates enzymatic turnover. Embo J *21*, 1456–1464.

Hayashi, T., Seki, M., Maeda, D., Wang, W., Kawabe, Y.-I., Seki, T., Saitoh, H., Fukagawa, T., Yagi, H., and Enomoto, T. (2002). Ubc9 is essential for viability of higher eukaryotic cells. Exp Cell Res *280*, 212–221.

Hecker, C.-M., Rabiller, M., Haglund, K., Bayer, P., and Dikic, I. (2006). Specification of SUMO1- and SUMO2-interacting motifs. J Biol Chem *281*, 16117–16127.

Hemelaar, J., Borodovsky, A., Kessler, B.M., Reverter, D., Cook, J., Kolli, N., Gan-Erdene, T., Wilkinson, K.D., Gill, G., Lima, C.D., et al. (2004). Specific and covalent targeting of conjugating and deconjugating enzymes of ubiquitin-like proteins. Mol Cell Biol *24*, 84–95.

Hershko, A., and Ciechanover, A. (1998). The ubiquitin system. Annu Rev Biochem *67*, 425–479.

Hetzer, M., Bilbao-Cortés, D., Walther, T.C., Gruss, O.J., and Mattaj, I.W. (2000). GTP hydrolysis by Ran is required for nuclear envelope assembly. Mol Cell *5*, 1013–1024.

Hicke, L., and Dunn, R. (2003). Regulation of membrane protein transport by ubiquitin and ubiquitin-binding proteins. Annu Rev Cell Dev Biol *19*, 141–172.

Hoelz, A., Debler, E.W., and Blobel, G. (2011). The structure of the nuclear pore complex. Annu Rev Biochem *80*, 613–643.

Hopper, A.K., Traglia, H.M., and Dunst, R.W. (1990). The yeast RNA1 gene product necessary for RNA processing is located in the cytosol and apparently excluded from the nucleus. J Cell Biol *111*, 309–321.

Hu, T., Guan, T., and Gerace, L. (1996). Molecular and functional characterization of the p62 complex, an assembly of nuclear pore complex glycoproteins. J Cell Biol *134*, 589–601.

Hutchison, C.A., Phillips, S., Edgell, M.H., Gillam, S., Jahnke, P., and Smith, M. (1978). Mutagenesis at a specific position in a DNA sequence. J Biol Chem *253*, 6551–6560.

Hutten, S., and Kehlenbach, R.H. (2006). Nup214 is required for CRM1-dependent nuclear protein export in vivo. Mol Cell Biol *26*, 6772–6785.

Hutten, S., and Kehlenbach, R.H. (2007). CRM1-mediated nuclear export: to the pore and beyond. Trends Cell Biol *17*, 193–201.

Hutten, S., Flotho, A., Melchior, F., and Kehlenbach, R.H. (2008). The Nup358-RanGAP complex is required for efficient importin alpha/beta-dependent nuclear import. Mol Biol Cell *19*, 2300–2310.

Hutten, S., Wälde, S., Spillner, C., Hauber, J., and Kehlenbach, R.H. (2009). The nuclear pore component Nup358 promotes transportin-dependent nuclear import. J Cell Sci *122*, 1100–1110.

Izaurralde, E., Kutay, U., Kobbe, von, C., Mattaj, I.W., and Görlich, D. (1997). The asymmetric distribution of the constituents of the Ran system is essential for transport into and out of the nucleus. Embo J *16*, 6535–6547.

Jäkel, S., Albig, W., Kutay, U., Bischoff, F.R., Schwamborn, K., Doenecke, D., and Görlich, D. (1999). The importin beta/importin 7 heterodimer is a functional nuclear import

receptor for histone H1. Embo J *18*, 2411–2423.

Jäkel, S., Mingot, J.-M., Schwarzmaier, P., Hartmann, E., and Görlich, D. (2002). Importins fulfil a dual function as nuclear import receptors and cytoplasmic chaperones for exposed basic domains. Embo J *21*, 377–386.

Johnson, E.S., and Gupta, A.A. (2001). An E3-like factor that promotes SUMO conjugation to the yeast septins. Cell *106*, 735–744.

Johnson, E.S., Schwienhorst, I., Dohmen, R.J., and Blobel, G. (1997). The ubiquitin-like protein Smt3p is activated for conjugation to other proteins by an Aos1p/Uba2p heterodimer. Embo J *16*, 5509–5519.

Joseph, J., Tan, S.-H., Karpova, T.S., McNally, J.G., and Dasso, M. (2002). SUMO-1 targets RanGAP1 to kinetochores and mitotic spindles. J Cell Biol *156*, 595–602.

Kagey, M.H., Melhuish, T.A., and Wotton, D. (2003). The polycomb protein Pc2 is a SUMO E3. Cell *113*, 127–137.

Kalab, P., and Heald, R. (2008). The RanGTP gradient - a GPS for the mitotic spindle. J Cell Sci *121*, 1577–1586.

Kalab, P., Weis, K., and Heald, R. (2002). Visualization of a Ran-GTP gradient in interphase and mitotic Xenopus egg extracts. Science *295*, 2452–2456.

Kaminsky, R., Denison, C., Bening-Abu-Shach, U., Chisholm, A.D., Gygi, S.P., and Broday, L. (2009). SUMO regulates the assembly and function of a cytoplasmic intermediate filament protein in C. elegans. Dev. Cell *17*, 724–735.

Kehlenbach, R.H., Assheuer, R., Kehlenbach, A., Becker, J., and Gerace, L. (2001). Stimulation of nuclear export and inhibition of nuclear import by a Ran mutant deficient in binding to Ran-binding protein 1. J Biol Chem *276*, 14524–14531.

Kiseleva, E., Goldberg, M.W., Allen, T.D., and Akey, C.W. (1998). Active nuclear pore complexes in Chironomus: visualization of transporter configurations related to mRNP export. J Cell Sci *111 (Pt 2)*, 223–236.

Klein, U.R., Haindl, M., Nigg, E.A., and Muller, S. (2009). RanBP2 and SENP3 function in a mitotic SUMO2/3 conjugation-deconjugation cycle on Borealin. Mol Biol Cell *20*, 410–418.

Komander, D., and Rape, M. (2012). The ubiquitin code. Annu Rev Biochem *81*, 203–229.

Kotaja, N., Karvonen, U., Jänne, O.A., and Palvimo, J.J. (2002). PIAS proteins modulate transcription factors by functioning as SUMO-1 ligases. Mol Cell Biol *22*, 5222–5234.

Laemmli, U.K. (1970). Cleavage of structural proteins during the assembly of the head of bacteriophage T4. Nature *227*, 680–685.

Lange, A., Mills, R.E., Lange, C.J., Stewart, M., Devine, S.E., and Corbett, A.H. (2007). Classical nuclear localization signals: definition, function, and interaction with importin alpha. J Biol Chem *282*, 5101–5105.

Lee, G.W., Melchior, F., Matunis, M.J., Mahajan, R., Tian, Q., and Anderson, P. (1998). Modification of Ran GTPase-activating protein by the small ubiquitin-related modifier SUMO-1 requires Ubc9, an E2-type ubiquitin-conjugating enzyme homologue. J Biol

Chem *273*, 6503–6507.

Lee, J.H., Park, S.M., Kim, O.S., Lee, C.S., Woo, J.H., Park, S.J., Joe, E.-H., and Jou, I. (2009). Differential SUMOylation of LXRalpha and LXRbeta mediates transrepression of STAT1 inflammatory signaling in IFN-gamma-stimulated brain astrocytes. Mol Cell *35*, 806–817.

Lee, S.J., Matsuura, Y., Liu, S.M., and Stewart, M. (2005). Structural basis for nuclear import complex dissociation by RanGTP. Nature *435*, 693–696.

Lee, Y.-K., Thomas, S.N., Yang, A.J., and Ann, D.K. (2007). Doxorubicin down-regulates Kruppel-associated box domain-associated protein 1 sumoylation that relieves its transcription repression on p21WAF1/CIP1 in breast cancer MCF-7 cells. J Biol Chem *282*, 1595–1606.

Li, S.-J., and Hochstrasser, M. (2003). The Ulp1 SUMO isopeptidase: distinct domains required for viability, nuclear envelope localization, and substrate specificity. J Cell Biol *160*, 1069–1081.

Li, S.J., and Hochstrasser, M. (1999). A new protease required for cell-cycle progression in yeast. Nature *398*, 246–251.

Liu, B., Gross, M., Hoeve, ten, J., and Shuai, K. (2001). A transcriptional corepressor of Stat1 with an essential LXXLL signature motif. Proc Natl Acad Sci USA *98*, 3203–3207.

Macara, I.G. (2001). Transport into and out of the nucleus. Microbiol. Mol. Biol. Rev. *65*, 570–94, table of contents.

Mahajan, R., Delphin, C., Guan, T., Gerace, L., and Melchior, F. (1997). A small ubiquitin-related polypeptide involved in targeting RanGAP1 to nuclear pore complex protein RanBP2. Cell *88*, 97–107.

Mahajan, R., Gerace, L., and Melchior, F. (1998). Molecular characterization of the SUMO-1 modification of RanGAP1 and its role in nuclear envelope association. J Cell Biol *140*, 259–270.

Mandel, M., and Higa, A. (1970). Calcium-dependent bacteriophage DNA infection. J Mol Biol *53*, 159–162.

Martin, N., Schwamborn, K., Schreiber, V., Werner, A., Guillier, C., Zhang, X.-D., Bischof, O., Seeler, J.-S., and Dejean, A. (2009). PARP-1 transcriptional activity is regulated by sumoylation upon heat shock. Embo J *28*, 3534–3548.

Matunis, M.J., Coutavas, E., and Blobel, G. (1996). A novel ubiquitin-like modification modulates the partitioning of the Ran-GTPase-activating protein RanGAP1 between the cytosol and the nuclear pore complex. J Cell Biol *135*, 1457–1470.

Melchior F. (1998). Nuclear protein import in a permeabilized cell assay. Methods Mol Biol. 88:265-73.

Melchior, F., Paschal, B., Evans, J., and Gerace, L. (1993). Inhibition of nuclear protein import by nonhydrolyzable analogues of GTP and identification of the small GTPase Ran/TC4 as an essential transport factor. J Cell Biol *123*, 1649–1659.

Melchior, F., Sweet, D.J., and Gerace, L. (1995). Analysis of Ran/TC4 function in nuclear protein import. Meth Enzymol *257*, 279–291.

Mendoza, H.M., Shen, L.N., Botting, C., Lewis, A., Chen, J., Ink, B., and Hay, R.T. (2003). NEDP1, a highly conserved cysteine protease that deNEDDylates Cullins. J Biol Chem *278*, 25637–25643.

Meulmeester, E., Kunze, M., Hsiao, H.H., Urlaub, H., and Melchior, F. (2008). Mechanism and consequences for paralog-specific sumoylation of ubiquitin-specific protease 25. Mol Cell *30*, 610–619.

Miller, M.J., Barrett-Wilt, G.A., Hua, Z., and Vierstra, R.D. (2010). Proteomic analyses identify a diverse array of nuclear processes affected by small ubiquitin-like modifier conjugation in Arabidopsis. Proc Natl Acad Sci USA *107*, 16512–16517.

Mingot, J.M., Kostka, S., Kraft, R., Hartmann, E., and Görlich, D. (2001). Importin 13: a novel mediator of nuclear import and export. Embo J *20*, 3685–3694.

Miyauchi, Y., Yogosawa, S., Honda, R., Nishida, T., and Yasuda, H. (2002). Sumoylation of Mdm2 by protein inhibitor of activated STAT (PIAS) and RanBP2 enzymes. J Biol Chem *277*, 50131–50136.

Monecke, T., Güttler, T., Neumann, P., Dickmanns, A., Görlich, D., and Ficner, R. (2009). Crystal structure of the nuclear export receptor CRM1 in complex with Snurportin1 and RanGTP. Science *324*, 1087–1091.

Moore, M.S., and Blobel, G. (1994). A G protein involved in nucleocytoplasmic transport: the role of Ran. Trends Biochem Sci *19*, 211–216.

Morita, Y., Kanei-Ishii, C., Nomura, T., and Ishii, S. (2005). TRAF7 sequesters c-Myb to the cytoplasm by stimulating its sumoylation. Mol Biol Cell *16*, 5433–5444.

Moutty, M.-C., Sakin, V., and Melchior, F. (2011). Importin α/β mediates nuclear import of individual SUMO E1 subunits and of the holo-enzyme. Mol Biol Cell *22*, 652–660.

Murtas, G., Reeves, P.H., Fu, Y.-F., Bancroft, I., Dean, C., and Coupland, G. (2003). A nuclear protease required for flowering-time regulation in Arabidopsis reduces the abundance of SMALL UBIQUITIN-RELATED MODIFIER conjugates. Plant Cell *15*, 2308–2319.

Mühlhäusser, P., Müller, E.C., Otto, A., and Kutay, U. (2001). Multiple pathways contribute to nuclear import of core histones. EMBO Rep *2*, 690–696.

Nacerddine, K., Lehembre, F., Bhaumik, M., Artus, J., Cohen-Tannoudji, M., Babinet, C., Pandolfi, P.P., and Dejean, A. (2005). The SUMO pathway is essential for nuclear integrity and chromosome segregation in mice. Dev. Cell *9*, 769–779.

Nachury, M.V., and Weis, K. (1999). The direction of transport through the nuclear pore can be inverted. Proc Natl Acad Sci USA *96*, 9622–9627.

Nachury, M.V., Maresca, T.J., Salmon, W.C., Waterman-Storer, C.M., Heald, R., and Weis, K. (2001). Importin beta is a mitotic target of the small GTPase Ran in spindle assembly. Cell *104*, 95–106.

Nakielny, S., Siomi, M.C., Siomi, H., Michael, W.M., Pollard, V., and Dreyfuss, G. (1996). Transportin: nuclear transport receptor of a novel nuclear protein import pathway. Exp Cell Res *229*, 261–266.

Nemergut, M.E., Mizzen, C.A., Stukenberg, T., Allis, C.D., and Macara, I.G. (2001).

Chromatin docking and exchange activity enhancement of RCC1 by histones H2A and H2B. Science *292*, 1540–1543.

Nie, M., Xie, Y., Loo, J.A., and Courey, A.J. (2009). Genetic and proteomic evidence for roles of Drosophila SUMO in cell cycle control, Ras signaling, and early pattern formation. PLoS ONE *4*, e5905.

Oh, S.-M., Liu, Z., Okada, M., Jang, S.-W., Liu, X., Chan, C.-B., Luo, H., and Ye, K. (2010). Ebp1 sumoylation, regulated by TLS/FUS E3 ligase, is required for its anti-proliferative activity. Oncogene *29*, 1017–1030.

Ohno, M., Fornerod, M., and Mattaj, I.W. (1998). Nucleocytoplasmic transport: the last 200 nanometers. Cell *92*, 327–336.

Ohtsubo, M., Kai, R., Furuno, N., Sekiguchi, T., Sekiguchi, M., Hayashida, H., Kuma, K., Miyata, T., Fukushige, S., and Murotsu, T. (1987). Isolation and characterization of the active cDNA of the human cell cycle gene (RCC1) involved in the regulation of onset of chromosome condensation. Genes Dev *1*, 585–593.

Ohuchi, T., Seki, M., Branzei, D., Maeda, D., Ui, A., Ogiwara, H., Tada, S., and Enomoto, T. (2008). Rad52 sumoylation and its involvement in the efficient induction of homologous recombination. DNA Repair (Amst.) *7*, 879–889.

Ortiz de Montellano, P.R., David, S.K., Ator, M.A., and Tew, D. (1988). Mechanism-based inactivation of horseradish peroxidase by sodium azide. Formation of meso-azidoprotoporphyrin IX. Biochemistry *27*, 5470–5476.

Owerbach, D., McKay, E.M., Yeh, E.T.H., Gabbay, K.H., and Bohren, K.M. (2005). A proline-90 residue unique to SUMO-4 prevents maturation and sumoylation. Biochem Biophys Res Commun *337*, 517–520.

Paine P.L., Moore,L.C. and Horowitz,S.B. (1975). Nuclear envelope permeability. Nature, 254, 109–114.

Palancade, B., and Doye, V. (2008). Sumoylating and desumoylating enzymes at nuclear pores: underpinning their unexpected duties? Trends Cell Biol *18*, 174–183.

Panté, N., and Kann, M. (2002). Nuclear pore complex is able to transport macromolecules with diameters of about 39 nm. Mol Biol Cell *13*, 425–434.

Paraskeva, E., Izaurralde, E., Bischoff, F.R., Huber, J., Kutay, U., Hartmann, E., Lührmann, R., and Görlich, D. (1999). CRM1-mediated recycling of snurportin 1 to the cytoplasm. J Cell Biol *145*, 255–264.

Pay, A., Resch, K., Frohnmeyer, H., Fejes, E., Nagy, F., and Nick, P. (2002). Plant RanGAPs are localized at the nuclear envelope in interphase and associated with microtubules in mitotic cells. Plant J. *30*, 699–709.

Pemberton, L.F., Rosenblum, J.S., and Blobel, G. (1999). Nuclear import of the TATA-binding protein: mediation by the karyopherin Kap114p and a possible mechanism for intranuclear targeting. J Cell Biol *145*, 1407–1417.

Pichler, A., Gast, A., Seeler, J.S., Dejean, A., and Melchior, F. (2002). The nucleoporin RanBP2 has SUMO1 E3 ligase activity. Cell *108*, 109–120.

Pichler, A., Knipscheer, P., Oberhofer, E., van Dijk, W.J., Körner, R., Olsen, J.V., Jentsch, S.,

Melchior, F., and Sixma, T.K. (2005). SUMO modification of the ubiquitin-conjugating enzyme E2-25K. Nat Struct Mol Biol *12*, 264–269.

Pichler, A., Knipscheer, P., Saitoh, H., Sixma, T.K., and Melchior, F. (2004). The RanBP2 SUMO E3 ligase is neither HECT- nor RING-type. Nat Struct Mol Biol *11*, 984–991.

Pinto, M.P., Carvalho, A.F., Grou, C.P., Rodríguez-Borges, J.E., Sá-Miranda, C., and Azevedo, J.E. (2012). Heat shock induces a massive but differential inactivation of SUMO-specific proteases. Biochim Biophys Acta.

Plechanovova, A., Jaffray, E.G., McMahon, S.A., Johnson, K.A., Navrátilová, I., Naismith, J.H., and Hay, R.T. (2011). Mechanism of ubiquitylation by dimeric RING ligase RNF4. Nat Struct Mol Biol *18*, 1052–1059.

Potts, P.R., and Yu, H. (2005). Human MMS21/NSE2 is a SUMO ligase required for DNA repair. Mol Cell Biol *25*, 7021–7032.

Rangasamy, D., Woytek, K., Khan, S.A., and Wilson, V.G. (2000). SUMO-1 modification of bovine papillomavirus E1 protein is required for intranuclear accumulation. J Biol Chem *275*, 37999–38004.

Reichelt, R., Holzenburg, A., Buhle, E.L., Jarnik, M., Engel, A., and Aebi, U. (1990). Correlation between structure and mass distribution of the nuclear pore complex and of distinct pore complex components. J Cell Biol *110*, 883–894.

Renart, J., Reiser, J., and Stark, G.R. (1979). Transfer of proteins from gels to diazobenzyloxymethyl-paper and detection with antisera: a method for studying antibody specificity and antigen structure. Proc Natl Acad Sci USA *76*, 3116–3120.

Renault, L., Kuhlmann, J., Henkel, A., and Wittinghofer, A. (2001). Structural basis for guanine nucleotide exchange on Ran by the regulator of chromosome condensation (RCC1). Cell *105*, 245–255.

Reverter, D., and Lima, C.D. (2005). Insights into E3 ligase activity revealed by a SUMO-RanGAP1-Ubc9-Nup358 complex. Nature *435*, 687–692.

Ribbeck, K., and Görlich, D. (2001). Kinetic analysis of translocation through nuclear pore complexes. Embo J *20*, 1320–1330.

Ribbeck, K., Kutay, U., Paraskeva, E., and Görlich, D. (1999). The translocation of transportin-cargo complexes through nuclear pores is independent of both Ran and energy. Curr Biol *9*, 47–50.

Ribbeck, K., Lipowsky, G., Kent, H.M., Stewart, M., and Görlich, D. (1998). NTF2 mediates nuclear import of Ran. Embo J *17*, 6587–6598.

Rodriguez, M.S., Dargemont, C., and Hay, R.T. (2001). SUMO-1 conjugation in vivo requires both a consensus modification motif and nuclear targeting. J Biol Chem *276*, 12654–12659.

Rodriguez, M.S., Desterro, J.M., Lain, S., Midgley, C.A., Lane, D.P., and Hay, R.T. (1999). SUMO-1 modification activates the transcriptional response of p53. Embo J *18*, 6455–6461.

Rosas-Acosta, G., Russell, W.K., Deyrieux, A., Russell, D.H., and Wilson, V.G. (2005). A universal strategy for proteomic studies of SUMO and other ubiquitin-like modifiers. Mol Cell Proteomics *4*, 56–72.

Rothenbusch, U., Sawatzki, M., Chang, Y., Caesar, S., and Schlenstedt, G. (2012). Sumoylation regulates Kap114-mediated nuclear transport. Embo J.

Rout, M.P., Aitchison, J.D., Magnasco, M.O., and Chait, B.T. (2003). Virtual gating and nuclear transport: the hole picture. Trends Cell Biol *13*, 622–628.

Rout, M.P., Aitchison, J.D., Suprapto, A., Hjertaas, K., Zhao, Y., and Chait, B.T. (2000). The yeast nuclear pore complex: composition, architecture, and transport mechanism. J Cell Biol *148*, 635–651.

Rout, M.P., and Blobel, G. (1993). Isolation of the yeast nuclear pore complex. J Cell Biol *123*, 771–783.

Rush, M. G., Drivas, G. and D'Eustachio, P. D. (1996). The small nuclear GTPase Ran: how much does it run? BioEssays 18, 103-112.

Rytinki, M.M., Kaikkonen, S., Pehkonen, P., Jääskeläinen, T., and Palvimo, J.J. (2009). PIAS proteins: pleiotropic interactors associated with SUMO. Cell Mol Life Sci *66*, 3029–3041.

Sachdev, S., Bruhn, L., Sieber, H., Pichler, A., Melchior, F., and Grosschedl, R. (2001). PIASy, a nuclear matrix-associated SUMO E3 ligase, represses LEF1 activity by sequestration into nuclear bodies. Genes Dev *15*, 3088–3103.

Saitoh, H., and Hinchey, J. (2000). Functional heterogeneity of small ubiquitin-related protein modifiers SUMO-1 versus SUMO-2/3. J Biol Chem *275*, 6252–6258.

Saitoh, H., Pu, R., Cavenagh, M., and Dasso, M. (1997). RanBP2 associates with Ubc9p and a modified form of RanGAP1. Proc Natl Acad Sci USA *94*, 3736–3741.

Saitoh, H., Sparrow, D.B., Shiomi, T., Pu, R.T., Nishimoto, T., Mohun, T.J., and Dasso, M. (1998). Ubc9p and the conjugation of SUMO-1 to RanGAP1 and RanBP2. Curr Biol *8*, 121–124.

Sampson, D.A., Wang, M., and Matunis, M.J. (2001). The small ubiquitin-like modifier-1 (SUMO-1) consensus sequence mediates Ubc9 binding and is essential for SUMO-1 modification. J Biol Chem *276*, 21664–21669.

Sanger, F., Nicklen, S., and Coulson, A.R. (1977). DNA sequencing with chain-terminating inhibitors. Proc Natl Acad Sci USA *74*, 5463–5467.

Sasaki, T., Kojima, H., Kishimoto, R., Ikeda, A., Kunimoto, H., and Nakajima, K. (2006). Spatiotemporal regulation of c-Fos by ERK5 and the E3 ubiquitin ligase UBR1, and its biological role. Mol Cell *24*, 63–75.

Scheffzek, K., Klebe, C., Fritz-Wolf, K., Kabsch, W., and Wittinghofer, A. (1995). Crystal structure of the nuclear Ras-related protein Ran in its GDP-bound form. Nature *374*, 378–381.

Schmidt, D., and Muller, S. (2002). Members of the PIAS family act as SUMO ligases for c-Jun and p53 and repress p53 activity. Proc Natl Acad Sci USA *99*, 2872–2877.

Schulz, S., Chachami, G., Kozaczkiewicz, L., Winter, U., Stankovic-Valentin, N., Haas, P., Hofmann, K., Urlaub, H., Ovaa, H., Wittbrodt, J., et al. (2012). Ubiquitin-specific protease-like 1 (USPL1) is a SUMO isopeptidase with essential, non-catalytic functions. EMBO Rep.

Schwarz, S.E., Matuschewski, K., Liakopoulos, D., Scheffner, M., and Jentsch, S. (1998).

The ubiquitin-like proteins SMT3 and SUMO-1 are conjugated by the UBC9 E2 enzyme. Proc Natl Acad Sci USA *95*, 560–564.

Schwoebel, E.D., Talcott, B., Cushman, I., and Moore, M.S. (1998). Ran-dependent signal-mediated nuclear import does not require GTP hydrolysis by Ran. J Biol Chem *273*, 35170–35175.

Seewald, M.J., Körner, C., Wittinghofer, A., and Vetter, I.R. (2002). RanGAP mediates GTP hydrolysis without an arginine finger. Nature *415*, 662–666.

Shen, T.H., Lin, H.-K., Scaglioni, P.P., Yung, T.M., and Pandolfi, P.P. (2006). The mechanisms of PML-nuclear body formation. Mol Cell *24*, 331–339.

Shin, E.J., Shin, H.M., Nam, E., Kim, W.S., Kim, J.-H., Oh, B.-H., and Yun, Y. (2012). DeSUMOylating isopeptidase: a second class of SUMO protease. EMBO Rep.

Siomi, H., and Dreyfuss, G. (1995). A nuclear localization domain in the hnRNP A1 protein. J Cell Biol *129*, 551–560.

Sivaraman, T., Kumar, T.K., Jayaraman, G., and Yu, C. (1997). The mechanism of 2,2,2-trichloroacetic acid-induced protein precipitation. J. Protein Chem. *16*, 291–297.

Smith, A., Brownawell, A., and Macara, I.G. (1998). Nuclear import of Ran is mediated by the transport factor NTF2. Curr Biol *8*, 1403–1406.

Smith, A.E., Slepchenko, B.M., Schaff, J.C., Loew, L.M., and Macara, I.G. (2002). Systems analysis of Ran transport. Science *295*, 488–491.

Smith, L.M., Fung, S., Hunkapiller, M.W., Hunkapiller, T.J., and Hood, L.E. (1985). The synthesis of oligonucleotides containing an aliphatic amino group at the 5' terminus: synthesis of fluorescent DNA primers for use in DNA sequence analysis. Nucleic Acids Res. *13*, 2399–2412.

Smith, L.M., Sanders, J.Z., Kaiser, R.J., Hughes, P., Dodd, C., Connell, C.R., Heiner, C., Kent, S.B., and Hood, L.E. (1986). Fluorescence detection in automated DNA sequence analysis. Nature *321*, 674–679.

Smith, M., Bhaskar, V., Fernandez, J., and Courey, A.J. (2004). Drosophila Ulp1, a nuclear pore-associated SUMO protease, prevents accumulation of cytoplasmic SUMO conjugates. J Biol Chem *279*, 43805–43814.

Song, J., Durrin, L.K., Wilkinson, T.A., Krontiris, T.G., and Chen, Y. (2004). Identification of a SUMO-binding motif that recognizes SUMO-modified proteins. Proc Natl Acad Sci USA *101*, 14373–14378.

Stade, K., Vogel, F., Schwienhorst, I., Meusser, B., Volkwein, C., Nentwig, B., Dohmen, R.J., and Sommer, T. (2002). A lack of SUMO conjugation affects cNLS-dependent nuclear protein import in yeast. J Biol Chem *277*, 49554–49561.

Stehmeier, P., and Muller, S. (2009). Phospho-regulated SUMO interaction modules connect the SUMO system to CK2 signaling. Mol Cell *33*, 400–409.

Sternsdorf, T., Jensen, K., Reich, B., and Will, H. (1999). The nuclear dot protein sp100, characterization of domains necessary for dimerization, subcellular localization, and modification by small ubiquitin-like modifiers. J Biol Chem *274*, 12555–12566.

Stewart, M. (2007). Molecular mechanism of the nuclear protein import cycle. Nat Rev Mol Cell Biol *8*, 195–208.

Stewart, M., Kent, H.M., and McCoy, A.J. (1998). Structural basis for molecular recognition between nuclear transport factor 2 (NTF2) and the GDP-bound form of the Ras-family GTPase Ran. J Mol Biol *277*, 635–646.

Subramaniam, S., Sixt, K.M., Barrow, R., and Snyder, S.H. (2009). Rhes, a striatal specific protein, mediates mutant-huntingtin cytotoxicity. Science *324*, 1327–1330.

Swaminathan, S., Kiendl, F., Körner, R., Lupetti, R., Hengst, L., and Melchior, F. (2004). RanGAP1*SUMO1 is phosphorylated at the onset of mitosis and remains associated with RanBP2 upon NPC disassembly. J Cell Biol *164*, 965–971.

Takahashi, Y., Kahyo, T., Toh-E, A., Yasuda, H., and Kikuchi, Y. (2001). Yeast Ull1/Siz1 is a novel SUMO1/Smt3 ligase for septin components and functions as an adaptor between conjugating enzyme and substrates. J Biol Chem *276*, 48973–48977.

Takahashi, Y., Mizoi, J., Toh-E, A., and Kikuchi, Y. (2000). Yeast Ulp1, an Smt3-specific protease, associates with nucleoporins. J Biochem *128*, 723–725.

Tanaka, K., Nishide, J., Okazaki, K., Kato, H., Niwa, O., Nakagawa, T., Matsuda, H., Kawamukai, M., and Murakami, Y. (1999). Characterization of a fission yeast SUMO-1 homologue, pmt3p, required for multiple nuclear events, including the control of telomere length and chromosome segregation. Mol Cell Biol *19*, 8660–8672.

Tatham, M.H., Geoffroy, M.-C., Shen, L., Plechanovova, A., Hattersley, N., Jaffray, E.G., Palvimo, J.J., and Hay, R.T. (2008). RNF4 is a poly-SUMO-specific E3 ubiquitin ligase required for arsenic-induced PML degradation. Nat Cell Biol *10*, 538–546.

Tatham, M.H., Kim, S., Jaffray, E., Song, J., Chen, Y., and Hay, R.T. (2005). Unique binding interactions among Ubc9, SUMO and RanBP2 reveal a mechanism for SUMO paralog selection. Nat Struct Mol Biol *12*, 67–74.

Taylor, D.L., Ho, J.C.Y., Oliver, A., and Watts, F.Z. (2002). Cell-cycle-dependent localisation of Ulp1, a Schizosaccharomyces pombe Pmt3 (SUMO)-specific protease. J Cell Sci *115*, 1113–1122.

Thomas, F., and Kutay, U. (2003). Biogenesis and nuclear export of ribosomal subunits in higher eukaryotes depend on the CRM1 export pathway. J Cell Sci *116*, 2409–2419.

Ulrich, H.D. (2008). The fast-growing business of SUMO chains. Mol Cell *32*, 301–305.

Vetter, I.R., Arndt, A., Kutay, U., Görlich, D., and Wittinghofer, A. (1999). Structural view of the Ran-Importin beta interaction at 2.3 A resolution. Cell *97*, 635–646.

Villa Braslavsky, C.I., Nowak, C., Görlich, D., Wittinghofer, A., and Kuhlmann, J. (2000). Different structural and kinetic requirements for the interaction of Ran with the Ran-binding domains from RanBP2 and importin-beta. Biochemistry *39*, 11629–11639.

Walther, T.C., Pickersgill, H.S., Cordes, V.C., Goldberg, M.W., Allen, T.D., Mattaj, I.W., and Fornerod, M. (2002). The cytoplasmic filaments of the nuclear pore complex are dispensable for selective nuclear protein import. J Cell Biol *158*, 63–77.

Wang, J., Chen, L., Wen, S., Zhu, H., Yu, W., Moskowitz, I.P., Shaw, G.M., Finnell, R.H., and Schwartz, R.J. (2011). Defective sumoylation pathway directs congenital heart disease. Birth Defects Res. Part a Clin. Mol. Teratol. *91*, 468–476.

Wälde, S., Thakar, K., Hutten, S., Spillner, C., Nath, A., Rothbauer, U., Wiemann, S., and Kehlenbach, R.H. (2012). The nucleoporin Nup358/RanBP2 promotes nuclear import in a cargo- and transport receptor-specific manner. Traffic *13*, 218–233.

Weger, S., Hammer, E., and Heilbronn, R. (2005). Topors acts as a SUMO-1 E3 ligase for p53 in vitro and in vivo. FEBS Lett *579*, 5007–5012.

Welchman, R.L., Gordon, C., and Mayer, R.J. (2005). Ubiquitin and ubiquitin-like proteins as multifunctional signals. Nat Rev Mol Cell Biol *6*, 599–609.

Wen, W., Meinkoth, J.L., Tsien, R.Y., and Taylor, S.S. (1995). Identification of a signal for rapid export of proteins from the nucleus. Cell *82*, 463–473.

Werner, A., Flotho, A., and Melchior, F. (2012). The RanBP2/RanGAP1(∗)SUMO1/Ubc9 Complex Is a Multisubunit SUMO E3 Ligase. Mol Cell *46*, 287–298.

Wessel, D., and Flügge, U.I. (1984). A method for the quantitative recovery of protein in dilute solution in the presence of detergents and lipids. Anal Biochem *138*, 141–143.

Wiese, C., Wilde, A., Moore, M.S., Adam, S.A., Merdes, A., and Zheng, Y. (2001). Role of importin-beta in coupling Ran to downstream targets in microtubule assembly. Science *291*, 653–656.

Wong, K.H., Todd, R.B., Oakley, B.R., Oakley, C.E., Hynes, M.J., and Davis, M.A. (2008). Sumoylation in Aspergillus nidulans: sumO inactivation, overexpression and live-cell imaging. Fungal Genet. Biol. *45*, 728–737.

Wood, L.D., Irvin, B.J., Nucifora, G., Luce, K.S., and Hiebert, S.W. (2003). Small ubiquitin-like modifier conjugation regulates nuclear export of TEL, a putative tumor suppressor. Proc Natl Acad Sci USA *100*, 3257–3262.

Wu, J., Matunis, M.J., Kraemer, D., Blobel, G., and Coutavas, E. (1995). Nup358, a cytoplasmically exposed nucleoporin with peptide repeats, Ran-GTP binding sites, zinc fingers, a cyclophilin A homologous domain, and a leucine-rich region. J Biol Chem *270*, 14209–14213.

Wu, K., Yamoah, K., Dolios, G., Gan-Erdene, T., Tan, P., Chen, A., Lee, C.-G., Wei, N., Wilkinson, K.D., Wang, R., et al. (2003). DEN1 is a dual function protease capable of processing the C terminus of Nedd8 and deconjugating hyper-neddylated CUL1. J Biol Chem *278*, 28882–28891.

Yang, Q., Rout, M.P., and Akey, C.W. (1998). Three-dimensional architecture of the isolated yeast nuclear pore complex: functional and evolutionary implications. Mol Cell *1*, 223–234.

Yaseen, N.R., and Blobel, G. (1999). GTP hydrolysis links initiation and termination of nuclear import on the nucleoporin nup358. J Biol Chem *274*, 26493–26502.

Yokoyama, N., Hayashi, N., Seki, T., Panté, N., Ohba, T., Nishii, K., Kuma, K., Hayashida, T., Miyata, T., and Aebi, U. (1995). A giant nucleopore protein that binds Ran/TC4. Nature *376*, 184–188.

Zhang, C., and Clarke, P.R. (2000). Chromatin-independent nuclear envelope assembly induced by Ran GTPase in Xenopus egg extracts. Science *288*, 1429–1432.

Zhang, F.-P., Mikkonen, L., Toppari, J., Palvimo, J.J., Thesleff, I., and Jänne, O.A. (2008a).

Sumo-1 function is dispensable in normal mouse development. Mol Cell Biol *28*, 5381–5390.

Zhang, H., Saitoh, H., and Matunis, M.J. (2002). Enzymes of the SUMO modification pathway localize to filaments of the nuclear pore complex. Mol Cell Biol 22, 6498–6508.

Zhang, X.-D., Goeres, J., Zhang, H., Yen, T.J., Porter, A.C.G., and Matunis, M.J. (2008b). SUMO-2/3 modification and binding regulate the association of CENP-E with kinetochores and progression through mitosis. Mol Cell *29*, 729–741.

Zhong, S., Müller, S., Ronchetti, S., Freemont, P.S., Dejean, A., and Pandolfi, P.P. (2000). Role of SUMO-1-modified PML in nuclear body formation. Blood *95*, 2748–2752.

Zhu, S., Goeres, J., Sixt, K.M., Békés, M., Zhang, X.-D., Salvesen, G.S., and Matunis, M.J. (2009). Protection from isopeptidase-mediated deconjugation regulates paralog-selective sumoylation of RanGAP1. Mol Cell *33*, 570–580.

Zhu, S., Zhang, H., and Matunis, M.J. (2006). SUMO modification through rapamycin-mediated heterodimerization reveals a dual role for Ubc9 in targeting RanGAP1 to nuclear pore complexes. Exp Cell Res *312*, 1042–1049.

Zou, T., Liu, L., Rao, J.N., Marasa, B.S., Chen, J., Xiao, L., Zhou, H., Gorospe, M., and Wang, J.-Y. (2008). Polyamines modulate the subcellular localization of RNA-binding protein HuR through AMP-activated protein kinase-regulated phosphorylation and acetylation of importin alpha1. Biochem J *409*, 389–398.

ABBREVIATIONS

General Abbreviations

~	approximately
~	thioster bond in context of sumoylation
aa	amino acids
A.nidulans	*Aspergillus nidulans*
APS	Ammonium persulfate
A.thaliana	*Arabidopsis thaliana*
ATP	Adenosine-5′-triphosphate
BSA	Bovine serum albumin
C-	Carboxyl-
C.elegans	*Caenorhabditis elegans*
CNBr	Cyanogenbromide
cNLS	classical nuclear localization signal
Da	Dalton
DeSI1	DeSumoylating isopeptidase 1
D.melanogaster	*Drosophila melanogaster*
DMEM	Dulbecco's modified eagle medium
DMP	Dimethyl pimelimidate
DMSO	Dimethyl sulfoxide
DNA	Deoxyribonucleic acid
dNTP	2′-deoxynucleoside-5′-triphosphate
ddNTP	2′,3′-deoxynucleoside-5′-triphosphate
DTT	Dithiothreitol
E-	Enzyme-
ECL	Enhanced chemical luminescence
E.coli	*Escherichia coli*
EDTA	ethylenediaminetetraacetic acid
FBS	Fetal bovine serum
GDP	Guanosine-5′-diphosphate
GMP-PNP	5'-Guanylyl imidodiphosphate
GST	Glutathione *S*-transferase
GTP	Guanosine-5′-triphosphate
H2A and H2B	Histone 2A and 2B
HCl	Hydrochloric acid
HDAC4	Histone deacetylase 4
HEAT	Huntingtin, elongation factor 3, protein phosphatase 2A, and the yeast kinase TOR1

HeLa	Henrietta Lacks
HEPES	4-(2-hydroxyethyl)-1-piperazineethanesulfonic acid
HF	High fidelity
HIV	Human immunodeficiency virus
IDCR	Ionic detergent compatibility reagent
IF	Immunofluorescence
IgG	Immunoglobulin G
Imp	Importin
IP	Immunoprecipitation
IPTG	Isopropyl β-D-1-thiogalactopyranoside
ISG15	IFN-stimulated gene 15
kDa	Kilodalton
LB	Luria-Bertani
MAPL	Mitochondrial-anchored protein ligase
Mg	Magnesium
mRNA	Messenger ribonucleic acid
N-	Amino- in context of protein
NaOH	Sodium hydroxide
NCS	Newborn calf serum
Nedd8	Neural precursor cell expressed developmentally down-regulated protein 8
NEM	*N*-Ethylmaleimide
NES	Nuclear export signal
NLS	Nuclear localization signal
NPC	Nuclear pore complex
Nt	nucleotide
NTF2	Nuclear transport factor 2
NTRs	Nuclear transport receptors
NuMa	Nuclear mitotic apparatus protein 1
Nups	Nucleoporins
OH	Hydroxyl
PAGE	Polyacrylamide gel electrophoresis
PBS	Phosphate buffered saline
PBST	Phosphate buffered saline tween
Pc2	Polycomb 2
PCR	Polymerase chain reaction
PIAS	Protein inhibitors of activated STATs
PKI	Protein kinase inhibitor

PML	Promyelocytic leukemia
PMSF	Phenylmethylsulfonyl fluoride
PTMs	Posttranslational Modifications
Ran	Ras-related nuclear protein
RanBP1 and 2	Ran-binding protein 1 and 2
RanGAP1	Ran GTPase-activating protein 1
Ras	Rat sarcoma
RCC1	Regulator of chromosome condensation 1
Rev	Regulator of virion expression
RHES	Ras Homolog Enriched in Striatum
RNA	Ribonucleic acid
SAB	Sumoylation assay buffer
SAE1 and 2	SUMO-activating enzyme subunit 1 and 2
SDS	sodium dodecyl sulfate
SENP	SUMO/Sentrin specific protease
S.cerevisiae	*Saccharomyces cerevisiae*
S.pombe	*Schizosaccharomyces pombe*
SIM	SUMO-interaction motif
SMT3	Suppressor of Mif2 3
SOC	Super Optimal broth with Catabolite repression
SUMO	Small Ubiquitin-like Modifier
TAE	Tris/acetate/EDTA
TB	Transport buffer
TCA	Trichloroacetic acid
TE	Tris/EDTA
TEMED	Tetramethylethylenediamine
TLS	Translocation in liposarcoma
TOPORS	Topoisomerase I Binding, arginine/serine-Rich
Tpx2	Targeting protein for Xklp2
Tris	Tris (hydroxymethyl) aminomethane
Ub	Ubiquitin
Ubc9	Ubiquitin-conjugating enzyme 9
Ubls	Ubiquitin-like modifiers
Ulp1 and 2	Ubiquitin-like protease 1 and 2
Urm1	Ubiquitin-related modifier 1
Uspl1	Ubiquitin-specific protease-like 1
Usp25	Ubiquitin-specific protease 25
UV	Ultraviolet

v/v	volume/volume
w/v	weight/volume

Physical units

A	ampere
°C	degree Celsius
g	gram
x g	acceleration of gravity on earth
h	hour
L	liter
M	molar (mol/L)
min	minute
OD	optical density
pH	negative common logarithm of the proton concentration
rpm	rotations per minute
sec	second
V	volt

Prefixes

k	kilo 10^3
c	centi 10^{-2}
m	milli 10^{-3}
μ	micro 10^{-6}
n	nano 10^{-9}
p	pico 10^{-12}

Code for amino acids

A	Ala	alanine
C	Cys	cysteine
D	Asp	aspartate
E	Glu	glutamate
F	Phe	phenylalanine
G	Gly	glycine
H	His	histidine
I	Iso	isoleucine
K	Lys	lysine
L	Leu	leucine
M	Met	methionine

N	Asn	asparagine
P	Pro	proline
Q	Gln	glutamine
R	Arg	arginine
S	Ser	serine
T	Thr	threonine
V	Val	valine
W	Trp	tryptophane
Y	Tyr	tyrosine
X		any amino acid
ψ		bulky hydrophobic residue

CURRICULUM VITAE

Personal Data

Name:	Volkan Sakin
Date & Place of Birth:	April 23rd, 1984 in Diyarbakir, Turkey
Nationality:	Turkish

Education

Since October 2008

PhD student in the laboratory of Prof. Dr. Frauke Melchior
Started at the Department of Biochemistry I
University of Göttingen and continued after the lab move (April 2009)
at DKFZ-ZMBH Alliance, University of Heidelberg

2007-2008

MSc-PhD Program Molecular Biology, University of Göttingen &
International Max Planck Research School (IMPRS)
Master's examination: 1.25 (excellent)

2002-2007

BSc Program Molecular Biology and Genetics
Middle East Technical University / Ankara, Turkey
CPGA: 3.71 / 4.00

1999-2002

High School
Ankara Science High School / Ankara, Turkey
CGPA: 5.00 / 5.00

Scientific Activities

May-June 2008

Lab rotation project:
„Investigating the role of phosphatases in UV-induced DNA damage response"
Supervision: Prof. Dr. Matthias Dobbelstein
Department of Molecular Oncology, University of Göttingen

March-May 2008

Lab rotation project:
„Functional characterization of CDYL1b in different cell types"
Supervision: Dr. Wolfgang Fischle
Chromatin Biochemistry Group MPI for Biophysical Chemistry

January-February 2008   Lab rotation project:
„Characterization of Lysine Linkages of Mixed SUMO1-Ubiquitin
chains by *in vivo* and *in vitro* Approaches"
Supervision: Prof. Dr. Frauke Melchior
Department of Biochemistry I, University of Göttingen

June-September 2006   Research Internship:
„Investigating the role of TIMP3 and OSF2 in N-Ras transformed cells"
Supervision: Prof. Dr. Angel G. Pellicer, M.D.
Pathology Department, New York University School of Medicine

Teaching Experience

2011 & 2012   Supervising tutor for one week for the 3-week practical course
„Antibodies – essential tools in molecular cell biology"
in MCB Master Program, ZMBH, University of Heidelberg

June-July 2010   Supervision of lab rotation student Anna Kołodziejczyk
for 6-weeks, ZMBH, University of Heidelberg

Publications

Moutty, M.C., Sakin, V., and Melchior, F. (2011). Importin α/β mediates nuclear import of individual SUMO E1 subunits and of the holo-enzyme. Mol Biol Cell. 22(5): 652-60.

Sakin V., Eskiocak U., Kars M.D., Iseri O.D., Gunduz U. (2008). hTERT gene expression levels and telomerase activity in drug-resistant MCF-7 cells. Exp Oncol. 30(3): 202-5